



NTNU – Trondheim
Norwegian University of
Science and Technology

Analysis and design of solar based systems for heating and cooling of buildings

Igor Shesho

Master's Thesis

Submission date: July 2014

Supervisor: Vojislav Novakovic, EPT

Co-supervisor: Laurent Georges, EPT

Norwegian University of Science and Technology
Department of Energy and Process Engineering



MASTER THESIS

Analysis and design of solar based systems for heating and cooling of buildings

Igor Shesho

Supervisor: Vojislav Novakovic

Co-supervisor: Laurent Georges

Submission date: July 2014

Norwegian University of Science and Technology
Department of Energy and Process Engineering

EPT-M-2014-145

MASTER THESIS

for

Student Igor Shesho

Spring 2014

Analysis and design of solar based systems for heating and cooling of buildings*Analyse og design av systemer for bruk av solenergi for oppvarming og kjøling av bygninger***Background and objective**

According to the IEA (International Energy Agency) buildings represent 32% of the total final energy consumption and converted in terms of primary energy this will be around 40%. Inspected deeper, the heating energy consumption represents over 60% of the total energy demand in the building. Space heating and hot water heating account for over 75% of the energy used in single and multi-family homes. Solar energy can meet up to 100% of this demand.

Solar technologies can supply the energy for all of the building's needs—heating, cooling, hot water, light and electricity—without the harmful effects of greenhouse gas emissions created by fossil fuels. Usually the maximum demand for cooling coincides with the maximum availability of solar radiation, whereas conventional electrical-compressor chillers have the problem of providing their minimum capacity in the hottest hours.

The main objective of this thesis is optimizing solar driven air-conditioning systems through developing innovative combinations of solar heating, cooling and storage techniques in regard to primary energy savings and economic viability. The objective will be achieved through transient dynamic simulations and a holistic approach for various configurations between solar heating and cooling technologies, energy storage and auxiliary conventional heating and cooling devices.

This assignment is realized as a part of the collaborative project “Sustainable Energy and Environment in Western Balkans” that aims to develop and establish five new internationally recognized MSc study programs for the field of “Sustainable Energy and Environment”, one at each of the five collaborating universities in three different WB countries. The project is funded through the Norwegian Programme in Higher Education, Research and Development in the Western Balkans, Programme 3: Energy Sector (HERD Energy) for the period 2011-2014.

The following tasks are to be considered:

1. Literature review of solar based systems for heating and cooling of buildings.
2. Define the solar heating and cooling components, reference system and various configurations of the SHC technologies subject for optimization

3. Numerical modelling of the solar heating and cooling system components (solar collectors, storage tanks, absorption chiller, heat pump)
4. Dynamic simulation and optimization of the defined solar air-conditioning configurations
5. Simulation results, analysis and conclusions
6. Make a draft proposal (8-10 pages) for a scientific paper based on the performed work in the master thesis.

-- ” --

When the thesis is evaluated, emphasis is put on processing of the results, and that they are presented in tabular and/or graphic form in a clear manner, and that they are analyzed carefully.

The thesis should be formulated as a research report with summary both in English and Norwegian, conclusion, literature references, table of contents etc. During the preparation of the text, the candidate should make an effort to produce a well-structured and easily readable report. In order to ease the evaluation of the thesis, it is important that the cross-references are correct. In the making of the report, strong emphasis should be placed on both a thorough discussion of the results and an orderly presentation.

The candidate is requested to initiate and keep close contact with his/her academic supervisor(s) throughout the working period. The candidate must follow the rules and regulations of NTNU as well as passive directions given by the Department of Energy and Process Engineering.

Risk assessment of the candidate's work shall be carried out according to the department's procedures. The risk assessment must be documented and included as part of the final report. Events related to the candidate's work adversely affecting the health, safety or security, must be documented and included as part of the final report. If the documentation on risk assessment represents a large number of pages, the full version is to be submitted electronically to the supervisor and an excerpt is included in the report.

Pursuant to “Regulations concerning the supplementary provisions to the technology study program/Master of Science” at NTNU §20, the Department reserves the permission to utilize all the results and data for teaching and research purposes as well as in future publications.

The final report is to be submitted digitally in DAIM. An executive summary of the thesis including title, student's name, supervisor's name, year, department name, and NTNU's logo and name, shall be submitted to the department as a separate pdf file. Based on an agreement with the supervisor, the final report and other material and documents may be given to the supervisor in digital format.

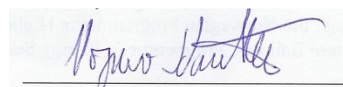
- Work to be done in lab (Water power lab, Fluids engineering lab, Thermal engineering lab)
 Field work

Department of Energy and Process Engineering, 20. February 2014



Olav Bolland
Department Head

Research Advisor: Lauren Georges, NTNU



Vojislav Novakovic
Academic Supervisor

Acknowledgement

This assignment is realised as a part of the collaborative project “Sustainable Energy and Environment in Western Balkans” that aims to develop and establish five new internationally recognized MSc study programs for the field of “Sustainable Energy and Environment”, one at each of the five collaborating universities in three different WB countries. The project is funded through the Norwegian Programme in Higher Education, Research and Development in the Western Balkans, Programme 3: Energy Sector (HERD Energy) for the period 2011-2014.

First off all I would like specially to thank and express my sincere gratitude to my supervisor, Professor Vojislav Novakovic for providing me the opportunity to work, research and broaden my perspectives on such reputable University - NTNU.

Secondly I want to thank to my co-supervisor Laurent Georges for his advices and guidance, helping me in setting the foundation of this thesis.

Also I want to thank to Associate professor Natasa Nord who helped me in the part of building simulation.

I am thankful to my professors from Macedonia: Slave Armenski, Done Tashevski and Mile Dimitrovski for their advices, who contributed in writing this thesis.

Last but not the least I want to give special thanks to my family for their support and encouragement during my stay in Trondheim.

Igor Shesho

Abstract

It is well known that building sector in most of the countries consumes more than 40 % from the primary energy. Also the increased requirements for thermal comfort especially for cooling involve a considerable consumption of energy. Increased consumption of energy causes rising environmental issues like increasing the greenhouse gasses emissions/pollution, global warming etc. Thus the European Union established directive as a common framework of measures for the promotion of energy efficiency. Due to the implementation of the recommended energy efficiency measures new buildings have low heating and cooling energy consumption and also the Article 9 from the EU directive requires that “Member States shall ensure that by 31 December 2020 all new buildings are nearly zero-energy buildings; and after 31 December 2018, new buildings occupied and owned by public authorities are nearly zero-energy buildings”. This opens the possibility of efficient harnessing the renewable energies since they are usually utilized at low temperature levels.

The Macedonian renewable energy market regarding the residential heating and cooling systems mostly is covered by wood pellets, less with heat pumps and the solar energy is mainly present in solar thermal systems for heating domestic hot water. Therefore the main idea of this thesis is to analyze the thermal performance of solar assisted air-conditioning systems and their feasibility for conditions in Macedonia.

Thermal performance of the solar thermal systems are estimated using numerical methods and software since the solar processes are transient in nature been driven by time dependent forcing functions and loads. The system components are defined with mathematical relationships that describe how components function. They are based on first principles (energy balances, mass balances, rate equations and equilibrium relationships) at one extreme or empirical curve fits to operating data from specific machines such as absorption chillers. The component models are programmed i.e. they represent written subroutines which are simultaneously solved with the executive program. In this thesis for executive program is chosen TRNSYS containing library with solar thermal system component models.

Validation of the TRNSYS components models is performed i.e. the simulation results are compared with experimental measurements.

With the simulations are determined the long-term system performance i.e. data are obtained for the energy consumption, solar fraction, collector efficiency also it is performed parametric analysis to determine the influence of specific parameters like collector area, tilt and orientation, mass flow rate etc. to the system performance. In this thesis are considered only the residential buildings.

Reference solar assisted air-conditioning system is defined for the analysis purposes, which is numerically modeled in TRNSYS defined with the component models and their interconnections. The solar system main components are: solar collectors, storage tank, auxiliary heater, absorption machine reference building as load generator and the hydraulic components.

Analysis starts with assessment the solar thermal system performances when is used only for providing heat energy for the heating system. In this case as parametric variables are considered: heating system type (radiator and underfloor), specific building heat energy consumption defined with three building types differencing only in thermal insulation , collector type, collector area and storage tank volume. Solar fractions are in the range from 8% for radiator heating system, building type I i.e. specific heat consumption of 70 kWh/m² a, 16 m² collector area, storage tank 1000 l-radiator heating up to 52% solar fraction for underfloor heating system, building type III i.e. specific heat consumption of 57 kWh/m² a for 64 m² collector area, storage tank 2000 l.

Another analysis is performed for solar assisted cooling system in order to determine the solar fractions and efficiencies for different collector areas, storage tanks. The obtained results reveals the solar fraction regarding the ratio between specific collector area : 0,1 m² / m²_{conditioned} can cover almost 30% , 0,2 m² / m²_{conditioned} covers 50% and 0,4 m² / m²_{conditioned} can cover 70% of the total required heating energy for driving the absorption chiller. Also is the influence of installing cold storage tank between the absorption chiller and building cooling system.

At the end is made life cycle cost analysis for the solar assisted air-conditioning systems with electrical heater or heat pump as auxiliary sources. Solar collector systems applied only for heating and DHW with heat pump as auxiliary heat source and building with specific heat consumption of have payback period starting from 7,5 years while the solar assisted cooling system have negative NPV values which indicates that economically is not profitable measure. Solar assisted cooling is not feasible since the electricity price in Macedonia is cheap and also the absorption chiller price is relatively high. But it can provide more than 50 % savings in primary energy if as conventional is considered the electrical energy.

Nomenclature and abbreviations

Symbols:

If no other units are mentioned in the text, the following units are used

Q_u	[kJ/h]	- Useful gain from the collector
A_c	[m ²]	- Collector aperture area
S	[kJ/h m ²]	- Solar radiation absorbed per collector unit area
U_L	[kJ/h m ² K]	- Overall collector heat loss coefficient
T_i	[K]	- Fluid inlet temperature
F_R	[-]	- Collector heat removal factor
τ	[-]	- Collector absorber transmittance
α	[-]	- Collector absorber absorbance
I_T	[kJ/h m ²]	- Total radiation incident on the solar collector
I_{bT}	[kJ/h m ²]	- Beam radiation incident on the solar collector
I_{dsT}	[kJ/h m ²]	- Sky diffuse radiation on the solar collector
I_{dgT}	[kJ/h m ²]	- Ground-reflected diffuse radiation on the solar collector
IAM	[-]	- incidence angle modifier
θ_{sky}	[-]	- Effective incidence angles for sky diffuse
θ_{ground}	[-]	- Effective incidence angles for and ground reflected
η_0	[-]	- Optical efficiency (conversion factor)
a_1	[W/m ² K]	- Heat transfer coefficient
a_2	[W/m ² K]	- Temperature depending heat transfer coefficient
I_T	[W/m ²]	- Solar radiation at which the measurement is performed
G_b, G_d	[W/m ²]	- Beam and diffuse solar irradiance
c_1	[W/m ² K]	- Heat transfer coefficient
c_2	[W/m ² K]	- Temperature depending heat transfer coefficient
c_5	[W/m ² K]	- Temperature depending heat transfer coefficient
T_m	[K]	- Mean fluid temperature inlet/outlet solar collector
T_a	[°C]	- Ambient temperature where the collector is installed
ΔT_{db}	[°C]	- Temperature difference dead band controller
γ_{hr1}	[-]	- Control signal (0-1) for auxiliary heater
U	[kJ/kg K]	- Overall heat transfer coefficient
C_p	[kJ/kg K]	- Specific heat capacity
COP	[-]	- Coefficient Of Performance
$Q_{surf,I}$	[kJ/h]	- Convective heat gain from inner surface of zone
$Q_{inf,I}$	[kJ/h]	- Infiltration gains
$Q_{vent,I}$	[kJ/h]	- Ventilation gains
$Q_{g,c,I}$	[kJ/h]	- Internal convective
$Q_{cplg,I}$	[kJ/h]	- Gains due to connective air flow
$Q_{r,wi}$	[kJ/h]	- Radiative gains for the wall surface temperature node
$Q_{g,r,i,wi}$	[kJ/h]	- Radiative airnode internal gains received by wall
$Q_{sol,wi}$	[kJ/h]	- Solar gains through zone windows received by walls,
$Q_{long,I}$	[kJ/h]	- Long-wave radiation exchange
$Q_{wall-gain}$	[kJ/h]	- Predfiend heat flow to the wall or window surface.
$\Delta\Delta t$	[K]	- Characteristic temperature function

Q_{SH}	[kJ/h]	- Extracted heat energy from the storage tank
\dot{m}	[kg/h]	- mass flow rate

Abbreviations

ETC	- Evacuated tube collector
FPC	- Flat plate collector
BHE	- Borehole heat exchanger
GCHP	- Ground coupled heat pump
PV	- Photovoltaic
DEC	- Desiccant cooling system
FPC	- Flat plate collector
CPC	- Compound parabolic collectors
SAC	- Solar air-conditioning
HVAC	- Heating Ventilation Air-conditioning
DHW	- Domestic Hot Water
CSHPSS	- Central Solar Heating Plants with Seasonal Storage
ROI	- Return of investment
SC	- Solar cooling
PER	- Primary Energy Ratio

Sub scripts

<i>in</i>	- inlet
<i>out</i>	- outlet
<i>avg</i>	- average
<i>amb</i>	- ambient
<i>b</i>	- beam radiation
<i>ds</i>	- sky diffuse radiation
<i>dg</i>	- ground reflected radiation
<i>D</i>	- Desorber
<i>A</i>	- Absorber
<i>C</i>	- Condenser
<i>E</i>	- Evaporator
<i>th</i>	- Thermal
<i>el</i>	- Electrical
<i>sol</i>	-Solar

Contents

Acknowledgement	i
Abstract.....	ii
Nomenclature.....	iv
and abbreviations	iv
List of figures.....	ix
List of tables	xii
Chapter 1.....	1
1. Introduction	1
1.1 Background.....	2
1.2 Objectives	3
1.3 Literature review.....	3
1.4 Structure of the report.....	6
Chapter 2.....	8
2. Technologies for active solar thermal systems	8
2.1 Solar assisted space heating and DHW system	9
2.2 Solar cooling systems	17
2.3 Solar cooling technologies.....	22
Chapter 3.....	31
3. Numerical modeling of solar thermal system.....	31
3.1 Energy simulation software	31
3.2 Numerical components models.....	34
3.3 Modeling solar thermal assisted air-conditioning system	52
Chapter 4.....	57
4. System and Components validation.....	57
4.1 Solar circuit component validation	57
4.2 Absorption chiller validation	62
Chapter 5.....	66

5. Performance evaluation of solar air-conditioning system	66
5.1 Performance indicators	68
Chapter 6.....	72
6. Simulation results and analysis.....	72
6.1 Reference building modeling and simulation	72
6.3 Analysis of the solar thermal system in cooling mode for the building	82
6.4 Techno-economic analysis.....	89
Chapter 7.....	101
7. Summary and recommendations for further work.....	101
APPENDICIES	106
Appendix A.....	107
Technical data solar thermal storage	107
Appendix B.....	109
Technical data flat plate solar collector	109
Appendix C.....	111
Technical data vacuum tube collector	111
Appendix D.....	113
Parameters value for the absorption chillers.....	113
Appendix E.....	114
Cooling tower performance data	114
Appendix F	115
Appendix G – Draft proposal scientific paper	116

List of figures

Figure 1. Solar thermal Market in EU27 and Switzerland [14].....	5
Figure 2. Total and newly installed capacity in EU27 and Switzerland [14].....	6
Figure 3. Direct collector loop: (a) pump control; (b) three-way valve control.....	11
Figure 4. Indirect collector loop: a) Internal heat exchanger b) plate heat exchanger	12
Figure 5. Typical solar-thermal system for space heating and DHW (adapted from Beckman et al.1977).....	13
Figure 6. Solar air heating system (adapted from Beckman et al.1977).....	14
Figure 7. Scheme of drainback space heating and water heating system (gravity return) [15].....	14
Figure 8. Schematic diagram of a domestic water-to-air heat pump system.....	15
Figure 9. Schematic diagram of a domestic water-to-water heat pump system.....	16
Figure 10. Schematic diagram of combination solar energy and ground source heat pump.....	17
Figure 11. Scheme of a solar cooling plant: 1 = solar collector field; 2 = hot storage; 3 = auxiliary boiler; 4 = absorption chiller; 5 = cold storage; 6 =compression chiller; 7 = cooling towers.....	18
Figure 12. Simplified scheme of solar cooling plant.....	18
Figure 13. Overview on physical ways to convert solar radiation into cooling/air-conditioning [16]...	19
Figure 14. COP-curves of sorption chillers and the upper thermodynamic limit (ideal) [16].....	20
Figure 15. Solar electric vapor-compression cooling cycle.....	21
Figure 16. a) Vapor compression chiller b) Absorption(thermally driven) chiller.....	24
Figure 17. Schematic diagram of an single stage absorption chiller (LiBr-H ₂ O)	25
Figure 18. Simple schematic drawing of an (solar driven) absorption chiller.....	29
Figure 19. Transversal and longitudinal directions	40
Figure 20. Stratified Fluid Storage Tank	41
Figure 21. Graphical representation of energy flows into a node	43
Figure 22. Energy balance for he auxiliary heater model.....	44
Figure 23. Radiative energy flows considering one wall	50

Figure 24. Two-node window model used in th TYPE56 energy balance equation	51
Figure 25. Subsystems definition of solar cooling system	53
Figure 26. Functional scheme presenting inter conections between components of the system moddeled in TRNSYS	53
Figure 27. Scheme of the experimental installation	57
Figure 28. TRNSYS model for the experimental installation of solar thermal collector system.....	59
Figure 29. Measured and simulated temperatures for the collector inlet as marked on	61
Figure 30. Measured and simulated temperatures at the collector outlet	61
Figure 31. Measured and simulated temperatures inside storage tank	61
Figure 32. Hourly measured and simulated solar radiation for the specific day	62
Figure 33. Measured ratios of external to internal heat transfer coefficients	65
Figure 34. Measured cooling capacity for design and variable flow rates, by Kühn et al. 2005&2007.....	65
Figure 35. Solar cooling system variables [44]	67
Figure 36. Monthly energy consumption for the three building “types”.....	74
Figure 37. Hourly dry bulb ambient temperatures for Skopje, R.Macedonia	74
Figure 38. Cross section of the active layer for the underfloor heating	76
Figure 39. Solar fraction for Building I, radiator and underfloor heating in regard of collector array area and strorage volume	80
Figure 40. Solar fraction for heating with storage tank 1500l regard of collector array area building type	81
Figure 41. Monthly average zone temperature, only heating analysed	81
Figure 42. Scheme of the collector array conection 16/2	85
Figure 43. Monthly values of solar fraction for different tilt angles and tracking azimuth for solar assited cooling system	86
Figure 44. Solar fraction and fan cooling tower energy consumption for system with and without storage tank for solar assited cooling system	87
Figure 45. Monthly average storage tank temperture and solar collector yield in regard of system with/without cold storage tank for solar assited cooling system	87
Figure 46. Solar fraction and thermal efficiency in regard of collector area for solar assited cooling system	88
Figure 47. Hourly heating loads and useful heat yield for different collector array areas and constat storage tank of 1000 l and one case for 64 m ² with 2000 l.....	91
Figure 48. Hourly heating loads and collector energy yield for different areas ten day period	91

Figure 49. Payback time for solar thermal systems for two building types regarding the specific heat energy consumption	98
Figure 50. Primary energy consumption for solar thermal systems in regard of two buildings with different specific heat energy consumption 57 kWh/m ² a and 70 kWh/m ² a.....	99
Figure 51. Specific absorption chiller costs per kW cooling power [48]	99

List of tables

Table 1. Technical data for collector type Camel Solar Flat plate 2.0-4	55
Table 2. Technical data for collector type Camel Solar Vacuum tube SC 15	58
Table 3. Storage tank technical details	59
Table 4. Technical data for different market available small absorption chillers	63
Table 5. Averaged measured performance data by Kühn (2005) of a 10kW absorption chiller	64
Table 6. Energy and thermal flows of solar cooling systems	67
Table 7. Legend of the performance indicators	69
Table 8. Calculation procedures for solar thermal system performance indicators.....	71
Table 9. Reference building physical and thermal performance data	73
Table 10. Active layer TYPE data	75
Table 11. Parametric analysis of solar assisted heating system with radiators	78
Table 12. Parametric analysis of solar assisted underfloor heating system	79
Table 13. Cooling tower design parameters	83
Table 14. Monthly average solar fractions and efficiency in regard of collector area and storage volume	84
Table 15. Monthly average solar fractions and thermal efficiency in regard of collector array interconnections.....	84
Table 16. Solar fractions and thermal efficiency for solar assisted cooling system in regard of collector orientation i.e. azimuth	85
Table 17. Average solar fraction and thermal efficiency of solar cooling system in regard of collector area and storage tank volume for solar assisted cooling system	88
Table 18. Solar fraction and thermal efficiency for different specific vacuum collector areas storage volumes for solar assisted cooling system	88
Table 19. Annual energy balance, energy and system costs, CO ₂ emissions for conventional heat source systems obtained with simulations, specific heat energy consumption 70 kWh/m ² a	92
Table 20. Solar thermal system energy performance, costs, parameters and CO ₂ emissions, primary energy consumption for building with specific heat energy consumption 70 kWh/m ² a, – part I	93

Table 21. Solar thermal system energy performance, costs, parameters and CO ₂ emissions, primary energy consumption for building with specific heat energy consumption 70 kWh/m ² a, – part II.....	93
Table 22. Solar thermal system energy performance, costs, parameters and CO ₂ emissions, primary energy consumption for building with specific heat energy consumption 57 kWh/m ² a, – part I	94
Table 23. Solar thermal system energy performance, costs, parameters and CO ₂ emissions, primary energy consumption for building with specific heat energy consumption 57 kWh/m ² a, – part II.....	94
Table 24. LCCA for solar thermal system assisted building heating with specific heat energy consumption 70 kWh/m ² a.....	97
Table 25. LCCA for solar thermal system assisted building heating with specific heat energy consumption 57 kWh/m ² a.....	98
Table 26. Solar thermal system energy performance, costs, parameters and CO ₂ emissions, primary energy consumption for building with specific cooling energy consumption 12 kWh/m ² a.....	100

Chapter 1

1. Introduction

In the past twenty years the uncontrolled or mildly said “demanded” industry development accompanied by the increased thermal comfort demand and the limited energy resources naturally activated and imposed the need of the forgotten term of energy efficiency. In the past, the cheap/affordable energy sources, high building energy consumption and the modest technology development were the main limiting factors in the viability of utilization renewable energy sources.

Undertaken measures started with limiting the energy consumption through different directives and regulations which translated into actions meant: improving efficiencies of existing systems, decreasing the energy demand, up to developing new technologies, and all of that with one purpose - doing more with less. Now with the implementation of the buildings directives such as the Energy Performance Building Directive 2002/91/EC the EU 2020 strategy, technology development enabled the renewable energy sources to be feasible for implementation in buildings air-conditioning systems.

From the climatic point of view, the World Meteorological Organization - WMO (2012) has determined that the “long term warming trend” continues, being the period of 2001 – 2011 the world’s warmest decade since 1850. This trend has a significant impact in the energy sector, both in the generation and the demand sides. Regard to the demand side, various studies has been conducted, in particular with the change in thermal energy loads in buildings; a number of them have been summarized by Yau and Pean (2011). Although the studies presented in the mentioned review follow different methodologies, it is noticeable an increase tendency in energy demand due to the effects of climate change. Considering the above, the integration of renewable energy sources is a valuable strategy to reduce and/or offset the increase in cooling load; especially with the use of active solar systems, because cooling loads are in phase with the amount of solar irradiation.

A significant contribution to the primary energy consumption of first and second world countries is being made by the rapidly increasing use of electrical air-conditioning units worldwide.

Chapter 1. Introduction

Worldwide sales of room air-conditioners of all types amount to approximately 50 Mio. units p.a., with the U.S. China and Japan being the three main markets. In Europe, commercial air conditioning has a share of 4% of the total annual electricity consumption while residential air conditioning accounts only for 0.4%. Although the latter number is still comparatively low, Europe has seen a seven-fold increase of residential air-conditioning sales between 1990 and 2004. The reasons for the growing use of air-conditioning are twofold. First, the comfort demands from both building users and owners have increased. The standard of living of the present generation is higher than in the past, especially in private buildings. . Second, the trend towards commercial buildings with large glazed facades has increased the internal heat load to be removed by air-conditioning. Third, electricity prices are comparatively low. The additional cost caused by the use of air-conditioning units is not in the order of magnitude to influence the consumer behavior significantly.

The obvious consequence of this growing air-conditioning use is increased power consumption. Outside Europe, another consequence of excessive air-conditioning are locally higher temperatures in metropolitan areas, commonly referred to as heat islands. As a part, these inner-city temperature peaks are the result of heat conveyed from building inside to outside, released at a temperature level above ambient temperature. Both these consequences are strong arguments for alternative air-conditioning or cooling methods.

Priority is given to buildings and transport sector. Through directives to improve building energy efficiency (energy performance of buildings directive or EPBD), the European Union recognized high potential for energy savings from buildings and promote the installation of solar thermal systems in the building sector. Solar technologies can supply the energy for all of the building's needs—heating, cooling, hot water, light and electricity—without the harmful effects of greenhouse gas emissions created by fossil fuels thus solar applications can be used almost anywhere in the world and are appropriate for all building types. The heat energy demand for heating the building and/or DHW determines the solar collectors area which often can exceed the available optimal area for installation of the collectors. Thus collectors are connected in arrays which opens a variety of combinations regarding the number of collectors hydraulics and layout.

1.1 Background

It is well known that according the IEA(International Energy Agency) buildings represents 32% of the total final energy consumption and converted in terms of primary energy this will be around 40%. Inspected deeper, the heating energy consumption represents over 60% of the total energy demand in the building. Space heating and hot water heating account for over 75% of the energy used in single and multi-family homes.

Chapter 1. Introduction

Solar technologies can supply the energy for all of the building's needs—heating, cooling, hot water, light and electricity—without the harmful effects of greenhouse gas emissions created by fossil fuels. Usually the maximum demand for cooling coincides with the maximum availability of solar radiation, whereas conventional electrical-compressor chillers have the problem of providing their minimum capacity in the hottest hours.

As mentioned before in 2010 the European commission adopted communication “Energy 2020” that defines new strategy toward 2020 for a competitive, sustainable and secure energy [1].

Without a doubt, the European goal of covering 20% of energy needs with renewable energy can only be reached with a significant increase of renewable energy capacities in the heating sector. The explosion of crude oil and natural gas prices along with increasing import dependency have further increased public attention and interest.

1.2 Objectives

In this work/thesis the main accent is given on solar energy. The main objective is assessment of thermal performance of the solar driven air-conditioning systems through analysis of different innovative combination of solar heating, cooling and storage techniques in regard of primary energy savings and economic feasibility compared to pre-defined reference system for the weather conditions in R.Macedonia. Objective will be achieved through transient dynamic simulations and a holistic approach for various configurations between solar heating and cooling technologies, energy storage and auxiliary conventional heating and cooling devices. Representative building with different specific heat and cooling energy will be defined in order to analyze the performance of the solar assisted air-conditioning systems.

1.3 Literature review

Solar thermal systems for hot water production are already mandatory in new buildings according to solar ordinances in Spain [2], Portugal, Italy, Greece and other European countries [3].

Systems combining production of domestic hot water (DHW) and space heating systems are well suited to middle and high latitudes, due to significantly higher solar radiation in the transitional period around winter (September-October and March-May) and the significant heating demand in these latitudes at that time [4].

Installations with large solar collector areas and small size heat storage capacity can cover around 50% of the total heat demand. This percentage can be higher in some cases of large storage capacities and primary energy savings up to 80% [5]. Simulations of central solar heating plants with seasonal storage (CSHPSS) have shown that the solar fraction of such systems varies between

Chapter 1. Introduction

50% and 100% [6, 7]. The heat produced by the collectors may be stored in thermal energy storages in order to provide domestic hot water and space heating when required [8].

Solar air conditioning refers to any air conditioning system that uses solar power. This can be done through solar thermal energy conversion, passive solar and photovoltaic conversion.

The addition of a solar cooling facility makes the system complete, covering all building thermal and cooling demands. These systems which are combination of solar heating and cooling seem to be proved advantageous since high cooling load coincident with high solar radiation and consequently the readily available solar energy from the existing solar collector can be exploited by a heat driven machine. The use of the solar collector is then extended to a whole year, making the system financially attractive, when the number of annual full-load hours is high [9]. Furthermore since the cooling machine is heat driven, the building electrical load share reduce the problems associated with peak power demand during summer are minimized. Depending on the size of solar collector field, hot water storage, local climatic conditions and building loads, these solar driven systems can cover 10-60% of the combined space heating/cooling and DHW demand at southern, northern and central European countries [10].

Urban areas are of particular interest where adverse outdoor conditions, as a result of higher outdoor pollution and the urban heat island effect, encourage the use of mechanical air-conditioning with a direct impact on peak electrical energy use [11]. Application of the solar energy for air-conditioning in the commercial sector can be said that is relatively new. In the study of Lamp and Ziegler [12] they give an overview of the European research on solar-assisted air conditioning up to 1996. It is investigated that the application of renewable technologies in the European tourism industry and identified a large number of solar thermal systems but only a few solar cooling systems [13].

Regarding the large scale application as main obstacles, beside the high first cost, also there is the lack of practical experience and acquaintance among engineers with the design, control and operation of these systems. For smaller scale systems, there is no market available technology. Therefore, the development of low power cooling and air conditioning systems is of particular interest. Heat-driven cooling technologies include mainly closed cycles (absorption, adsorption) and open cycles (desiccant systems which will be detail described in the next chapter.

Despite their ecological advantages, solar cooling systems also have to yield an economic advantage for the customer. At present, investment costs are higher for solar cooling systems than for comparable compressor based cooling units. Thus, the full potential of solar cooling is far from being realized, however building owners, occupants and architects are becoming more and more sensitive towards energy issues. The economic advantage of solar cooling systems results from

much lower operation costs which include the costs for power, water and maintenance. Especially the electrical power consumption of a solar cooling system influences the economics strongly. The main idea of such a system is to use thermal energy for most of the process work, thus the remaining power consumption should be kept as low as possible.

1.3.1 Solar thermal market in Europe

In this part are presented the results from the report of the European Solar Thermal Industry federation for the current situation of the solar thermal market in Europe i.e. it is given overview for ten year trend from 2002 – 2012.

The European Union market continues to suffer from the constraints imposed by the financial and economic crises affecting most of the continent, resulting in a sluggish construction sector and reduction of public support schemes for solar thermal. The annual market has been contracting since the peak year of 2008. The 2.41 GW_{th} sold in 2012 are well above the 2007 sales (2 GW_{th} / 2.88 mio m²) but are a far cry from the 3.36 GW_{th} (4.8 mio m²) reached in 2008. Over the past ten years, there was a continuous steep uptrend in the growth rate up to 2008; followed by a decline, steeper in the first two years (2009, 2010) and then flattening out (2011, 2012). The variation in the newly installed capacity is illustrated with the blue line in the graph on the right. In spite of the decrease recorded over the last four years, the annual market size has doubled, over the past decade at an average annual growth rate of 10%. Using the same comparison over the last five years (2007-2012), we can observe an absolute growth in the annual sales of 20% and an average annual growth rate of 3.6%

Figure 1. Residential applications still represent the bulk of the solar thermal market. Nevertheless, large installations are increasing apace. Large size systems above 35 kW_{th} (50 m²) for commercial heating and cooling applications have shown a positive development, but it is mainly for very large systems (above 350 kW_{th} / 500 m²) that the market has been moving rapidly.

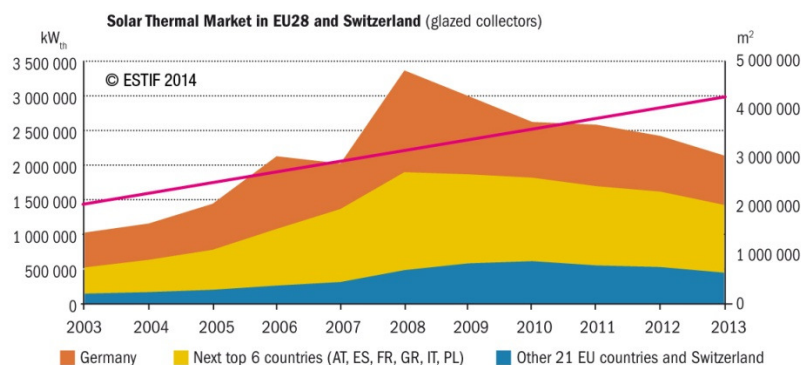


Figure 1. Solar thermal Market in EU27 and Switzerland [14]

Chapter 1. Introduction

In 2012 confirmed Denmark as the land of large solar district heating, with a total of 71.4 MWth (102 000 m²) installed, contributing to a total installed capacity of 196 MWth (280 000 m²), solely in large solar thermal plants, that account for 65% of the European total installed capacity in large systems, Figure 2 with regard to industrial process heat, several pilot projects have been implemented, with other large ones in the pipeline. This is clearly a market segment to watch closely in the coming years.

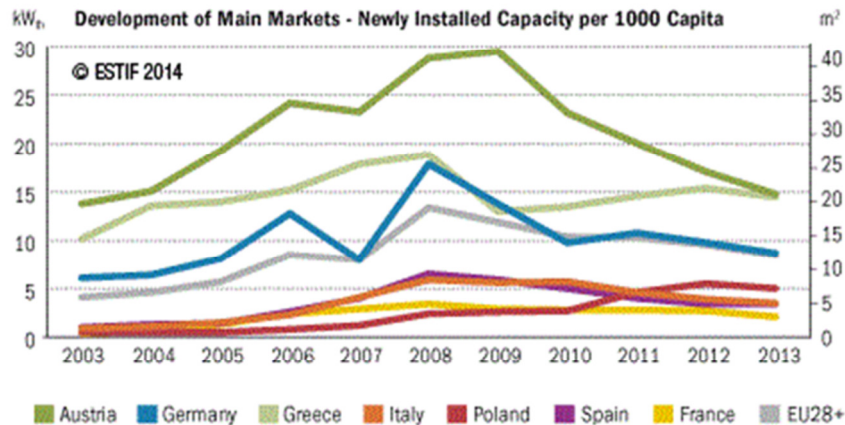


Figure 2. Total and newly installed capacity in EU27 and Switzerland [14]

Despite a below expectation growth of the total installed capacity (the evolution is shown by the grey bars in the graph referred to above, the lighter shade of grey indicates the increment from the newly installed capacity in 2012), solar thermal plays an increasingly important role in the European energy strategy, namely through the National Renewable Energy Action Plans. The 28 GW_{th} in operation generate an estimated 20 TWh_{th} of solar thermal energy while contributing to a saving of 2.5 Mt CO₂ [14].

1.4 Structure of the report

The rest of the report is structured as follows. Chapter 2 gives overview for the existing technologies for active solar systems. First is given general description of the solar assisted space heating and DHW systems. Further are elaborated several physical configurations of active solar heating systems and combinations with heat pumps. Second part from this chapter continues with solar cooling technologies and components with special accent on the absorption, adsorption chillers and desiccant cooling technologies, thermodynamic limitations and performances.

Chapter 3 concerns to the separate component models used in the simulation of the solar assisted air-conditioning system like solar collector, storage tank, auxiliary heater, absorption chiller, hydraulics etc. Simply said it is given overview of the mathematical relations which

Chapter 1. Introduction

describe how component models function. The elaborated component models are contained within TRNSYS and Tess library.

Chapter 4 is dedicated to procedure of validation for the previously mentioned component models in Chapter 3. Experimental set up of the system or component are modeled in TRNSYS and simulation results are compared with the measured ones.

Chapter 5 deals with performance evaluation of solar air-conditioning system. There are given performance indicators and procedures for calculation of system thermal performance.

In Chapter 6 is described the numerical development of the simulated system i.e. component models characteristics with their interconnections, input data and simulation boundaries. Further continues with developing different scenarios subject for simulations and analysis. Each of the simulation results are subject of analysis in regard of which are drawn conclusions and recommendations.

In the last Chapter 7 are condensed all of the results, analysis, conclusions covered within previous chapters. At the end are given recommendation for further work. At the end are given the Appendices.

Chapter 2

2. Technologies for active solar thermal systems

The term “active solar systems” is commonly applied to assemblies of equipment that provide heating, cooling or hot water in dwellings and commercial buildings.

The distinction between active and passive systems is sometimes made according to other criteria, as follows. Auxiliary energy is generally required to make the transfer fluid circulate in active systems (forced circulation), whereas natural circulation (of air) takes place in passive buildings. System operation is managed by a specific control device in active solutions, whereas passive systems are more or less self-regulating.

Usually excluded is equipment that supplies electricity or products of biological processes. Also excluded are materials and designs that by permitting the passive supply of solar energy to a building, usually through windows or other transparent and translucent surfaces, can reduce the demand for conventional energy.

Active solar space systems use collectors to heat a fluid, storage units to store solar energy until needed and distribution equipment to provide the solar energy to the heated spaces in a controlled manner. Additionally complete system includes pumps or fans for transferring the energy to storage or to the load; these require a continuous availability of non-renewable energy, generally in the form of electricity.

The load can be space cooling, heating or combination of these two with hot water supply. When is combined with conventional heating equipment solar heating provides the same level of comfort, temperature stability and reliability like conventional system.

It will be separately described the technology of solar space heating and cooling processes. In further analysis will be used combination of solar space heating and cooling system with DHW system.

2.1 Solar assisted space heating and DHW system

A solar system for space and water heating can be designed to suit any particular application, residential or commercial, new or retrofit. It is technically feasible to design a solar system that can provide 100% of heating needs of a building but generally it is uneconomical to do so. Practical solar heating systems are designed to displace up to 50% of conventional fuel needs and require auxiliary heating systems that are fully capable of supplying the total heating load when no solar energy is being collected and when stored solar energy has been depleted.

When space heating systems serve occupied buildings it is economical to include heating of domestic hot water (DHW) in the system. For residential systems during the summer when there is no space heating load, the entire solar system can be devoted to water heating so that solar can supply a substantial portion if not all of the DHW heating needs. However for large commercial systems summer operation to provide a relatively small DHW demand may not be worthwhile.

The solar loop also known as the collector loop, comprises the components which collect solar energy (electromagnetic radiation from the sun), convert it to heat and transfer the heat to the storage. The basic component of the solar loop is a set of solar collectors through which a heat-transfer fluid circulates. This fluid is generally water or an anti-freeze solution, such as mono-ethylene glycol + water, but other fluids (e.g. air or an organic thermal fluid) can also be used. Several types of collectors exist on the market. The most common for low-temperature applications are flat-plate solar collectors , however other types can also be used, such as evacuated tubular collectors (ETC).

The solar loop is completed by a piping circuit, a circulation pump, and several safety and maintenance devices (e.g., an expansion tank, a filter, an air bleed, a safety valve, and a non-return valve). The heat from the solar loop is usually transferred to a heat storage device, either directly or through a heat-exchanger when different fluids are used in the collectors and in the storage. The solar loop is controlled by a differential thermostat which switches the pump on and off to ensure that fluid circulates only if a net gain of energy is possible.

Storage is required because energy demand and solar availability rarely coincide. Storage is generally as sensible heat (sometimes latent heat) and the most common form is an insulated water tank. A thermal stratification is observed in storage tanks: hot water, lighter than cold water, rises to the top of the tank. In well-designed systems, this physical phenomenon is enhanced to improve the performance. The connection with the load in the distribution loop varies according to the application.

Chapter 2. Technologies for active thermal solar systems

The size of a solar system (primarily the collector area and storage volume) for a particular building depends on the portion of the total load the system is expected to provide. Size also depends on climate and location. The type of the system whether air or liquid based depends in part on the application and to a large extent on the designers choice. Very often large systems may be subdivided into several small systems to better suit the application. Smaller systems may be easier to control, provide better overall efficiency and cost collectively less than a system with one large collector array and storage.

Solar heating systems are as adaptable technically for commercial applications as for residential applications, except that for very large buildings, available area for collector placement may constrain system size. For most residential applications, selecting an air- or liquid based system is largely a matter of designer or owner preferences. Air-based solar system can be as effective as liquid-based systems, and costs for equally sized systems are essentially the same. Heat transport in large air ducts is more expensive than a liquid through pipes.

Regarding new building or retrofit, there is considerable freedom in selecting a solar system type for a new building and in designing that system to provide an arbitrary (but economical) fraction of the total load. Orientation of the building, slope of the roof for mounting collectors, location and space thermal energy storage and type of heat distribution system can be selected according to system choice. Options are fewer for retrofit application. Building orientation is fixed, roof slope may not be suitable for collector mounting, choice of storage location and size may be limited and some interior changes may be necessary to accommodate the heat transport subsystem. The existing heating and distribution system may also restrict the selection of solar system type and design.

The size of the solar system is logically based on economics. Among the economic figures of merit are total capital investment (first cost), least cost for energy, life cycle cost, life cycle cost savings, payback, and return of investment (ROI). While positive life-cycle cost savings and short-term payback are criteria most readily understood by homeowners a high ROI is usually the criterion for commercial systems.

While other, noneconomic factors can affect choice of system size for residential applications, using solar systems that can provide from 30% to perhaps 50% of the total annual heating requirements is a practical choice. Sizes of commercial systems, while also dictated by economic constraints also depend on availability of suitable locations for collectors.

Solar radiation availability and heating demand are inversely related; in sunny winter climates, the need for space heating is low while in areas with prevailing clouds in winter, temperatures are generally low and heating demand is high. It is commonly assumed that solar heating systems are

therefore suitable for climates between these two extremes. While solar radiation is least during the coldest periods of winter the fall and spring periods may provide substantial opportunity for displacement of conventional heating fuels.

2.1.1 Physical configurations of active solar heating systems

Although it is possible to imagine a large variety of active solar systems (even with a simple application such as space or water heating), there are far fewer possibilities for the solar loop itself. A small number of basic designs exist, with only a few variants, and these are independent of the application. A distinction can be made between a solar loop without a heat exchanger (direct loop), and one with a heat-exchanger (indirect loop).

In this simple configuration of direct loop Figure 3(a), solar heat from the collector is transferred directly to the storage (or to the distribution loop when there is no storage in the system). The same fluid circulates throughout, consequently the direct loop is unsuitable when anti-freeze fluid is required in the collector. The direct loop is usually controlled by a differential thermostat (between the collector outlet and the bottom of the storage tank). This thermostat controls the circulation pump and lets it operate only if the temperature difference between the two sensors is greater than some set value.

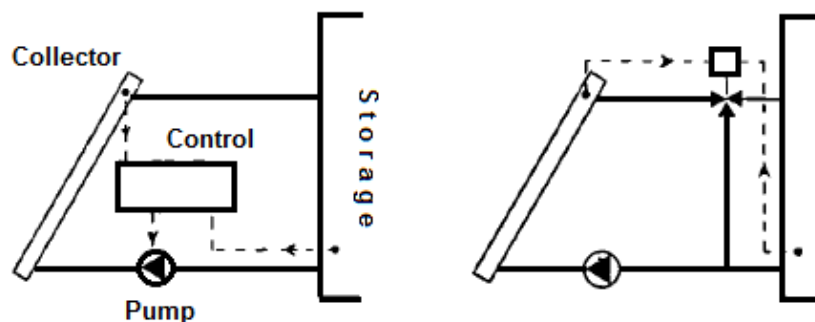


Figure 3. Direct collector loop: (a) pump control; (b) three-way valve control

In a variant of this system Figure 3 (b), the pump operates continuously during daylight hours and the differential thermostat controls a three-way valve. These two types of control are roughly equivalent in terms of thermal performance. Therefore the former type (the simplest) is often preferred. Nevertheless, it is preferable to avoid starting and stopping the pump too frequently.

Frost protection of a collector loop is usually achieved by the use of an anti-freeze solution, but this is rarely used as a storage fluid owing to its cost. A heat-exchanger is therefore required between the collector loop and the storage. The simplest case is that of a heat-exchanger submerged within the storage tank, most often in the lower part. This design is often used for single-family

Chapter 2. Technologies for active thermal solar systems

solar water heaters. The control strategies mentioned above still apply here with similar sensor locations. As a general rule, this configuration does not allow the storage to remain stratified when the collector operates, thus low flow-rates are not suitable.

Another combination is with indirect loop with external heat exchanger i.e. plate type. In this loop, the primary side of a tubular or plate heat-exchanger is inserted in the collector loop, and the secondary side is connected to the storage Figure 4.

A secondary pump is needed and the control is more sophisticated. One simple configuration has the primary pump PI working continuously (during daylight hours), while a differential thermostat between the collector outlet and the bottom of the storage controls the secondary pump P2. Another possible solution for large collector arrays has been proposed. This solution incorporates three temperature sensors, one at the collector outlet (SO), one at the heat exchanger inlet (collector loop, SO1), and one at the bottom of the storage (SI). The control operates the primary pump PI as soon as $TSO > TS1$; after a delay, the pump is then controlled by the sensor SO1 which replaces SO. The primary pump goes on working only if $TSO' > TS1$; in this case, the secondary pump P2 is also switched on. For large plants, many sophisticated control strategies have been proposed in the past, including attempts at optimum control of several storage tanks at different temperatures. In most cases however, the practical operating problems outweighed the improvement in performance.

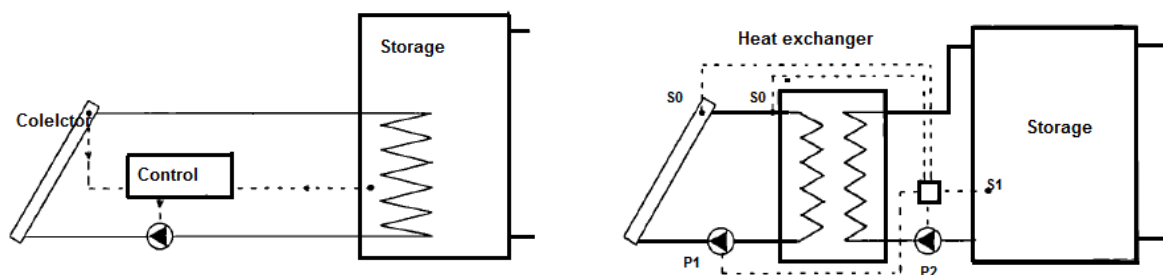


Figure 4. Indirect collector loop: a) Internal heat exchanger b) plate heat exchanger

On the Figure 5 is presented schematic diagram of a typical space heating system. The system consists of three loops-collector, storage and load. In addition as previously mentioned, most space-heating systems are integrated with a domestic water-heating system to improve the yearlong solar load factor.

Since space heating is relatively low-temperature use of solar energy, a thermodynamic match of collector to task indicates that an efficient flat plate collector or low-concentration solar collector is the device of choice.

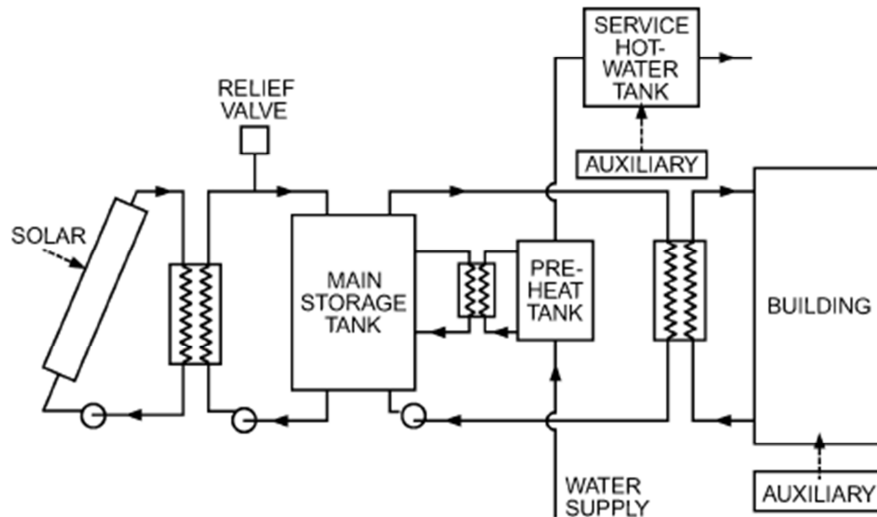


Figure 5. Typical solar-thermal system for space heating and DHW (adapted from Beckman et al.1977)

The collector fluid loop contains fluid manifolds, the collectors the collector pump and heat exchanger, an expansion tank and other subsidiary components. A collector heat exchanger and antifreeze in the collector loop are normally used in all solar space heating systems since the existence of a significant demand implies the existence of some subfreezing weather.

The storage loop contains the storage tank and pump as well as the tube side of the collector heat exchanger. To capitalize on whatever stratification may exist in the storage tank, fluid entering the collector heat exchanger is generally removed from the bottom of the storage. This strategy ensures that the lowest temperature fluid available in the collector loop is introduced at the collector inlet for high efficiency.

On the Figure 6 shows assumed configuration for a solar air heater with pebble-bed storage unit. Energy for domestic hot water is provided by heat exchange from air leaving the collector to a domestic water preheat tank as in the liquid system. The hot water is further heated if necessary by a conventional water heater. During summer operation, a seasonal, manually operated storage bypass damper is used to avoid heat loss from the hot bed into the building.

The standard solar domestic water heater collector heats either air or liquid. Collected energy is transferred by a heat exchanger to a domestic water preheat tank that supplies solar-heated water to a conventional water heater. The water is further heated to the desired temperature by conventional fuel if necessary.

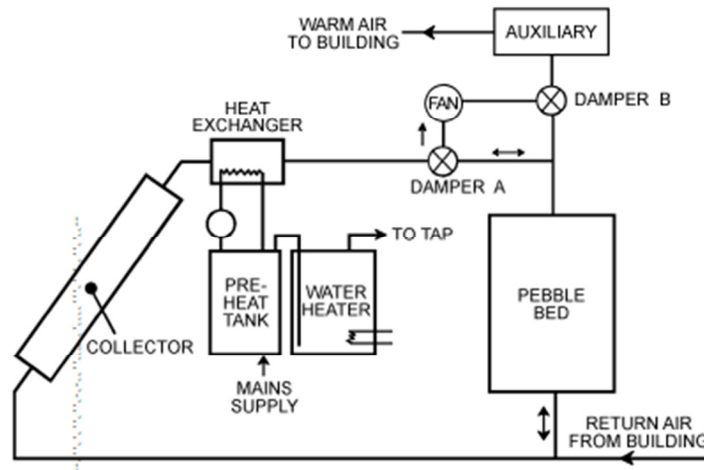


Figure 6. Solar air heating system (adapted from Beckman et al.1977)

Another possible system for combined space heating and DHW is the drainback solar system. In this case, a large atmospheric pressure storage tank is used from which water is pumped to the collector by pump P1 in response to the differential thermostat T_1 . Drainback is used to prevent freezing because the amount of antifreeze required would be prohibitively expensive. Service hot water is obtained by placing a heat exchanger coil in the tank near the top, where even if stratification occurs the hottest water will be found.

Standby heat becomes increasingly important as heating requirements increase. The heating load winter availability of solar radiation and cost and availability of the auxiliary energy must be determined. It is rarely cost-effective to do the entire heating job for either space or service hot water by using the solar heat collection and storage system alone. On the Figure 7 is presented solar drainback system for space heating and DHW. The space heating is provided by heat exchanger water-air placed in the ventilation duct of the building.

The storage tank has two heat-exchangers for indirect fluid heating for the space heating which is serial connected with the auxiliary heater and another for the DHW.

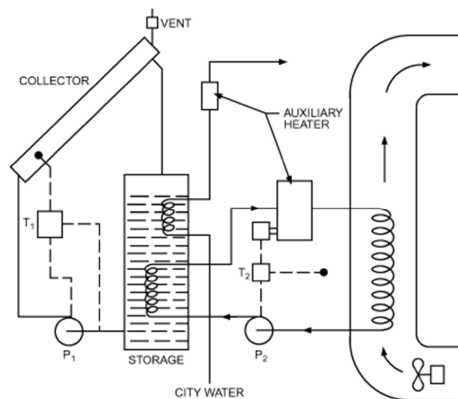


Figure 7. Scheme of drainback space heating and water heating system (gravity return) [15]

A disadvantage of system depicted in Figure 7 is that water must be circulated against full static head losses as well as friction head losses in the supply piping and through the collector.

2.1.2 Solar energy and heat pumps

The solar energy can be used as supplementary thermal energy for the heat source of the heat pumps. It can be used to preheat the air entering the heat pump evaporator or regenerate the ground temperature for the ground source heat pumps.

Heat pumps are usually vapor compression refrigeration machines, where the evaporator can take heat into the system at low temperatures and the condenser can reject heat from the system at high temperatures.

Heat pumps have been used in combination with solar systems in residential and commercial applications. The additional complexity imposed by such a system and extra costs are offset by the high coefficient of performance and the lower operating temperature of the collector subsystem. A schematic of common residential heat pump system is shown in Figure 8.

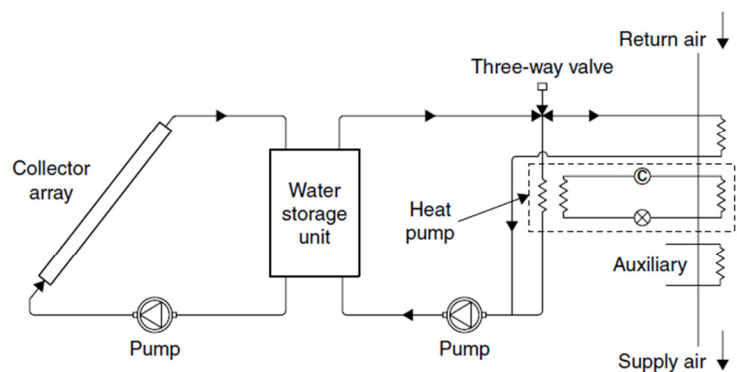


Figure 8. Schematic diagram of a domestic water-to-air heat pump system

During favorable weather conditions it is possible with this arrangement to have solar energy delivered directly to the forced air system while the heat pump is kept off. The arrangement shown on Figure 8 is a series configuration where the heat pump evaporator is supplied with energy from the solar system. Energy from collector system is supplied directly to the building when the temperature of the water in the storage temperature is high. When the storage temperature cannot satisfy the load the heat pump is operated thus it benefits from relatively high temperature of the solar energy system which is higher than the ambient and thus increases the heat pump's COP.

A parallel arrangement is also possible where the heat pump serves as an independent auxiliary energy source for the solar energy system as shown in Figure 9. In this case a water-water heat pump is used.

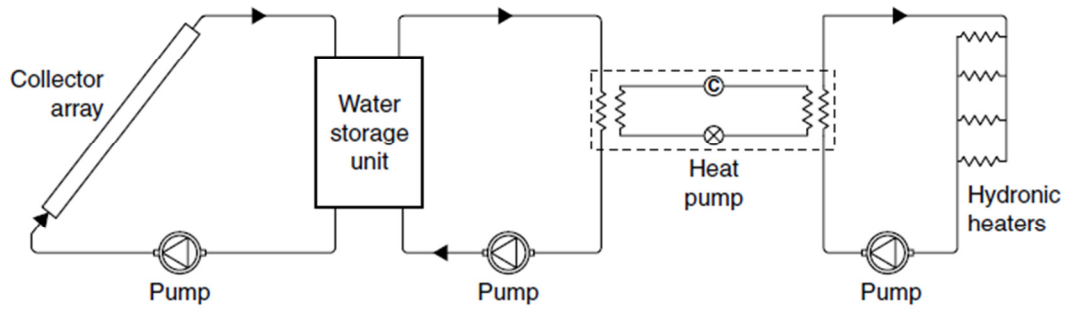


Figure 9. Schematic diagram of a domestic water-to-water heat pump system

The series connection is usually preferred because it allows all the solar collector power to be used, leaving the tank at low temperature which allows the solar energy system to work more efficiently the next day.

At the ground source heat pumps most embedded heat exchangers for private residences are installed either horizontally or vertically in the ground. Interest in vertical heat exchangers, also called borehole heat exchangers (BHE), has increased in the housing sector over the last decade because they offer better performances. Indeed, horizontal heat exchangers are directly affected by local climatic conditions as they are buried at depths between 0.80 and 1.50 m, while boreholes can exploit the ground temperature regularity below 6 m in depth, which ensures good performance throughout the year whatever the local climatic conditions. However, it should be pointed out that the high cost of boreholes is the major drawback of BHE systems, as installation requires drilling technologies. Nevertheless, the soil surface area occupied by a BHE is very small compared to that occupied by a horizontal ground heat exchanger, an advantage in areas of high land prices.

Nevertheless, the use of a geothermal heat pump (GHP) with BHE to heat and/or to cool buildings can create annual imbalances in the ground loads. In the case of heating dominated buildings, a thermal heat depletion of the soil can occur, which progressively decreases the heat pump's entering fluid temperature. On the contrary, cooling-dominated buildings heat the soil, which progressively increases the heat pump's entering fluid temperature. As a consequence, the heat pump's performance coefficient decreases and the installation gradually becomes less efficient. One solution for this problem could be combining solar collectors and the Ground Coupled Heat Pump (GCHP). This type of system has been increasingly recognized since the oil crisis in the 1970s, but the technology has not been widely adopted. In addition, experimental and theoretical results on the combination of thermal solar collectors with a GCHP used in heating dominated detached houses are relatively scarce.

The schematic diagram of the combination solar energy with ground source heat pump is presented on Figure 10. Solar heat is used in priority to heat DHW and is injected into the ground

via boreholes only when the DHW temperature setting is reached. The advantage of this operation is that it contributes to the balance of the ground loads, optimizes the use of solar heat provided by solar collectors and prevents overheating problems. The heat pump can be used in heating mode or in cooling mode. In cooling mode, heat is injected into the ground which also contributes to the balance of the ground loads.

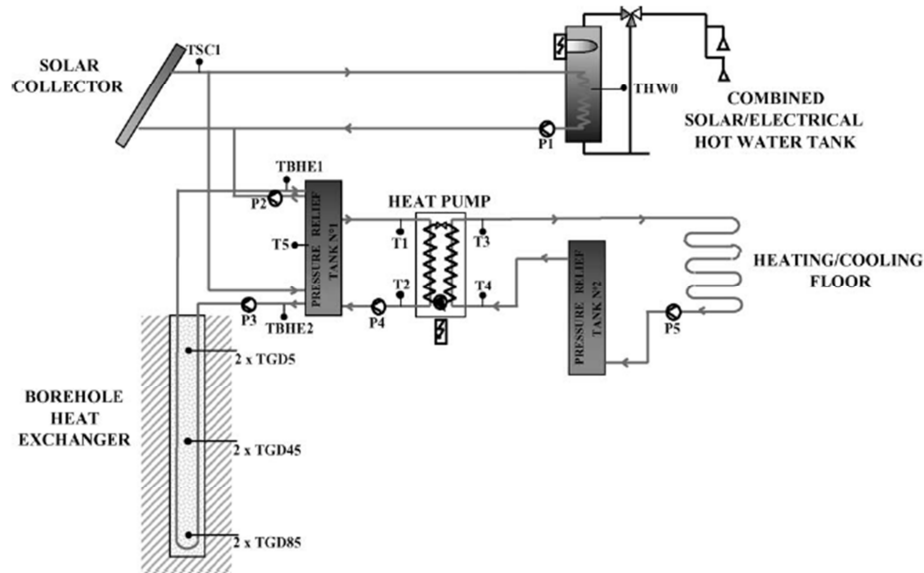


Figure 10. Schematic diagram of combination solar energy and ground source heat pump

It should be noted that regarding the control strategy compared to conventional heating or cooling, system controlling this installation is relatively complex. The power provided by geothermal energy is nearly the same throughout the year, as opposed to solar energy for which the power provided depends on solar radiations. To ensure proper operation of the installation, it is simpler to use two existing control systems: one adapted to ground-coupled heat pump systems and another adapted for solar heating systems. However, these two control systems must have good operational flexibility in order to ensure that the GCHP system combines well with the solar collector.

2.2 Solar cooling systems

In 2011, worldwide, about 750 solar cooling systems were installed, including installations with small capacity (<20kW) (Mugnier and Jakob, 2012). Recently a number of very large installations have been completed or are under construction. Examples are the system at the headquarters of the CGD bank in Lisbon, Portugal with a cooling capacity of 400 kW and a collector field of 1 560m²; and the system installed at the United World College in Singapore, completed in 2011, with a cooling capacity of 1 470 kW and a collector field of 3 900m².

Chapter 2. Technologies for active thermal solar systems

Solar cooling of buildings is an attractive idea. Cooling is important in space conditioning of most buildings in warm climates and in large buildings in cooler climates. The biggest advantage is that cooling loads and solar availability are approximately in phase. The combination of solar cooling and heating should greatly improve use factors on collectors compared to heating alone. Solar air conditioning can be accomplished by three classes of systems: absorption cycles, desiccant cycles and solar mechanical processes. In

Figure 11 is presented general scheme of solar assisted absorption cooling system. The cooling demand can be satisfied by the absorption chiller, the compression chiller or the cold storage. The thermal power needed by the absorption chiller is supplied by the solar collector field, the auxiliary heater or the hot storage. Cooling towers for the chillers heat rejection complete the scheme.

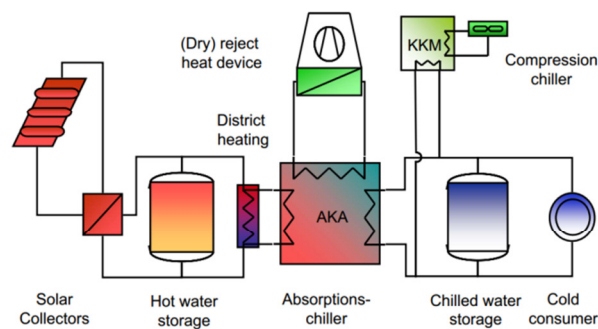


Figure 11. Scheme of a solar cooling plant: 1 = solar collector field; 2 = hot storage; 3 = auxiliary boiler; 4 = absorption chiller; 5 = cold storage; 6 = compression chiller; 7 = cooling towers

In order to reduce the plant complexity (and the cost of the system) some simplified configurations can be drawn. In the simplest solar cooling plant presented on Figure 12, (1 + 4 + 7) the entire thermal load is satisfied by a totally solar driven absorption chiller. In this case, the absorption chiller has to be sized with respect to the pick demand ($Q_E \geq Q_{L,max}$). The solar collector field must be oversized, because it has to drive the chiller also during the periods of low irradiation ($Q_{Coll} \geq Q_G$).

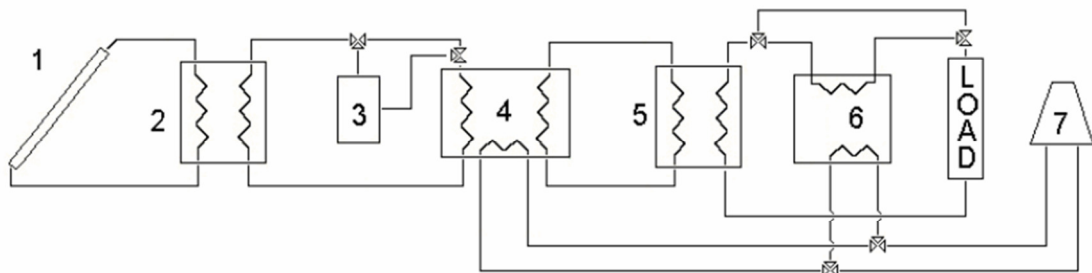


Figure 12. Simplified scheme of solar cooling plant

In order to avoid wasting the heat collected, a hot storage can be inserted between the solar field and the absorption chiller (1 + 2 + 4 + 7). The storage capacity must be evaluated by matching the

thermal power produced by the collectors and the chiller heat demand. When $Q_{Coll} > Q_G$, the heat surplus is stored in the tank; when $Q_{Coll} < Q_G$, the hot storage is needed to drive the absorption chiller: this situation typically occurs at the beginning and at the end of the day, when the solar radiation level is not high enough to drive the chiller at its lowest capacity. The collector area is partially reduced with respect to the previous case: in fact, when the irradiation is low, the hot storage can contribute to supply the chiller generator. To significantly reduce the collector area, an auxiliary boiler could be introduced (1 + 3 + 4 + 7). In this case, a fraction of the energy input to the generator can be supplied by the burner. The heat collected by the solar devices is wasted for few time, when the building load is low and the solar radiation is high ($Q_{Coll} > Q_G$).

2.3.1 Thermodynamic schemes and limits for solar cooling systems

From a thermodynamic point of view there are many processes conceivable for the transformation of solar radiation in cooling. Solar cooling technologies can be broadly classified according to Figure 13.

. Although the conversion of electricity by photovoltaic and the subsequent use of this electricity in a classical motor driven vapor compression chiller is a technically feasible concept, it is not further considered here. Reason is that in industrialized countries, which have a well-developed electricity grid, the maximum use of photovoltaic is achieved by feeding the produced electricity into the public grid. From an economic point of view this is even more valid if the price for electricity generated by solar energy is higher than that of electricity from conventional sources (e.g., feed-in laws in Germany or Spain). From the thermally driven technologies, which may use a solar thermal collector to provide heat to drive a cooling process, the technologies based on heat transformation are best developed. Therefore only these technologies are considered further.

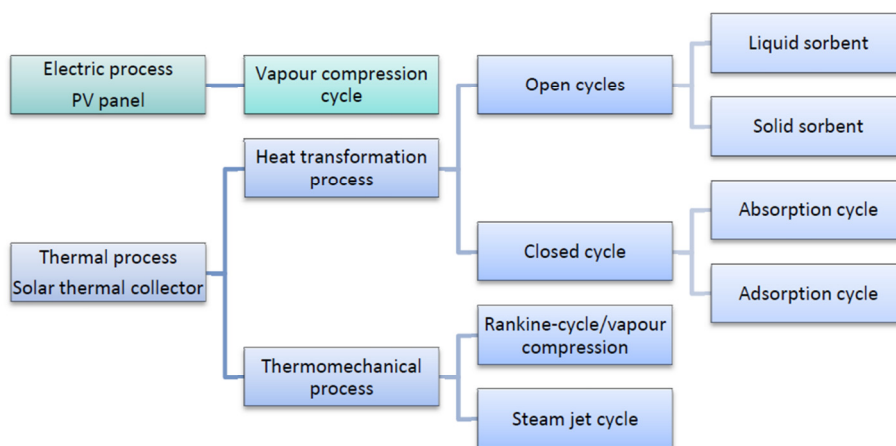


Figure 13. Overview on physical ways to convert solar radiation into cooling/air-conditioning

[16]

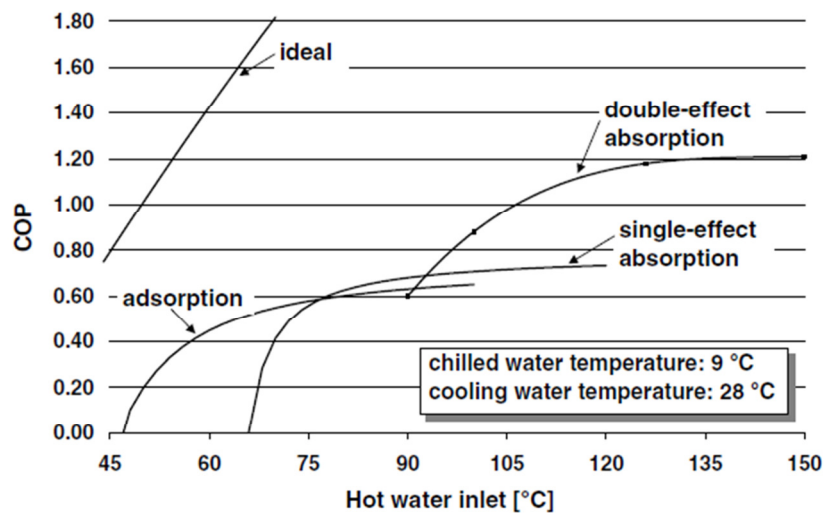


Figure 14. COP-curves of sorption chillers and the upper thermodynamic limit (ideal) [16]

From the above presented technologies this report will concentrate on those for small to scale A/C applications, which are currently available in the market.

In contrast, solar cooling systems based on the Rankine cycle have not been subject of further study, due to their complexity and higher costs. Therefore this technology will not be further discussed in this work.

Double effect absorption cycles have considerably higher COPs at around 1.1 - 1.4, but require significantly higher driving temperatures between 120°C and 170°C, so that the energetic and economic performance of the solar thermal cooling system is not necessarily better.

Vapor-compression cycle chillers are the most common for air-conditioning applications in commercial and residential buildings, since the technology is mature and significant improvements have been done in order to increase the COP. Therefore, coupling this cycle with PV, as seen in Figure 15 is an option worth. Furthermore, this cycle has been subject of study as part of innovative applications for hybrid photovoltaic/thermal collectors to produce electricity and heat to drive a hybrid air conditioner system.

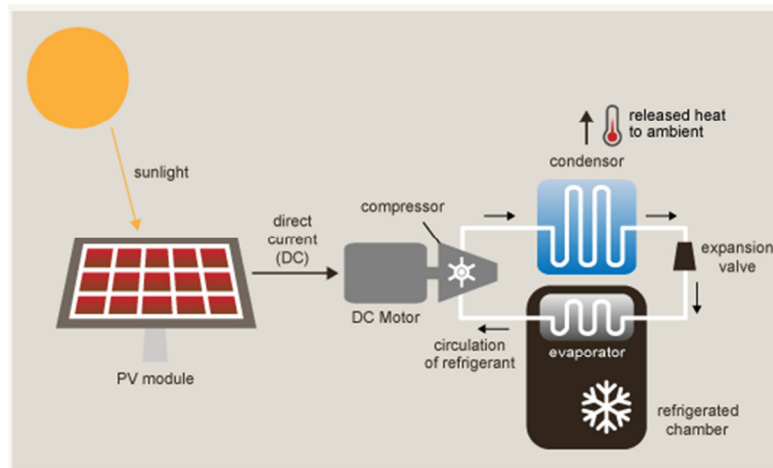


Figure 15. Solar electric vapor-compression cooling cycle

The use of a conventional vapor-compression chiller powered by photovoltaic panels for A/C has been proved technically viable in Turkey without the use of an auxiliary device to provide cooling [17]. This study concludes that the required panel area and COP vary depending on the evaporator temperature and the month of the year; which corresponds to a specific cooling capacity in the range of 0.10 – 0.35 kW/m². This value is lower in comparison with other technologies – see Table 1, because, although the chiller COP is high, the global efficiency of the whole system is reduced because of the current low efficiencies of PV modules, between 12% to 15%.

Solar refrigeration can also be applied by using thermal energy supplied from solar collectors, rather than electricity from PV cells; approach that has received particular attention for the past decades. Mainly because the efficiency of solar collectors is higher in comparison with PV modules, hence the former are able to use more of the received solar energy. Furthermore, with the use of solar thermal cooling it is possible to benefit from the existing infrastructure in residential and commercial buildings that currently provides hot domestic water – DHW– and in some regions space heating in winter and, reduce the environmental impact related with the use of refrigerants, as R-22 and R-410A, in conventional A/C systems.

Absorption chillers are available on the market in a wide range of capacities and designed for different applications. However, only very few systems are available in a range below 100 kW of cooling capacity. Today, also a few commercial systems for small power, e.g., below 30 kW, are available. Today absorption chillers are mainly applied if a ‘cheap’ heat source is available, such as waste heat, district heat or heat from co-generation plants. For air conditioning applications mainly absorption chillers using the sorption pair H₂O–LiBr are applied.

2.3 Solar cooling technologies

The key components of solar air conditioning systems are the solar collector subsystem and the thermally driven cooling subsystem. Additional key components are a heat rejection unit to reject the waste heat of the thermally driven chiller and storages (hot, cold).

Solar energy can be converted into cooling using two main principles:

- Electricity generated with photovoltaic modules can be converted into cooling using well-known refrigeration technologies that are mainly based on vapour compression cycles
- Heat generated with solar thermal collectors can be converted into cooling using thermally driven refrigeration or air-conditioning technologies. Most of these systems employ the physical phenomena of sorption in either an open or closed thermodynamic cycle. Other technologies, such as steam jet cycles or other cycles using a conversion of heat to mechanical energy and of mechanical energy to cooling are less significant

Techniques which allow the use of solar thermal collectors for air-conditioning of buildings regarding the thermally driven chillers can be distinguished in two main types:

- Closed cycle where thermally driven chillers are used to produce chilled water which can be used for any type of air-conditioning equipment
- Open cycles, also referred to as desiccant cooling systems, are used for direct treatment of air in a ventilation system.

Many details about components and systems for using solar thermal energy for air-conditioning application may be found in [18] .

Solar or waste heat driven closed absorption or adsorption chillers and open desiccant evaporative cooling systems (DEC) offer the potential to provide summer comfort conditions in buildings at low primary energy consumption. The future of many of the methods will depend on development beyond the cooling process itself. Temperature constrains in the operation of collector limit what can be expected of solar cooling processes.

In solar cooling system mostly used solar collectors are flat plate solar collectors (FPC), evacuated tube collectors (ETC), are stationary type and due to their temperature range as presented in Table 2 are the most commonly used for solar single-effect cooling systems. ETC, like FPC, are able to collect both beam and diffuse radiation; however has better overall performance than FPC, since their efficiency is greater at low incidence angles [15] and have less thermal losses [16].

Table 2. Solar collectors for single-effect absorption cooling systems

Collector type	Absorber type	Concentration ratio ¹	Temperature range ² °C
Flat plate collector - FPC	Flat	1	30-80 ³
Evacuated tube collector - ETC	Flat	1	50-200
Compound parabolic collector-CPC	Tubular	1-5	60-240

*1 Concentration ratio = the aperture area divided by the receiver/absorber area of the collector

*2 At nominal conditions

*3 There are collectors, using vacuum insulation or transparent insulation TI, which can achieve higher values. Also with the use of highly selective coatings, temperatures of 100 °C can be obtained [15].

Compound parabolic collectors (CPC) are able to reflect the incoming direct radiation to the absorber over wide-ranging angles. In contrast, its performance is significantly reduced when the amount of beam radiation is diminished in cloudy days.

The performance of a solar cooling system depends strongly on its components, how are interconnected and the control strategy adopted this includes the coupling between the chiller and the solar field. Situation that is particularly important for solar absorption systems, where there is a negative relation between the COP of the chiller and the efficiency of the solar collector. Since the former generally increases with the generator operating temperature while the performance of the solar collector is reduced. Therefore, there is an optimum temperature to drive the generator that maximizes the global efficiency of the solar system. This temperature is not a constant value, rather is a function of several parameters, as the ambient temperature and humidity, solar irradiation, which vary significantly during the operation of the system [19].

In the last decade, the main progress was made in the field of small capacity thermally driven chillers and SAC has significantly contributed to stimulate this development. Today, numerous systems from various manufacturers are offered on the market and have reached a considerable technical maturity. Most of the manufacturers are small start-up companies. Some of those companies achieved a status where they set up a manufacturing capacity on an industrial scale and others are on the way to follow.

However, solar cooling is still in the early stages of market development; costs need to be reduced through further development and increased deployment. A standardized, effective and simplified range of technology arrangements require development – particularly for single family and multi-family dwellings – to enable solar cooling to compete with conventional and supported renewable technologies and achieve widespread deployment. Quality assurance and system certification procedures are also needed to help stimulate the market by building buyer confidence.

2.3.1 Absorption cooling

The first evolution of an absorption system began in the 1700s. It was observed that in the presence of H_2SO_4 (sulfuric acid), ice can be made by evaporating pure H_2O (water) within an evacuated container. In 1810, it was found that ice could be produced from water in a couple of vessels connected together in the presence of sulfuric acid. As the H_2SO_4 absorbed water vapor (to reduce heat), ice formed on the surface of water. However, difficulties emerged with leakage and the corrosion of air into the void vessel. In 1859, a French engineer named Ferdinand Carre de signed a machine that used a working fluid pair of water and ammonia. This machine was used for making ice as well as storing food. In 1950, a new system was introduced with a water/lithium-bromide pair in gas working fluids for commercial purposes [20].

Currently, absorption chillers are the most common thermally-driven cooling process in solar cooling installations. Common absorption cooling pairs include ammonia-water and water-lithium bromide, with many sorption chillers available commercially over a range of capacities, but few at capacities of 100 kWth or less. The so-called “single effect” absorption chillers typically need heat with temperatures in the range of 70 to 100°C, and achieve a coefficient of performance (COP) of about 0.7.

The primary advantage of an absorption system is that it has a larger COP (coefficient of performance) than other thermally operated technologies.

In closed absorption cycles the refrigerant is conserved and reused repeatedly in successive cycles. Heat exchange but not fluid exchange takes place between the refrigerant and the atmosphere. Closed sorption cooling cycles work under the same principle as vapor-compression machines, except that the mechanical compressor is replaced by a thermally driven compressor:

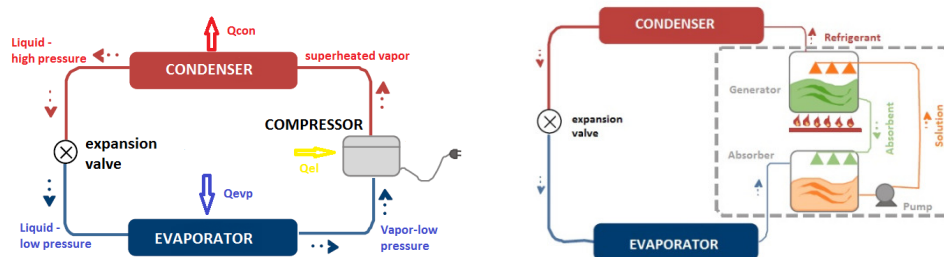


Figure 16. a) Vapor compression chiller b) Absorption(thermally driven) chiller

Absorption air-conditioning is compatible with solar energy since a large fraction of the energy required is thermal energy at temperatures that currently available flat-plate collectors can provide. Solar absorption air conditioning has been subject of investigation by a number of researchers [21-30].

Chapter 2. Technologies for active thermal solar systems

A single stage absorption chiller is essentially a three temperatures device. It removes a quantity of heat Q_E from a source at low temperature T_E , it rejects a quantity of heat Q_M to a source with a temperature close to the environment T_M , it is driven by a quantity of heat Q_G taken from a source at high temperature T_G . The quantity of heat Q_E is the refrigeration capacity of the chiller.

On Figure 16 is shown a schematic of an absorption refrigeration system. As mentioned before absorption refrigeration differs from vapor-compression air-conditioning only in the method of compressing the refrigerant. In absorption pressurization is accomplished by first dissolving the refrigerant in a liquid (the absorbent) in the absorber section, then pumping the solution to a high pressure with an ordinary liquid pump. The low boiling refrigerant is then driven from solution by the addition of heat in the generator. By this means the refrigerant vapor is compressed without the large input of high grade shaft work that the vapor-compression air-conditioning demands. On Figure 17, two vessels can be individuated, a condenser (C) and an evaporator (E). These are also found in many other refrigerating machines (like vapor compression chillers). A refrigerant, that in the present case is pure water, is condensed in the high pressure vessel C, until it reaches the state of saturated liquid (point 8). The condensation process releases the latent heat Q_C to an external stream. The refrigerant is then brought to the low pressure vessel E through a lamination valve or a U tube (point 9). Due to the lamination it is now a mixture of vapor and liquid. In the evaporator the liquid part of the refrigerant is brought to the state of saturated vapor. The evaporation takes place thanks to a quantity of heat Q_E extracted from an external stream.

If water vapor (point 10) is taken again to the high pressure level the cycle can be closed. How this is accomplished is the key of the absorption technology. The saturated vapor enters the vessel A, named absorber, which is at a pressure almost identical to that of the evaporator.

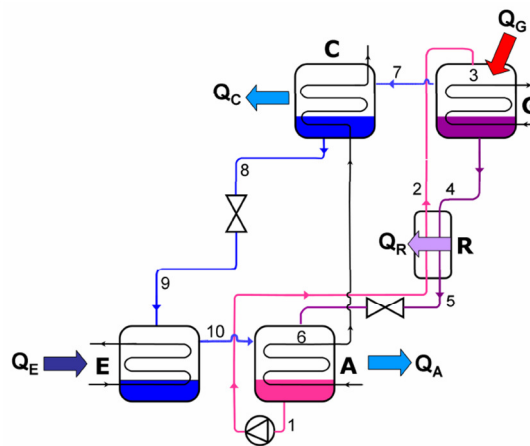


Figure 17. Schematic diagram of a single stage absorption chiller (LiBr-H₂O)

Chapter 2. Technologies for active thermal solar systems

For the thermodynamic analysis of the absorption system the principles of mass conservation and the first and second laws of thermodynamics are applied to each component of the system. Each component can be treated as a control volume with inlet and outlet streams, heat transfer and work interactions. In the system mass conservation includes the mass balance of each material of the solution. The governing equations of mass and type of material conservation for steady-state, steady-flow systems are [31]:

$$\sum \dot{m}_i - \sum \dot{m}_o = 0 \quad (1)$$

$$\sum (\dot{m}, x)_i - \sum (\dot{m}, x)_o = 0 \quad (2)$$

where \dot{m} is the mass flow rate and x is mass concentration of LiBr in the solution. The first law of thermodynamics yields the energy balance of each component of the absorption system as follows:

$$\sum (\dot{m}, h)_i - \sum (\dot{m}, h)_o + |Q_i - Q_o| + W = 0 \quad (3)$$

An overall-steady state energy balance on the absorption cooler indicates that the energy supplied to the generator and to the evaporator must equal the energy removed from the machine via the coolant flowing through the absorber and the condenser plus whatever net losses may occur to the surroundings

$$Q_G + Q_E = Q_A + Q_C + Q_{loss} \quad (4)$$

The useful output energy of the system for heating applications is the sum of the heat rejected from the absorber and the condenser while the input energy is supplied to the generator.

The thermal coefficient of performance COP is defined as the ratio of energy into the evaporator Q_E to the energy into the generator Q_G .

$$COP = \frac{Q_E}{Q_G} \quad (5)$$

The coefficient of performance is useful index of performance in solar cooling, where collector costs (and thus cost of Q_E) are important. Many LiBr-H₂O machines have nearly constant COP as the generator temperatures vary over the operating range as long as the temperatures are above the minimum.

Others types of COP can be defined. A COP_e is the ratio of cooling to electrical energy used to provide air and liquid flows, operate controls etc.

$$COP_e = \frac{Q_e}{\text{Electric Input}} \quad (6)$$

Solar fractions on the heating energy demand of the absorption chillers therefore need to be higher than about 50% to start saving primary energy [32].

The most common used refrigerant-absorber pairs are: Lithium Bromide (absorber) and water (refrigerant) LiBr-H₂O , and Ammonia (refrigerant) – Water(absorber) NH₃-H₂O. Because the LiBr-H₂O has high volatility ratio, it can operate at lower pressures and therefore at lower generator temperatures achievable by flat-plate collectors. A disadvantage of this system is that the pair tends to form solids. LiBr has tendency to crystalize when air cooled and system cannot be operated at or below the freezing point of the water. Therefore the LiBr-H₂O system is operated at evaporator temperatures of 5 °C or higher. Using the mixture of LiBr with some other salt as the absorber can overcome the crystallization problem. It over comes the problem of using a filter as the pair is not volatile, and it has a very high latent heat of vaporization. However, because water is used as the refrigerant in this pair, there are problems with low temperature operation at temperatures below 0°C. Moreover, the system requires vacuum conditions and at high concentrations, the pair tends to be crystalline. There are also issues of corrosion with some metals. A brief thermodynamic analysis of this pair is available in previous investigations [33, 34].

The ammonia-water system has advantage that it can be operated down to very low temperatures. However for temperatures much below 0°C water vapor must be removed from ammonia as much as possible to prevent ice crystals from forming. This requires a rectifying column after the boiler. Also ammonia is a safety Code Group B2 fluid (ASHRAE Standard 34-1992) which restricts its use indoors [35].

Single effect LiBr-H₂O absorption chillers operate with thermal COP limited to 0,7 and actual operating coefficients may be very much less due to cycling and other problems. Double effect chillers in which two generators in series are used can have COP values in the range 1.0 to 1.5. These improvements are obtained at the expense of considerable complication of the machines and will probably require the use of collector operating at temperatures beyond the range of flat-plate collectors.

2.3.2 Adsorption cooling

Adsorption cycles for refrigeration were first used in the early 1900s. Plank and Kuprianoff (1960) reported on manufactured machines using ammonia/CaCl and methanol/activated carbon. Hulse (1929) reported on a sulfur dioxide/silica gel machine for the air-conditioning of rail freight cars in the United States. Critoph (2012), in his historical review, reports on a domestic activated

Chapter 2. Technologies for active thermal solar systems

carbon/methanol refrigerator called 'Eskimo' and sold in the 1930s by the Norwegian Amundsen Refrigerator Company. In general, this technology was recognized in 19th century so its practical application in the field of refrigeration is relatively recent.

The concentration of adsorbate vapors in a solid adsorbent is a function of the temperature of the pair i.e. the mixture of adsorbent and adsorbate and the vapor pressure of the latter. The dependence of adsorbate concentration on temperature under constant pressure conditions makes it possible to adsorb or desorb the adsorbate by varying the temperature of the mixture.

An adsorbent – refrigerant working pair for a solar refrigerator requires following characteristics:

Refrigerant should have large latent heat of evaporation. A low heat of desorption under the envisaged operating pressure and temperature conditions and low thermal capacity.

The conventional adsorption cycle has been presented extensively in the literature [31-33] and it mainly includes two phases:

1. Adsorbent cooling with adsorption process which results in refrigerant evaporation inside the evaporator and thus in the desired refrigeration effect. At this phase the sensible heat and the adsorption heat are consumed by a cooling medium which is usually water or air

2. Adsorbent heating with desorption process also called generation which results in refrigerant condensation at the condenser and the heat release into the environment. The heat necessary for the generation process can be supplied by a low-grade heat source such as solar energy, waste heat etc.

When the temperature of the heating medium ranges from 60 to 95 °C, the coefficient of cooling efficiency for adsorption chillers is 0.6–0.7 [9–11]. With a solid sorbent, the coefficient of cooling efficiency (COP) in open systems is 0.6–1.0 (when the temperature of the heating medium ranges from 45 to 95 °C), whereas with a liquid sorbent the COP is about 1.0 (when the temperature of the heating medium ranges from 60 to 80 °C) [34].

Closed cycle adsorption cooling

A closed cycle desiccant system has been developed in which the refrigerant (water) is cycled. During the cooling process water previously condensed is injected into a flash evaporator and evaporates to provide cooling. The vapor is adsorbed in a zeolite desiccant which allows low (10 °C – 15 °C) temperature in the evaporator. The water evaporated from the zeolite (or silica gel) during regeneration is condensed in sensible exchanger by heat rejection to the surroundings. The condensed water is then recycled in the evaporator.

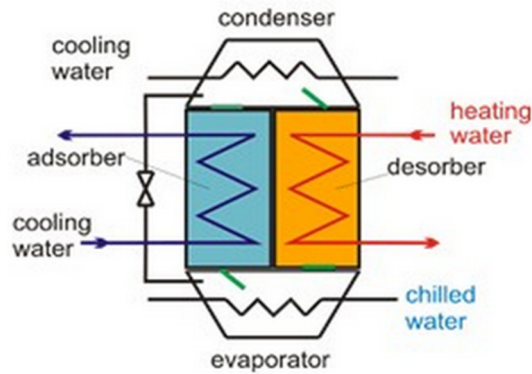


Figure 18. Simple schematic drawing of an (solar driven) adsorption chiller

In contrast to absorption chillers, adsorption chillers use solid sorption materials. Market available systems use water as refrigerant and silica gel as sorbent. Because of the fact that the solid sorbent cannot be circulated adsorption chillers consist of two separate chambers Figure 18, which both contain the adsorbent. Besides these two adsorbent chambers, there is one evaporator and one condenser (coupled to the heat sink).

The adsorbent containing the water is heated (by the solar collectors) and the adsorbed water is expelled as water vapor and condenses in the condenser and the condensed water is transferred to the evaporator. The adsorbent is cooled again, leading to a lower pressure in the sealed system where the water in the evaporator evaporates, taking up the heat from the chilled water circuit, after which water vapor is adsorbed in the adsorbent (adsorption heat is evacuated).

One of the first companies that offers commercial adsorption chillers is the SorTech AG, founded in 2002 as a spin-off of the German “Fraunhofer-Institut für Solare Energiesysteme ISEscale” solar cooling application. Starting from 2007 the SorTech chillers are silica gel based with cooling capacities starting from 5 kW to 15 kW per unit. In the meantime more than 200 projects mainly in Europe, but as well in Africa, North America, Asia, and Australia could be realized with cooling capacities up to 150 kW.

2.3.4 Open-cycle solar desiccant cooling

Characteristic for open systems, working as an aerial set is that they become particularly ineffective when the heat gains are significant. In that case the excess heat from the building is removed by increasing the air circulation in a room. A critical defect of open systems is the limited possibility of their use. They may be operated only in such conditions when the air is cooled at a central air-conditioning unit and when the air treatment depends on its cooling. An additional constraint is the inability to achieve a low temperature for the air supply. All these have negative

Chapter 2. Technologies for active thermal solar systems

impact on obtaining the desired levels of the supply air. Therefore, the adsorption refrigerating systems supplied by solar energy appears to be the most promising solution to the problem.

Solar desiccant air conditioning systems use a desiccant to remove moisture from an air stream. The dried air is processed by evaporative coolers to produce a relatively dry cool air stream which then cools the building space. Solar energy can be used to regenerate the desiccant. These systems offer the promise of a high thermal coefficient of performance using the moderately low temperatures compatible with solar collectors.

Mainly are used two types of desiccant systems: solid desiccant system in which the desiccant is a stationary bed or rotating matrix and liquid desiccant system in which desiccant is pumped round between air streams.

Air flows through the components in open-cycle systems and moisture and heat are transferred between the air stream the atmosphere and heat sources. The ambient serves as a heat sink for the discharged moisture regarding the closed cycle which only exchange heat with the surrounding atmosphere. The desiccant is regenerated with solar energy.

Warm and humid air (fresh air) enters the slowly rotating desiccant wheel and is dehumidified by adsorption of water. Because the air is heated up by the adsorption heat there is also installed a heat recovery wheel. The result is a significant pre-cooling of the supply air stream. After the pre-cooling the air is humidified and further cooled by a controlled humidifier according to the desired temperature and humidity of the supply air stream. The exhaust air stream (warm, humid) of the rooms is humidified close to the saturation point to exploit the full cooling potential in order to allow an effective heat recovery. To allow a continuous operation of the dehumidification process the sorption wheel has to be regenerated by applying heat in a comparatively low temperature range from 50-75°C

Chapter 3

3. Numerical modeling of solar thermal system

The method for the modeling is separated into three distinct stages: Building modeling stage and system plant modeling stage, and stage 3 manual calculations. This can be summarized in the following key stages:

Stage 1: Building model

- Development of building models (geometrics, construction details) for the building
- Apply future weather data to building model
- Simulate cooling demand from building models for various scenarios

Stage 2: TRNSYS solar model

- Development of solar powered absorption plant
- Apply loads generated from stage 1 model for specific future weather years
- Simulate cooling delivered by solar absorption cooling system

Stage 3: Manual calculations

- Calculate COP of solar powered cooling system
- Calculate additional cooling to be delivered by cooling/heating system

3.1 Energy simulation software

The development of solar simulation capabilities greatly assist in the promotion of practical solar systems. Simulations, like any other calculations are only as good as the models that are the basis of the program and the skill which they are used. Some of the programs that have been applied to solar processes have been written specifically for study of solar energy systems. Other were intended for non-solar applications but have had models of solar components added to them to make them useful for solar problems.

Simulations are numerical experiments and can give the same kinds of thermal performance information as physical experiments. They are however relatively quick and inexpensive and can

Chapter 3. Numerical modeling of solar thermal system

produce information on effect of design variable changes on system performance by series of experiments all using exactly the same loads and weather. These design variables could include selectivity of the absorbing surface, number of covers on the collector, collector area etc. With cost data and appropriate economy analysis, simulation results can be used to find least cost systems.

There are two basic kinds of data that can be obtained from simulations. First, integrated performance over extended periods can be determined. This is normally wanted for a year that represents the long-term average climate in which is proposed process would operate. A year is the time base of most economic studies, but information may be needed for other periods from days to spans of many years.

The extent to which simulations represent the operation of real physical systems depends on the level of detail included in the numerical experiment. Component models can vary in complexity, as can system. In principle simulations can be as detailed as the user wishes. In practice there may be factors in system operation which are difficult to simulate such as leaks in air systems and operation of real systems may be less ideal than the simulation indicates.

3.1.1 Review of simulation software's used in solar air-conditioning

Here are presented the results from the review i.e. the technical report of Subtask C, Task 38 where is given brief description of some simulation tools applicable in solar air-conditioning systems. These tools are the most commonly used by IEA task 38 participants.

SPARK

SPARK is a general simulation environment that supports the definition of simulation models and solution of these models via a robust and efficient differential/algebraic equation solver. In SPARK, the modeler describes the set of equations defining a model as equation-based objects. At the lowest level, an atomic object characterizes one equation and its variables. Then, macroscopic objects can be created as an assembly of various atomic or macroscopic objects.

SPARK has its own HVAC library based on some simple models.

ENERGY PLUS

EnergyPlus is an energy analysis and thermal load simulation program. Based on a user's description of a building from the perspective of the building's physical make-up, associated mechanical systems, etc., EnergyPlus will calculate the heating and cooling loads necessary to maintain thermal control set points, conditions throughout an secondary HVAC system and coil loads, and the energy consumption of primary plant equipment as well as many other simulation details that are necessary to verify that the simulation is performing as the actual building would. Many of the simulation characteristics have been inherited from the legacy programs of BLAST

Chapter 3. Numerical modeling of solar thermal system

and DOE-2. It is the intent of EnergyPlus to handle as many building and HVAC design options either directly or indirectly through links to other programs in order to calculate thermal loads and/or energy consumption on for a design day or an extended period of time (up to, including, and beyond a year).

EES

EES is an acronym for Engineering Equation Solver. The basic function provided by EES is the numerical solution of a set of algebraic equations. EES can also be used to solve differential and integral equations, do optimization, provide uncertainty analyses and linear and non-linear regression, convert units and check unit consistency and generate publication-quality plots.

EASYCOOL

EasyCool provides 11 pre-defined system configurations for solar thermally driven cooling applications, of which 4 configurations are foreseen for reference calculations (non-solar, conventional system solutions). The program reads annual time series with hourly building load data and meteorological data of the respective site (these data set has to be prepared in advance) and calculates annual energetics and economic performance data as well as environmental figures such as CO₂ savings.

INSEL

The acronym INSEL stands for INtegrated Simulation Environment Language. This graphical programming language has been developed at the Faculty of Physics of Oldenburg University (Germany) in the early 1990's and was originally designed for the modelling of renewable electrical energy systems. The graphical programming language INSEL is based on the principle of "structured programming" on blocks diagrams. It consists of connecting blocks in order to obtain block diagrams that express a solution for a certain simulation task.

TRNSYS

Trnsys is a widely used modular thermal process simulation program. Originally developed for solar energy applications, it now is used for simulation of wider variety of thermal processes. Subroutines are available that represents the components in typical solar energy systems.

TRNSYS is a complete and extensible simulation environment for the transient simulation of systems, including multi-zone buildings. It is used by engineers and researchers around the world to validate new energy concepts, from simple domestic hot water systems to the design and simulation of buildings and their equipment, including control strategies, occupant behavior, alternative energy systems (wind, solar, photovoltaic, hydrogen systems), etc. The simulation engine is programmed in Fortran and the source is distributed. The engine is compiled into a Windows Dynamic Link

Chapter 3. Numerical modeling of solar thermal system

Library (DLL), TRNDII. The TRNSYS kernel reads all the information on the simulation (which components are used and how they are connected) in the TRNSYS input file, known as the deck file (*.dck). It also opens additional input files (e.g. weather data) and creates output files.

Users can readily write their own component subroutines. By a simple language, the components are connected together in manner analogues to piping, ducting and wiring in a physical system. The DLL-based architecture allows users and third-party developers to easily add the custom component models, using all common programming languages (C, C++, PASCAL, FORTRAN, etc.). In addition, TRNSYS can be easily connected to many other applications, for pre- or post-processing or through interactive calls during the simulation (e.g. Microsoft Excel, Matlab, COMIS, etc.).

Current versions of TRNSYS have in executive program convergence promoters and other means of speeding computations. There are three integration algorithms in TRNSYS, the user can choose the one best suited to the problem at a hand. The one that is extensively used is the modified Euler method. It is essentially a first order predictor corrector algorithm using Euler's method for the predicting step and the trapezoid rule for the correction step.

TRNSYS applications include:

- Solar systems (solar thermal and PV)
- Low energy buildings and HVAC systems with advanced design features (natural ventilation, slab heating/cooling, double façade, etc.)
- Renewable energy systems
- Cogeneration, fuel cells
- Anything that requires dynamic simulation!

As an additional component library (also used in this work) is the developed by the company Thermal Energy System Specialist (TESS). The TESS Applications Library is an assortment of scheduling and setpoint applications that use the TRNSYS Simulation Studio plugin feature. These components are extremely useful for creating daily, weekly, monthly schedules, normalized occupancy, lighting, or equipment schedules, and setpoints for thermostats.

3.2 Numerical components models

Mathematical description of the used component models are given as described in the TRNSYS manual Mathematical references since all of the simulations are performed in TRNSYS.

3.2.1 Collector model – Flat plate collector

For the flat plate solar collector it is used the Type 539 from the TESS library. It is chosen this model because compared to Type 1 from the TRNSYS library it takes into consideration the influence of the capacitance effect to the temperature change.

The operation of most solar energy systems is inherently transient. There is no such thing as steady-state operation when one considers the transient nature of the driving forces. This observation has led to numerical studies by Klein, Wijesundera and others on the effects of collector heat capacity on collector performance. The effects can be regarded in two distinct parts. One part is due to the heating of the collector from its early morning low temperature to its final operating temperature in the afternoon. The second part is due to intermittent behavior during the day whenever the driving forces such as solar radiation and wind change rapidly.

The rate of useful gain for a flat-plate collector according the Duffie and Beckaman :

$$Q_u = A_c F_R [S - U_L (T_i - T_a)]^+ \quad (7)$$

Where

Q_u [kJ/h]	- useful gain from the collector
A_c [m ²]	- collector aperture area
S [kJ/h m ²]	- solar radiation absorbed per collector unit area
U_L [kJ/h m ² K]	- overall collector heat loss coefficient
T_i [K]	- fluid inlet temperature
F_R [-]	- collector heat removal factor based on collector inlet temperature

where the + sign implies the presence of a controller and that only positive values of the term in the brackets should be used. Operation of a forced – circulation collector will not be carried out when $Q_u < 0$ (or when $Q_u < Q_{min}$ where Q_{min} is a minimum level of energy gain to justify pumping the fluid through the system). In real systems, this is accomplished by comparing the temperature of the fluid leaving the collector (i.e. the top header) with the temperature of the fluid in the exit portion of the storage tank and running the pump only when the difference in temperatures is positive and energy can be collected.

The rate of useful gain is also given by:

$$Q_u = \dot{m} \cdot C_p (T_o - T_i) \quad (8)$$

Where \dot{m} is the output of the pump circulating through the collector.

If the storage unit is fully mixed sensible heat unit, its performance is given by equation:

$$(mC_p)_s \frac{dT_s}{dt} = Q_u - L_s - (UA)_s (T_s - T_a) \quad (9)$$

The equivalent equations for stratified water tank storage systems, pebble bed exchangers or heat of fusion systems are used in lieu of Equation 66(9) as appropriate. These equations are the

Chapter 3. Numerical modeling of solar thermal system

basic equations to be solved in the analysis of systems such as simple solar water heater with collector, pump, controller and storage tank. The rate of energy removal to meet all or part of a load is L_S and is time-dependent ; S and T_a are also time dependent.

If the collector is discretized into isothermal temperature nodes, the governing differential equation for node j can be expressed as:

$$C_j \frac{dT_j}{dt} = F'(S_j - A_j U_L (T_j - T_a)) - \dot{m} C_p (T_j - T_{in,j}) \quad (10)$$

Where:

$$C_j = \frac{C}{\#Nodes} \quad ; \quad A_j = \frac{A}{\#Nodes} \quad ; \quad S_j = \frac{S}{\#Nodes} \quad (11)$$

$$S = (\tau\alpha)_n IAM \cdot A \cdot I_T \quad (12)$$

$$T_{in,j} = T_{j-1} \text{ where } T_o = T_{in} \quad (13)$$

The dependence of $(\tau\alpha)$ on the angle of incidence of radiation on the collector varies from one collector to another and the standard test methods include experimental estimation of this effect. Collector tests are generally performed on clear days at normal incidence so that the transmittance - absorptance product $(\tau\alpha)$ is nearly the normal incidence value for beam radiation, $(\tau\alpha)_n$. The intercept efficiency, $F_R (\tau\alpha)_n$, is corrected for non-normal solar incidence by the factor $(\tau\alpha)/(\tau\alpha)_n$. By definition, $(\tau\alpha)$ is the ratio of the total absorbed radiation to the incident radiation. Thus, a general expression for $(\tau\alpha)/(\tau\alpha)_n$ i.e. the incident angle modifier (IAM) is written as:

$$IAM = \frac{(\tau\alpha)}{(\tau\alpha)_n} = \frac{I_{bT} \frac{(\tau\alpha)_b}{(\tau\alpha)_n} + I_{dsT} \frac{(\tau\alpha)_{ds}}{(\tau\alpha)_n} + I_{dgT} \frac{(\tau\alpha)_{dg}}{(\tau\alpha)_n}}{I_T} \quad (14)$$

where:

$(\tau\alpha)$	[0...1]	- Product of the cover transmittance and the absorber absorptance
$(\tau\alpha)_n$	[0...1]	- $(\tau\alpha)$ at normal incidence
$(\tau\alpha)_b$	[0...1]	- $(\tau\alpha)$ for beam radiation (depends on the incidence angle θ)
$(\tau\alpha)_{ds}$	[0...1]	- $(\tau\alpha)$ for sky diffuse radiation
$(\tau\alpha)_{dg}$	[0...1]	- $(\tau\alpha)$ for ground reflected radiation
I_T	[kJ/h m ²]	- Total radiation incident on the solar collector (Tilted surface)
I_{bT}	[kJ/h m ²]	- Beam radiation incident on the solar collector
I_{dsT}	[kJ/h m ²]	- Sky diffuse radiation on the solar collector (tilted surface)
I_{dgT}	[kJ/h m ²]	- Ground-reflected diffuse radiation on the solar collector (tilted surface)

A general expression has been suggested by Souka and Safwat (1966) for angular dependence of IAM for collectors with flat covers as:

$$IAM = 1 + b_0 \left(\frac{1}{\cos\theta} - 1 \right) \quad (15)$$

Chapter 3. Numerical modeling of solar thermal system

where θ is the incidence angle and b_0 is a constant called the incidence angle modifier coefficient – this equation follows the ASHRAE 93-77 convention, and b_0 is generally negative number. At larger angles of incidence, the linear relationship no longer applies, but most of the useful energy absorbed in a collector system will be at times when θ is less than 60° .

For flat-plate collectors, $(\tau\alpha)_b/(\tau\alpha)_n$ can be approximated:

$$\frac{(\tau\alpha)_b}{(\tau\alpha)_n} = 1 - b_0 \left(\frac{1}{\cos\theta} - 1 \right) - b_1 \left(\frac{1}{\cos\theta} - 1 \right)^2 \quad (16)$$

The incidence angle modifiers for both sky, $(\tau\alpha)_{ds}/(\tau\alpha)_n$, and ground diffuse, $(\tau\alpha)_{dg}/(\tau\alpha)_n$, are determined by defining equivalent incidence angles for beam radiation that give the same transmittance as for diffuse radiation.

In this component model 5 (five) optical modes can be selected in order to input the IAM data:

- Optical mode 1: perfect IAM $(\tau\alpha)/(\tau\alpha)_n=1$ for any incidence angle
- Optical mode 2: the user specifies the values of b_0 and b_1 in Equation 16
- Optical mode 3: values of $(\tau\alpha)_b/(\tau\alpha)_n$ versus θ are supplied in an external data file but the collector is assumed to be symmetrical so only one direction is provided in the data file
- Optical mode 5: values of $(\tau\alpha)_b/(\tau\alpha)_n$ versus θ are supplied in an external data file for both the longitudinal and transversal directions, this mode is usually used to simulate evacuated collectors

The effective incidence angles for sky diffuse and ground reflected radiations are:

$$\theta_{sky} = 59.68 - 0.1388\beta + 0.001497\beta^2$$

$$\theta_{gnd} = 90.00 - 0.5788\beta + 0.002693\beta^2$$

An estimate of the loss coefficient and transmittance-absorptance product at normal incidence can be made if the parameters of the collector efficiency test are known.

A general equation for solar thermal collector efficiency can be obtained from the Hottel-Whillier equation at steady-state conditions as:

$$\eta = \frac{Q_U}{A \cdot I_T} = \frac{\dot{m} C_p (T_o - T_i)}{A I_T} = F_R (\tau\alpha)_n - F_R U_L \frac{T_i - T_a}{I_T} \quad (17)$$

But today the collector efficiency equation has different form which is used in the collector efficiency certificates:

$$\eta = \eta_0 - a_1 \frac{T_m - T_a}{I_T} - a_2 \frac{(T_m - T_a)^2}{I_T} \quad (18)$$

where:

Chapter 3. Numerical modeling of solar thermal system

η_0 [-]	Optical efficiency (conversion factor)
a_1 [W/m ² K]	Heat transfer coefficient
a_2 [W/m ² K]	Temperature depending heat transfer coefficient
I_T [W/m ²]	Solar radiation at which the measurement is performed (usually 1000 W/m ²)

These parameters are available for collectors tested according to ASHRAE standards and rated by SRCC (ASHRAE, 2003; SRCC, 1995), as well as for collectors tested according to the recent European Standards on solar collectors (CEN, 2001).

Correction to the ideal efficiency curve

Analytical corrections are applied to the collector parameters to account for:

- Operations at flow rates different from the test conditions
- N_S identical collectors mounted in series
- Non-normal solar incidence

In order to account for conditions when the collector is operated at a flow rate other than the value at which it was tested, both $F_R (\tau\alpha)$ and $F_R U_L'$ are corrected to account for changes in F_R . The ratio, r_1 , by which they are corrected is given by:

$$r_1 = \frac{F_R U_L' |_{USE}}{F_R U_L' |_{TEST}} = \frac{F_R (\tau\alpha)_n |_{USE}}{F_R (\tau\alpha)_n |_{TEST}} = \frac{\frac{\dot{m} C_p}{AF'U_L} \left(1 - e^{-AF'U_L / \dot{m} C_p} \right) |_{USE}}{\frac{\dot{m}_{test} C_p}{AF'U_L} \left(1 - e^{-AF'U_L / \dot{m} C_p} \right) |_{TEST}} \quad (19)$$

That quantity can be calculated from the test conditions:

$$F'U_L = -\frac{\dot{m} C_p}{A} \ln \left(1 - \frac{F_R U_L' A}{\dot{m} C_p} \right) \quad (20)$$

For liquid collectors, $F'U_L$ calculated from the test conditions is approximately equal to $F'U_L$ at use conditions and can be used in both the numerator and denominator of Equation 19.

Calculation of the collector outlet temperature at steady-state conditions at normal incidence can be made with the equation:

$$T_o = T_i + \frac{A}{\dot{m} C_p} (F_R \tau \alpha_N I_T - F_R U_L (T_i - T_a)) \quad (21)$$

However, we rarely have steady-state conditions in a real system and there are many times where the mass of the collector impacts the collector outlet temperature. Equations 6610 and 12 may be combined to give the general differential equation for a node of the solar collector.

$$C_j \frac{dT_j}{dt} = F'(\tau\alpha)_n \cdot IAM \cdot A_j \cdot I_T - A_j F' U_L (T_j - T_a) - m C_p (T_j - T_{in,j}) \quad (22)$$

Without the collector heat removal factor, it becomes impossible to calculate the isolated collector fin efficiency factor (F'), the collector transmittance-absorptance product at normal incidence ($(\tau\alpha)_n$) and the collector heat loss coefficient (U_L) required solving the collector node energy balance.

Knowing the heat removal factor F_R the other terms can be calculated as:

$$F' = -\frac{\dot{m}_{test} C_{p,test}}{AU_L} \text{LOG} \left(1 - \frac{F_R AU_L}{\dot{m} C_p} \right) \quad (23)$$

The collector efficiency results can be presented as a function of the average collector temperature or the outlet collector temperature and not as a function of the collector inlet temperature.

$$\eta = \frac{Q_U}{AI_T} = F_{av}(\tau\alpha)_n - F_{av} U_L \frac{(T_{av} - T_a)}{I_T} = F_0 U_L \frac{(T_o - T_a)}{I_T} \quad (24)$$

3.2.1.1 Collector model – Evacuated Tube Collector

Evacuated tube collectors (ETCs) have demonstrated that the combination of selective surface and an effective convection suppressor can result in good performance at high temperatures. In the component model for the vacuum tube collector Type 538 is used from the TESS library.

The vacuum envelope reduces convection and conduction losses, so the collector can operate at higher temperatures than flat-plate collectors. Like flat-plate collectors they collect both direct and diffuse radiation. However their efficiency is higher at low incidence angles. This effect tends to give evacuated tube collectors an advantage over flat-plate collectors in terms of daylong performance.

With the Type 538 is modeled an evacuated tube solar collector with a quadratic efficiency curve and the off-normal radiation effects which can be treated with bi-axial incidence angle modifiers and the user has the option of controlling the flow rate through the collector to maintain a desired outlet temperature. The capacitance (mass) of the collector is not accounted for in this model; steady state conditions are assumed. The total collector array may consist of collectors connected in series and in parallel. The thermal performance of the total collector array is determined by the number of modules in series and the characteristics of each module.

Regarding the mathematical description of the evacuated tube collectors the only difference in the equations is in the IAM i.e. this type of collectors has biaxial Incidence Angle Modifiers.

The transversal incidence angle is measured in a plane that is perpendicular to both the collector aperture and the longitudinal plane. The corresponding IAM is referred to as the transversal IAM, or azimuthal modifier.

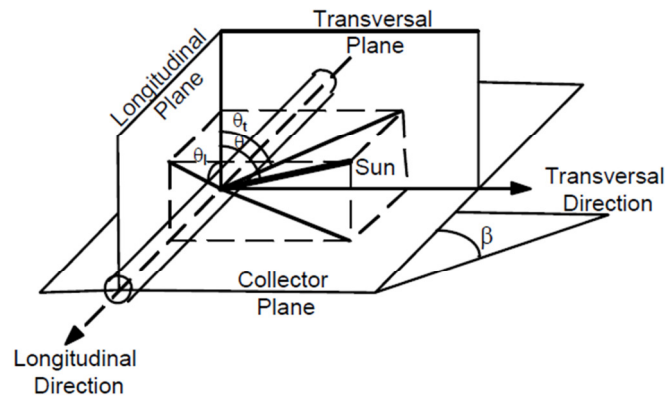


Figure 19. Transversal and longitudinal directions

The collector tube represented in Figure 19 is in the most common orientation, along a North-South axis (assuming the collector faces due South). If the collector was tested in a different configuration or if it is mounted with the tubes along an East-West axis, the IAM data obtained from a collector test may have to be adapted (by switching the longitudinal and transversal directions). In TRNSYS, "longitudinal" and "transversal" always refer to the plane of the collector and the sun as described here below, not to the tubes.

In most cases, collector test reports provide the transversal IAM for different transversal incidence angle values (and longitudinal angle = 0) and longitudinal IAM for different longitudinal incident angles (and transversal angle = 0). The data file requires the IAM for non-zero longitudinal and transversal angles.

3.2.2 Thermal energy storage model

Thermal energy storage is needed if a solar heating system is to provide heat overnight or during cloudy periods of the day. A variety of materials can be used for heat storage and the desirable characteristics are the following: easy to transfer heat from the heated fluid to the storage material; readily recoverable and supplied to the heating system; subject to little internal losses or losses to the environment; inexpensive; requiring minimal floor area or volume.

As is generally well known, offsets and intermittence make achieving the potential of solar technologies relatively complex. The bulk of energy production occurs at midday, if the sky is clear; and during summer. Meanwhile, consumption is higher during winter, especially at morning and night when space heating loads tend to be at their peak and occupants use more hot water. The diurnal offset is relatively easy to compensate for with water tanks (buffers) and other short term

storage methods like the use of the building's thermal mass. At the seasonal scale however, solutions are more complex and expensive.

Seasonal storage systems are much larger than short-term ones. Braun [36] evaluated that storage capacities per unit of collector area must be two to three orders of magnitude (100–1000 times) larger for seasonal storage than for overnight storage. Nevertheless, Fisch et al. reported investment costs per square meter of solar collector for large scale solar plants only twice as high for systems with seasonal storage than for systems with short-term storage. According to Braun et al., significant reductions in solar collector requirements for heating could be achieved by using seasonal storage at northern latitudes, where seasonal variations are large, and in cold climates, where DHW loads are much smaller than space heating loads. Since solar collectors tend to be expensive, there is definitely potential in developing more economical storage systems in order to obtain higher solar fractions for these heating tasks.

In the analyzed system for the storage tanks is used the Type 60c from the TRNSYS library which represents a stratified fluid storage tank with internal heaters and internal heat exchangers.

Water tank may operate with significant degrees of stratification, that is with the top of the tank hotter than the bottom. Many stratified tank models have been developed. They fall into either of two categories. In the first the multimode approach a tank is modeled as divided into N nodes (sections) with energy balances written for each section of the tank. The result is set of N differential equations that can be solved for temperatures of N nodes as function of time. In the second, the plug flow approach segments of liquid at various temperatures are assumed to move through the tank in plug flow and the models are essentially bookkeeping methods to keep track of the size temperature and position of the segments.

The used tank component it is modeled by assuming that the tank consists of N ($N \leq 100$) fully-mixed equal volume segments, as shown in

Figure 20

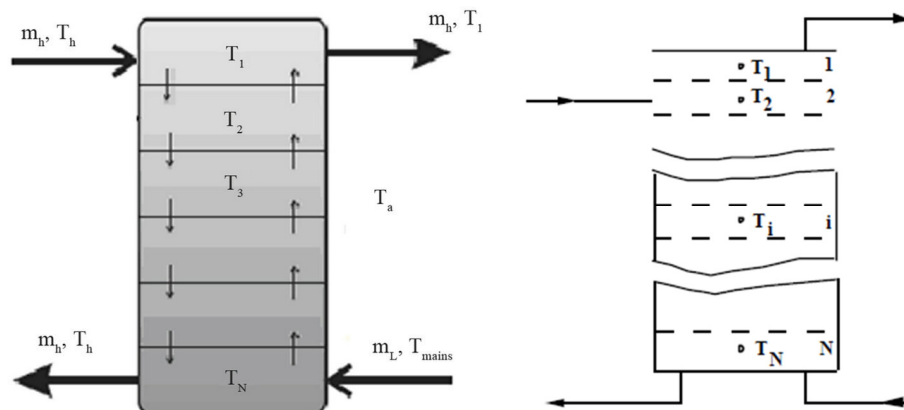


Figure 20. Stratified Fluid Storage Tank

Chapter 3. Numerical modeling of solar thermal system

The tank component locations are entered as heights, measured from the floor up, rather than node numbers. These components include: inlet and outlet flows, auxiliary heaters, thermostats, and heat exchangers. In the model there are two inlet modes available, one where the inlet height is variable i.e. the flow stream enters the node with the closes temperature. With sufficient nodes, this permits a maximum degree of stratification. The second mode the flows inlets are predefined by the user i.e. this mode is used in the analyzed model of this work. The temperature inversions that will occur during the simulation are eliminated by mixing of the appropriate adjacent nodes. The number of tank nodes is defined by the user and the tank is automatically divided by the program.

In this model are included two electric resistance heaters for which can be defined position in the tank and thermostat temperature limit. The heater can operate in two modes. Mode 1 allows the bottom heating element to be enabled only when the top element is satisfied. In this mode it is impossible the both heaters to be on simultaneously. It is usually used in the DHW systems. Mode 2 allows the opposite from mode 1 i.e. the both heaters can be on in same time. In the heaters control it is assumed dead band, The heater is enabled if the temperature of the node containing the thermostat is less than $(T_{set} - \Delta T_{db})$ or if it was on for the previous time step and the thermostat temperature is less than T_{set} .

Regarding the tank insulation tank may not be uniformly insulated. Also A pressure relief valve has been added to the storage tank to account for boiling effects. The user must specify the boiling temperature of the fluid; venting will release sufficient energy to keep the tank at the boiling temperature.

This Type 60c allows to be modeled three internal heat exchangers. There can be specified the dimensions of the heat exchangers, as well as the temperature and flow rate of the inside fluid. The inside fluid can be water, water/propylene glycol mixture or water/ethylene glycol mixture. Two wall conductivity parameters are used: one for the conductivity of the heat exchanger material itself, and one for the conductivity of the heat exchanger wall, which allows for contact resistance.

An energy balance about the i_{th} tank segment is presented on Figure 21

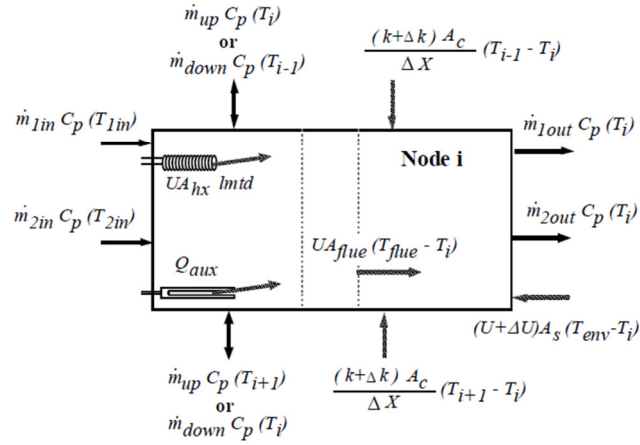


Figure 21. Graphical representation of energy flows into a node [37]

If all of the energy flows are combined in one equation, then the temperature for the temperature of node i is expressed as:

$$\begin{aligned}
 (M_i C_p) \frac{dT_i}{dt} = & \frac{(k + \Delta k) A_{c,i}}{\Delta x_{i+1 \rightarrow i}} (T_{i+1} - T_i) + \frac{(k + \Delta k) A_{c,i}}{\Delta x_{i+1 \rightarrow i}} (T_{i-1} - T_i) + (U_{\text{tank}} + \Delta U_i) A_{s,i} (T_{\text{enc}} - T_i) \\
 & UA_{\text{flue},i} (T_{\text{flue}} - T_i) + \dot{m}_{\text{down}} C_p (T_{i-1}) - \dot{m}_{\text{up}} C_p (T_{i-1}) - \dot{m}_{\text{down}} C_p (T_i) - \dot{m}_{\text{up}} C_p (T_{i+1}) + \gamma_{\text{hr1}} \dot{Q}_{\text{aux1}} \\
 & \gamma_{\text{hr2}} \dot{Q}_{\text{aux2}} + UA_{\text{hx1}} (lmt_{d1}) + UA_{\text{hx2}} (lmt_{d2}) + UA_{\text{hx3}} (lmt_{d3}) + m_{1in} C_p T_{1in} - m_{1out} C_p T_i + \\
 & + \dot{m}_{2in} T_{2in} - \dot{m}_{2out} C_p T_i
 \end{aligned} \quad (25)$$

Where the γ_{hr1} is the heater control signal. The temperatures of each of the N tank segments are determined by the integration of their time derivatives expressed in the above equation. At the end of each time step, temperature inversions are eliminated by mixing appropriate adjacent nodes.

3.2.3 Auxiliary heater

Practically sized solar system requires auxiliary heating to supply the portion of the heating load that the solar system cannot supply. System controls are commonly designed to use solar energy for heating and to rely on the auxiliary heating system whenever solar energy is not available and storage has been depleted. Even if the control strategy included provisions to share the load between the solar and auxiliary heating system during delivery, there is no assurance that an appropriate share of solar energy would always be available. The auxiliary heater must therefore be full capable of delivering heat at a rate sufficient to maintain comfort conditions during the coldest days.

In the simulation for the additional heating the fluid entering the absorption chiller or building heating system it is used model of proportionally controlled fluid heater. For the control is used external proportional control (an input signal between 0 and 1) is in effect as long as a fluid set

point temperature is not exceeded, so If the set point is exceeded, the proportional control is internally modified to limit the fluid outlet temperature

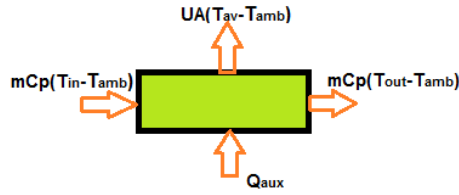


Figure 22. Energy balance for the auxiliary heater model

The outlet temperature when the heater is off from the energy balance equation can be calculated the outlet temperature:

$$T_{out} = \frac{mC_p T_{in} - UA \frac{T_{in}}{2} + UA T_{amb}}{\dot{m} C_p + \frac{UA}{2}} \quad (26)$$

This model also calculates the heater losses to the environment with the following equation:

$$\dot{Q}_{loss} = UA \left(\frac{T_{out} - T_{in}}{2} - T_{amb} \right) \quad (27)$$

$$\dot{Q}_{fluid} = \dot{m} C_p (T_{out} - T_{in}) \quad (28)$$

With the heater on and fluid flowing through the device the outlet temperature can be calculated

$$T_{out} = \frac{mC_p T_{in} - UA \frac{T_{in}}{2} + UA T_{amb} + \gamma_{htr} \eta_{htr} CAP_{htr}}{\dot{m} C_p + \frac{UA}{2}} \quad (29)$$

Where γ_{htr} is the heater control signal having a value between 0 and 1, and η_{htr} is the heater efficiency. The auxiliary energy imparted to the fluid by the heating element is given by equation

$$\dot{Q}_{aux} = \frac{\dot{m} C_p (T_{out} - T_{in}) - UA (T_{avg} - T_{amb})}{\eta_{htr}} \quad (30)$$

3.2.4 Controller model - Differential controller

The basic control strategy for space and water heating solar system is to maximize electrical energy collection and utilization and to minimize electrical energy use for collection and distribution. While a theoretically optimum strategy for each system with a specific load in a particular climate can be prescribed (Winn, Jonson and Moore 1974), practical control devices are generally not available to implement the optimum strategy for each system. Fortunately, even a simple controller performs reasonably well without inflicting severe penalties on the system. The

simplest controller is a differential thermostat that starts or stops an electric motor that operates a pump or valve.

The used differential controller in the simulations is the component Type 2 from the TRNSYS library. This controller generates a control function γ_0 that can have values of 0 or 1. The value of γ_0 is chosen as a function of the difference between upper and lower temperatures, T_H and T_L , compared with two dead band temperature differences, ΔT_H and ΔT_L . the new value of γ_0 is dependent on whether $\gamma_i = 0$ or 1. The controller is normally used with γ_0 connected to γ_i giving a hysteresis effect. For safety considerations, a high limit cut-out is included with the TYPE 2 controller. Regardless of the dead band conditions, the control function will be set to zero if the high limit condition is exceeded.

Mathematically, the control function is expressed as follows:

If the controller was previously on

$$\text{If } \gamma_i = 1 \text{ and } \Delta T_L \leq (T_H - T_L), \gamma_o = 1 \quad (31)$$

$$\text{If } \gamma_i = 1 \text{ and } \Delta T_L > (T_H - T_L), \gamma_o = 0 \quad (32)$$

If the controller was previously off

$$\text{If } \gamma_i = 0 \text{ and } \Delta T_H \leq (T_H - T_L), \gamma_o = 1 \quad (33)$$

$$\text{If } \gamma_i = 0 \text{ and } \Delta T_H > (T_H - T_L), \gamma_o = 0 \quad (34)$$

However, the control function is set to zero, regardless of the upper and lower dead band conditions, if $T_{IN} > T_{MAX}$. This situation is often encountered in domestic hot water systems where the pump is not allowed to run if the tank temperature is above some prescribed limit.

3.2.5 Absorption chiller model

Steady-state absorption chiller models are based on the internal mass and energy balances in all components, which depend on the solution pump flow rate and on the heat transfer between external and internal temperature levels. Several problems are associated with a single characteristic equation, which calculates all internal enthalpies only for the design conditions: if bubble pumps are used, the solution flow rate strongly depends on the generator temperature. Also if the external temperature levels differ significantly from design conditions, the internal temperature levels change and consequently the enthalpies. Therefore, in the current work, the internal energy balances were solved for each simulation time step as a function of the external entrance temperatures, so that changing mass flow rates can be considered in the model.

In TRNSYS library for the absorption chiller there is the model Type107 which uses a catalog data lookup approach to predict the performance of a single effect, hot water fired absorption chiller. the calculation routine has been developed as Type107 in TRNSYS-15 during the work for

Chapter 3. Numerical modeling of solar thermal system

IEA TASK25 to improve simulations with absorption chillers in solar assisted cooling systems. In this design, the heat required to desorb the refrigerant is provided by a stream of hot water. Since this component rely on catalog data, the performance of the machine can be predicted and interpolated within the range of available data but cannot be extrapolated beyond the range. Because of the catalog data lookup approach, Type107 is not applicable over every range of inlet conditions. In this component in the software catalog data are given but the lowest driving temperature is 108.89 which is unrealistically high and would produce reflect on the end results. Thus it was used the model Type 177 which is improvement from the Type 107 and it was develop in “Technische Universität Berlin” by the Jan Albers.

The part load performance of thermally driven heat pumps or chillers is dominated by the external driving temperatures of hot, chilled and cooling water. Thus heat transfer calculations are done for constant flow rates, normally. Under these conditions the transmission of the heat exchangers (i.e. their UA-values) can be assumed as constant and the characteristic equation method can be applied easily to describe the part load behavior of the heat pump taking varying external temperatures into account. With varying flow rates the assumption of constant heat transmission is not valid anymore. Nevertheless, heat transmission ratios can be derived, which implement the heat transmission variation into the method of characteristic equations. In addition, the temperature difference ratio z of logarithmic to arithmetic mean temperature differences is influenced by variable flow rates. Together with other well-known dimensionless numbers, such as the dimensionless heat transmission (NTU) or the ratio of heat capacity flow rates, they are implemented into an extended method of characteristic equations, which accounts for variable heat transmissions and loss parameters.

There are four Modes in the Type 177, and each of them is describe as follows:

- Mode 1 Standard mode which uses user supplied characteristic parameters. For some absorption chillers the parameters are given in a table.
- Special mode for the (old) Yazaki WFC-10 with a thermosyphon desorber. The (new) Yazaki WFC-10 SE cannot be simulated with this mode.
- Special mode for absorption chiller with variable solution flow rate
- Physical mode which uses user supplied values for the heat transmissions (i.e. UA-values) of all main heat exchangers (including the solution heat exchanger) and a fixed solution flow rate

The internal temperatures of the four heat exchangers (Desorber, Absorber, Condenser, Evaporator) can be combined by using Dühring’s rule for the saturation temperatures of sorbens and sorbate at condenser and evaporator pressure.

$$(T_D - T_A) = (T_C - T_E) B \quad (35)$$

Assuming equal heat fluxes inside and outside the ab-or adsorption chiller (i.e. adiabatic heat exchangers are assumed) the internal saturation temperatures T_X can be expressed as a function of the mean external temperatures t_X .

$$T_D = t_D - Q_E K_D / Y_D - Q_{D,x} / Y_D \quad (36)$$

$$T_E = t_E - Q_E K_E / Y_E \quad (37)$$

$$T_A = t_A - Q_E K_A / Y_A - Q_{A,x} / Y_A \quad (38)$$

$$T_C = t_C - Q_E K_C / Y_C \quad (39)$$

The coefficients K_X in equation (32-35) hold for the internal specific enthalpy differences at the corresponding heat exchangers related to the specific enthalpy difference at the evaporator. Y_X are the heat transmissions of the heat exchangers ($Y_X = U_X \cdot A_X$).

Defining a characteristic temperature difference ($\Delta\Delta t$):

$$\Delta\Delta t := (t_D - t_A) - (t_C - t_E) \cdot B \quad (40)$$

The characteristic equation for the cooling capacity:

$$Q_E = s_E \cdot \Delta\Delta t - s_E \cdot \Delta\Delta t_{\min E} \quad (41)$$

If the slope (s_E – which contains the enthalpy and heat transfer coefficients) and axis interval ($s_E \cdot \Delta\Delta t_{\min E}$) are constant, the part load of an ab- or adsorption chiller can be expressed as a linear function of $\Delta\Delta t$ only. It has been shown that under steady state conditions and constant solution flow rates or constant cycle times the assumption of constant parameters is permitted at many times.

It will be presented the mathematical reference for the Mode 3 of this component since only that was used in the simulations.

In mode 3 a modification of the extended method of characteristic equations described in [38] is used. it is based on fitted characteristic parameters from measurements or manufactures data sheets. The external flow rates of hot, chilled and cooling water have to be fixed at their rated values during the simulation. The solution flow rate may vary if the parameters are given for variable solution flow rates also. Two Pseudo-Dühring-Parameters (B^*_{E1} , B^*_{E2}) are used to define a characteristic temperature difference.

$$\Delta\Delta t^*_E = t_{Di} + (1 + B^*_{E1}) \cdot t_{ACi} + B^*_{E2} \cdot t_{Ei} \quad (42)$$

The characteristic equation for the cooling capacity

$$Q_E = q_{E2} \cdot (\Delta\Delta t^*_E)^2 + q_{E1} \cdot \Delta\Delta t^*_E + q_{E0} \quad (43)$$

can be used either in quadratic or linear form. For the latter case parameter q_{E2} is set to zero. For the driving heat the following equations apply:

$$\Delta\Delta t^*_D = t_{Di} + (1 + B^*_{D1}) \cdot t_{ACi} + B^*_{D2} \cdot t_{Ei} \quad (44)$$

$$Q_D = q_{D2} \cdot (\Delta\Delta t^*_D)^2 + q_{D1} \cdot \Delta\Delta t^*_D + q_{D0} \quad (45)$$

Basically the Pseudo-Dühring-Parameters in Equation (38) and (39) are different. Nevertheless mean values can be used (carefully) in both equations to simplify the fit procedure (e.g. of manufacturers data). The parameter description of the model are given in Appendix D.

$$B^*_1 = (B^*_{E1} + B^*_{D1}) / 2 \quad (46)$$

$$B^*_2 = (B^*_{E2} + B^*_{D2}) / 2 \quad (47)$$

3.2.6 Developing building numerical model

Energy requirements for space heating or service water heating can be calculated from basic principles of energy conservation. One of the most significant barriers in precise determining the buildings energy consumption is the lack of knowledge about the factors determining the energy use. Building energy consumption is mainly influenced by six factors: (1) climate, (2) building envelope, (3) building services and energy systems, (4) building operation and maintenance, (5) occupant activities and behavior and (6) indoor environmental quality provided. The latter three factors, related to human behavior, can have an influence as great as or greater than the former three. The user related aspects and behavior effects can be seen from the large spread in energy use for similar or identical buildings, but a distinction between the building-related and the user-related energy consumption cannot be established.

For the building simulation is used the Type 56 from the TRNSYS library. Type 56 describes a building with multiple thermal zones, i.e. rooms. The model uses data from wall and window materials and thicknesses. Each room has a homogenous temperature, and radiation heat between the rooms is based on the room area. Heat addition from solar direct and diffuse radiation is calculated for each room depending on window and heat transfer properties. Type 56 models the thermal behavior of a building divided into different thermal zones. In order to use this type, a separate pre-processing program must first be executed. The TRNBuild program reads in and processes a file containing the building description and generates two files (described later) that will be used by the TYPE 56 component during a TRNSYS simulation.

The level of detail of this type is compliant with the requirements of ANSI/ASHARE standard 140-2001. The level of detail of Type 56 also meets the general technical requirements of the European Directive on the Energy Performance of Buildings. During the last two decades TRNSYS is widely

Chapter 3. Numerical modeling of solar thermal system

employed in building energy simulations [39-41]. There exist systematic studies comparing the performance of this software against experimental results, as well as comparing the results from TRNSYS to other industry standards for building energy simulation.

In modeling the air conditioning equipment in the Type 56 model, the "energy rate" method can be used as a simplified model. The temperatures are set in advance for heating and cooling, set points for humidity control, maximum cooling and heating rates. These specifications can be different for each zone of the building. If it is required a more detailed model of the heating and cooling equipment, a "temperature level" approach is required. In this case, separate components are required to model the heating and/or cooling equipment. The outputs from the TYPE 56 zones are used as inputs to the equipment models, which in turn produce heating and cooling inputs to the TYPE 56 zones.

Type 56 needs a great amount of building data to calculate the thermal behavior of the building, these include geometry data, wall construction data, windows data,...etc. In the project initialization firstly are entered some general information about the project, like orientations of walls and windows required by the described building. Next step is defining zones in the building with the boundary surfaces (walls) materials, windows types thus defining the heat transfer coefficients. additional to weather data information such as: Radiation, ambient temperature, humidity,...etc. furthermore, it needs information such as SCHEDULE which may define the gain from the occupants during the day with intervals representing the time being occupant from the building owners

Short mathematical description of Type 56

All defined surfaces have thermal air nodes for which the calculations are performed. The system boundary for this energy balance includes the inside surface node of all surfaces of the zone. This balance deals with radiative and convective heat flow into and out of the airnode. The convective heat balance is determined by the equation:

$$Q_i = Q_{surf,i} + Q_{inf,i} + Q_{vent} + Q_{g,c,i} + Q_{cplg,i} \quad (48)$$

where:

$Q_{surf,i}$ convective heat gain from inner surface of zone (because of temperature difference between airnode temperature and surface temperature)

$Q_{inf,i}$ infiltration gains (airflow from outside only)

$Q_{vent,i}$ ventilation gains ((air flow from a user-defined source, like an HVAC system)

$Q_{g,c,i}$ internal convective gains (by people, equipment, illumination, radiators, etc.)

$Q_{cplg,i}$ gains due to (convective) air flow from airnode I or boundary condition, where

$$Q_{cplg,i} = V \cdot \rho \cdot c_p \cdot (T_{zone,i} - T_{air,i})$$

Regarding the radiative heat fluxes to the airnode graphical presentation is given on Figure 23

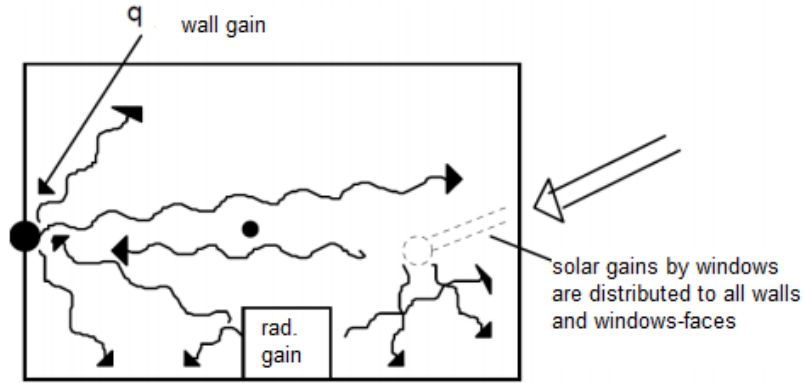


Figure 23. Radiative energy flows considering one wall

This balance is determined by the equation:

$$Q_{r,wi} = Q_{g,r,i,wi} + Q_{sol,wi} + Q_{long,,wi} + Q_{wall-gain} \quad (49)$$

Where:

$Q_{r,wi}$ radiative gains for the wall surface temperature node,

$Q_{g,r,i,wi}$ radiative airnode internal gains received by wall,

$Q_{sol,wi}$ the solar gains through zone windows received by walls,

$Q_{long,l}$ the long-wave radiation exchange between this wall and all other walls and windows ($\epsilon_i = 1$)

$Q_{wall-gain}$ the user-specified heat flow to the wall or window surface.

The walls are modeled according to the transfer function relationships of Mitalas and Arseneault defined from surface to surface (from outer to inner surface), which consider the wall as a black box. For any wall, the heat conduction at the surfaces are:

$$q_{s,i} = \sum_{k=0}^{n_{bs}} b_s^k T_{s,o}^k - \sum_{k=0}^{n_{cs}} c_s^k T_{s,i}^k - \sum_{k=0}^{n_{bs}} d_s^k q_{s,i} \quad (50)$$

$$q_{s,o} = \sum_{k=0}^{n_{as}} a_s^k T_{s,o}^k - \sum_{k=0}^{n_{cs}} b_s^k T_{s,i}^k - \sum_{k=0}^{n_{bs}} d_s^k q_{s,o} \quad (51)$$

These time series equations in terms of surface temperatures and heat fluxes are evaluated at equal time intervals. The superscript k refers to the term in the time series, and it specified by the user within the TRNBUILD description. The coefficients of the time series (a's, b's, c's, and d's) are determined within TRNBUILD program using the z-transfer function routines of literature.

Chapter 3. Numerical modeling of solar thermal system

A window is thermally considered as an external wall with no thermal mass, partially transparent to solar, but opaque to long-wave internal gains. In the energy balance calculation of the TYPE 56, the window is described as a 2-node model shown in Figure 24. Equation 50 is valid for

$$\begin{aligned} a_s^o &= b_s^o = c_s^o = d_s^o = U_{g,s} & \text{for } k > 0 \\ a_s^k &= b_s^k = c_s^k = d_s^k = 0 \end{aligned}$$

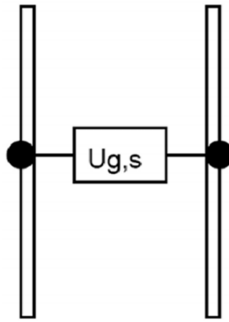


Figure 24. Two-node window model used in the TYPE56 energy balance equation

For the star network approach a zone is restricted to a single airnode. The long-wave radiation exchange between the surfaces within the airnode and the convective heat flux from the inside surfaces to the airnode air are approximated using the star network. This method uses an artificial temperature node (T_{star}) to consider the parallel energy flow from a wall surface by convection to the air node and by radiation to other wall and window elements.

A detailed window model has been incorporated into the TYPE 56 component using output data from the WINDOW 4.1 program developed by Lawrence Berkeley Laboratory, USA [42]. This window model calculates transmission, reflection and absorption of solar radiation in detail for windows with up to six panes. External and internal shading devices and an edge correction for different glazing spacer types are considered. Each glazing absorbs and reflects a part of the incoming solar radiation depending on the glazing material and the incidence angle. In the program WINDOW 4.1, the detailed calculation of reflection between the individual panes and the absorption and transmission of each pane is performed hemispherically for diffuse radiation and in steps of 10° incidence angle for direct solar radiation. Together with the thermal properties of the gas fillings and the conductivity and emissivity of the glazings, the optical data for the window is written to an ASCII file by the WINDOW 4.1 program. This output file has a standard format, which makes the results available for TRNSYS.

The optimum capacity of an energy storage system depends on the expected time dependence of solar availability, the nature of loads to be expected on the processes, the degree of reliability needed for the processes, the manner in which auxiliary energy is supplied and an economic

analysis that determines how much of the annual load should be carried by solar and how much by the auxiliary energy source.

The two principal materials used for storage are water for liquid-based systems and rock pebbles for air-based systems. Water has a high heat capacity and rocks have one-fifth as much (one third per unit volume) and both are inexpensive. The thermal energy storage (TES) system is one of the most appropriate methods of correcting the mismatch that occurs between the supply and demand of energy. Heat can be stored in sensible/latent form, and by thermo chemical techniques. In sensible heat storage (SHS), thermal energy is stored by raising the temperature of a solid or liquid. SHS systems utilize the heat capacity and change in temperature of the material during the process of charging and discharging. SHS characterized by temperature variation is a simpler technique, but occupies a larger volume.

The latent heat storage is based on heat absorption or release when a phase change material (PCM) undergoes a phase change. The latent heat storage by PCM in comparison with SHS, possesses a greater density of stored energy and operates in a narrower operational temperature range. Zalba have reviewed various aspects of latent heat storage systems, such as PCMs heat transfer and applications. PCMs are advantageous for the dynamic and static storage of thermal energy as they absorb and release large amounts of energy at specific temperature [34].

Storage mechanisms have been researched quite intensively in the frame of Task 32 [13] of the EA (International Energy Agency) SHC (Solar Heating and Cooling) program. A new joint IEA project [14], involving SHC Task 42 [15] and ECES (Energy Conservation through Energy Storage), concentrates on the storage materials involved.

3.3 Modeling solar thermal assisted air-conditioning system

Assessment of thermal performance of the solar air-conditioning system is performed through a dynamic simulation model with transient behavior implemented via thermal and mass storage terms as well as delay times. The model ie analyzed system generally consists of four main subsystems shown in Figure 25, as follows:

1. First subsitem composed of solar collectors with complete hydraulic fittings and control - differential controllers, plate heat exchangers ie this system is represented the source of thermal energy for heating or thermal enrgy for driving the cooling the absorption machine
2. Second is the subsystem for hot and cold storage which includes the storage tanks for hot / cold water that actually represents the connection between the heating system in the building ie absorpcionata cooling machine and the source of heat.

Chapter 3. Numerical modeling of solar thermal system

- The heating system introduced with heating / cooling devices, hydraulic armature heat exchangers and cooling absorption machine and eventually existing conventional sources of heat and / or cooling energy.

The fourth subsystem is the consumer of thermal energy ie the building . This system is represented by the thermal characteristics of the object, ie its orientation in space .

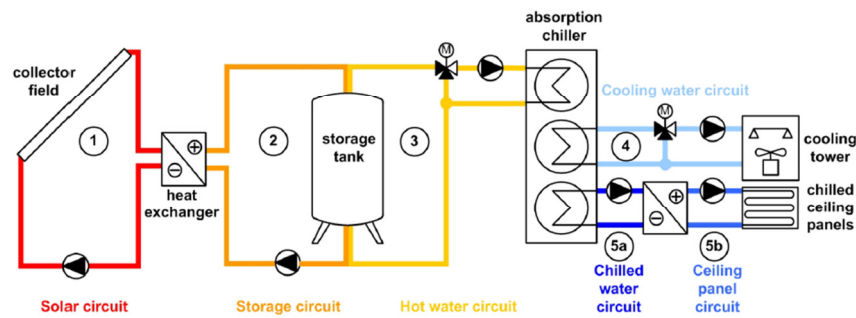


Figure 25. Subsystems definition of solar cooling system

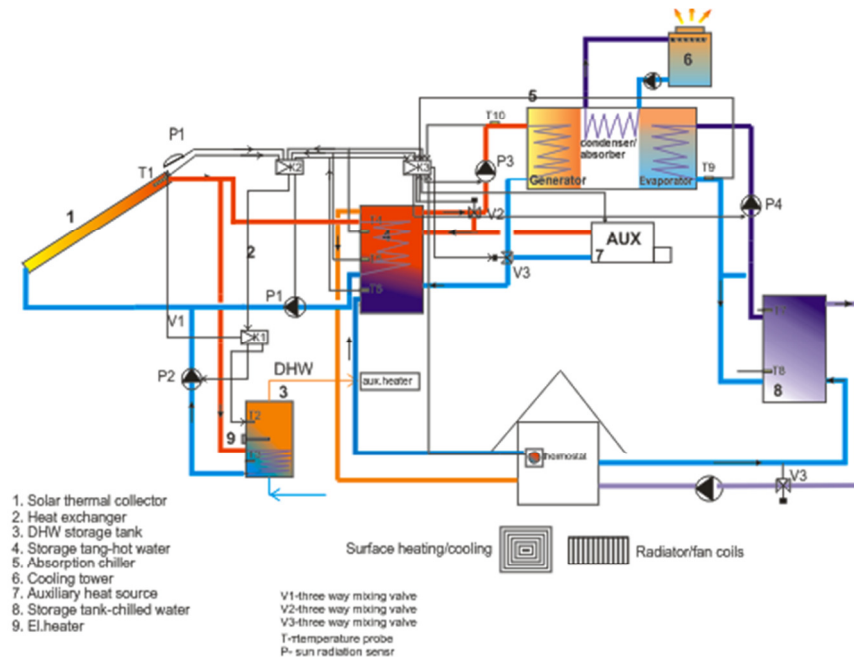


Figure 26. Functional scheme presenting inter connections between components of the system modeled in TRNSYS

The next picture shows the functional scheme according to which is made numerical modeling of the analyzed system in TRNSYS using previously described and validated components.

On Figure 26 is presented the analyzed solar assisted air-conditioning system. The main system components are: the solar collector array, two storage tanks, auxiliary heater, absorption chiller and the energy consumer i.e. the building which also incorporates the heating/cooling system components.

Chapter 3. Numerical modeling of solar thermal system

The working fluid from the solar collectors indirectly through heat exchangers is used to heat the domestic hot water in tank 3 or heat the fluid in the storage tank 4 further used as part of the heating energy in the building or part of the driving heat for the absorption chiller in summer. The circulation of the solar collectors working fluid for the storage tanks 3 and 4 is done by two separate circulating pumps P1 and P2, controlled by two differential controllers having mutual predefined control function further explained. First condition for the pumps to be switched on is the temperature difference between the collector outlet temperature and the fluid temperature in storage tank (3 or 4) to be greater than the set upper dead band. The control logic for switching between the two tanks is solved using the two controllers Type 2b (K1 and K2) one flow diverter Type 11f. The advantage has the controller K2 of the tank 4 i.e. the initial input control signal (on/off) for the controller of the DHW tank K1 is received from the controller K2 i.e. when the controller K2 is on, then the controller K1 is off.

The collector(s) thermal efficiency in the simulation is determined using the equation component from the TRNSYS library. The equation considers ratio between the useful energy gain from the all od the collectors transferred to the fluid and the total tilted radiation for the collector surface. The data for the quantity of useful energy gain and total radiation in the equation is read from the quantity integrator which integrates these values in the predefined period defined from the required value period thermal efficiency and energy i.e. daily, weekly, monthly, yearly or any other time interval.

Sub-system 1 – solar collectors

The solar collectors are connected in array where the number of serial and parallel connections is subject for further analysis in this work. As mentioned previously two collector types are used: flat plate collectors produced in Camel Solar type CS Full Plate 2.0-4 with technical characteristics given in Table 1, and the other type are the vacuum tube collectors with technical data given in Table 2.

Solar collectors parameters are varied and analyzed in order to estimate their impact on the total collected energy overall thermal efficiency and the solar fraction. Parameters analyzed in this work regarding solar collectors are:

- mass flow rate
- azimuth (orientation) of solar collectors (0° south, 90° West, -90° East one and two axis tracking, by azimuth and/or altitude)
- solar collector area – gross area of the array used in simulations 16 m^2 , 32 m^2 , 64 m^2
- slope (tilt) angle of collector installation

Chapter 3. Numerical modeling of solar thermal system

Table 1. Technical data for collector type Camel Solar Flat plate 2.0-4

Dimensions L x W x H	mm	2005 x 1005 x 85
Absorber aperture area	m ²	1.83
Absorptance, α	-	0.95
Emittance, ε	-	0.05
Transmittance	-	0.92
Conversion factor of the beam irradiance, $F'(\tau\alpha)_{en}$	-	0.795
Factor to determine the incidence angle modifier of the beam irradiance, b_0	-	0.138
Optical efficiency, η_0	-	0.791
Heat transfer coefficient a_1	W/m ² K	4.176
Temperature depending heat transfer coefficient a_2	W/m ² K ²	0.008
Incidence angle modifier diffuse radiation $K_{\theta d}$	-	0.988
Incidence angle modifier $K_{\theta} = 50^\circ$	-	0.935
Area related heat capacity c	kJ/m ² K	13.19
Volume flow rate,	l/m ² h	72
Peak power per collector unit $G=1000 \text{ W/m}^2$	W	1448



The differential controller settings are analyzed for their influence over the thermal efficiency, pump energy consumption and the solar fraction. In the controller, with the settings are considered the values for upper and lower dead band, parametrically analyzed in order to estimate their influence over system efficiency, electrical energy consumption and solar fraction. Since the storage tanks are modeled as stratified another parameter of interest is the position of the controllers probe (height) measuring the tank temperature.

All of the circulating pumps are modeled as constant flow pumps.

Second sub-system are the storage tanks as mentioned one is for DHW (3), other is for the heating system and driving the absorption chiller. The tank for DHW through all of the simulations has constant volume of 200l. The volume of storage tank 4 has been varied in the simulations in order to account for its influence on the system thermal efficiency and solar fraction. The storage volumes used in simulations are: 500l, 1000 l, 1500 l and 2000 l all of them are modeled with internal heat exchangers .

Technical data for the storage tanks used as input values in the model, like dimensions, heat exchanger data etc. are given in Appendix A

Chapter 3. Numerical modeling of solar thermal system

Another component is the auxiliary heater which adds energy to the fluid if the set temperature is not reached with the solar heat. Type 6 is used as auxiliary heater for the DHW while for the storage tank 4 is used Type 659 from the Tess library. Input parameters are the rated capacity, specific heat of the fluid and set point temperature while the heat loss to the surroundings is neglected. In most of the analyzed simulation scenarios the position of the auxiliary heater is outside of the storage tank, only one analysis is performed to assess the influence of the position of the auxiliary heater (inside or outside the storage tank) regarding the energy consumption.

The cooling energy is delivered by the absorption chiller modeled with Type 177 i.e. it is modeled LiBr/H₂O absorption chiller product of Sonenklima Suninverse 10, technical data given in Table 4. Cooling tower is modeled with component Type 510 closed circuit cooling tower, used to cool a liquid stream by evaporating water from the outside of coils containing the working fluid. The working fluid is completely isolated from the air and water in this type of system. Technical data are from cooling tower product of Baltimore Aircoil Company model details given in Annex 1.

In the last sun-system is presented the energy consumer i.e. the building. Multi zone Type 56 is used to model the thermal behavior of a building having multiple thermal zones. Within the same model are defined heating/cooling transfer devices such as underfloor heating and ventilation for the cooling part. Also for as cooling heat transfer device is used heat exchanger water-air modeled with Type 508a.

Internal (room) temperature in the building is maintained with thermostat Type 1502. The thermostat controller has commands for first stage heating at cool fluid temperatures, second stage heating at cooler fluid temperatures, and third-stage heating at even lower fluid temperatures. There is option to disable first stage heating during second stage and third stage heating, and to disable second stage heating during third stage heating.

In many heating applications, a desired fluid temperature may depend on the time of day or the day of the week. This variation of the heating set point temperatures are modeled here using an optional set back control function and a setback temperature difference.

Chapter 4

4. System and Components validation

4.1 Solar circuit component validation

In this part are presented and compared the results between the measurements of preassembled experimental solar collector system presented on

Figure 27. Scheme of the experimental installation and the results from the same system are modeled and simulated in TRNSYS. The validation is performed for the solar collector, storage tank and differential controller components.

The system has one flat plate solar collector connected with the internal heat exchanger of the storage tank. Control is provided by differential controller which is set to turn the circulation pump on when the temperature difference between the collector outlet temperature and the tank temperature is greater than five. The water from the storage tank is not discharged and the electric heater is turned off during the measurements. The fluid (water) flow rate is set to 7,5 lit/min.

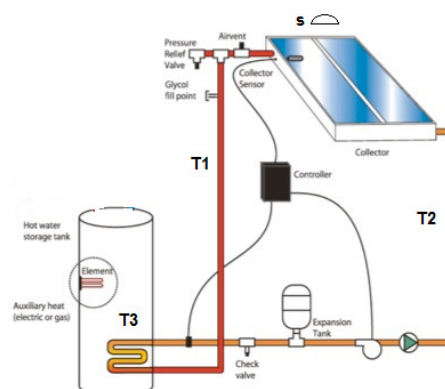


Figure 27. Scheme of the experimental installation

The measurements are made on an hour interval for the fluid inlet T1 and outlet T2 temperatures from the solar collector, tank fluid temperature T3 and the solar radiation measured

Chapter 4. System and Components validation

with the pyranometer S. The experimental setup of the analysed solar thermal system is placed in Skopje, R.Macedonia northern latitude of 42° and 21.43° east longitude.

The solar collector is evacuated tubular direct flow product of Camel Solar type Vacuum CS 15 Solar KeyMark certified. It is placed under tilt angle of 45° with south orientation i.e. azimuth angle of 0° . The collector thermal performance test results made according EN 12975 are presented in Table 2

Table 2. Technical data for collector type Camel Solar Vacuum tube SC 15

Dimensions L x W x H	mm	1990 x 1180 x 158
Number of absorber tubes	-	15
Absorptance, α	-	0.92-0.96
Emissance, ε	-	0.04-0.06
Conversion factor of the beam irradiance, $F'(\tau\alpha)_{en}$	-	0.695
Factor to determine the incidence angle modifier of the beam irradiance, b_0	-	0.138
Optical efficiency, η_0	-	0.738
Heat transfer coefficient a_1	W/m^2K	1.725
Temperature depending heat transfer coefficient a_2	W/m^2K^2	0.01
Incidence angle modifier diffuse radiation $K_{\theta d}$	-	1.203
Incidence angle modifier $K_{\theta} = 50^\circ$	-	0.935
Area related heat capacity c	kJ/m^2K	58.4
Volume flow rate,	l/m^2h	72
Aperture area per collector unit	m^2	1.42
Peak power per collector unit $G=1000 W/m^2$	W	1048



The area based collector power \dot{q} was modeled according the equation:

$$\dot{q} = F'(\tau\alpha)_{en} K_{ob}(\theta_i, \theta_i) G_b + F'(\tau\alpha)_{en} K_{od}(\theta) G_d - c_1(T_m - T_a) - c_2(T_m - T_a)^2 - c_5 \frac{dT_m}{dt} \quad (52)$$

With

$$K_{ob}(\theta_i, \theta_i) = K_{ob}(\theta_i, 0) \cdot K_{ob}(0, \theta_i)$$

Where

G_b, G_d	W/m^2	beam and diffuse solar irradiance
c_1	W/m^2K	heat transfer coefficient
c_2	W/m^2K	temperature depending heat transfer coefficient
c_5	W/m^2K	temperature depending heat transfer coefficient

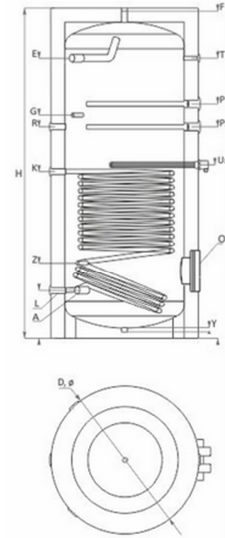
Chapter 4. System and Components validation

T_m	K	mean fluid temperature inlet/outlet solar collector
T_a	°C	ambient temperature where the collector is installed

Storage tank technical specification is presented in the Table 3

Table 3. Storage tank technical details

Capacity	l	150
Height	H, mm	1210
Diameter	D, mm	560
Insulation, rigid PU	mm	50
Coil capacity	l	4.56
Heat exchanger surface	m ²	0.74
Prolonged power according	kW	25
DIN 4708 80/60/45	m ³ /h	0.61
NL-power coefficient at 60°C	-	2.5
Coil outlet	L, mm	202
Cold water inlet	A, mm	202
Sensor sleeve for thermostat	G, mm	822
Coil inlet	K, mm	592
Hot water outlet	E, mm	868



The TRNSYS model components with their interconnections schematically are given on

Figure 28.

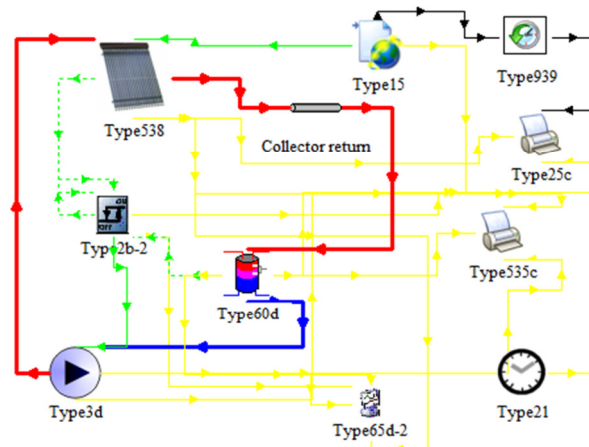


Figure 28. TRNSYS model for the experimental installation of solar thermal collector system

In the TRNSYS model for the solar collector model is used the collector Type 538 from the Tess library modeled with the technical data given in Table 2. The storage tank is modeled with the Type 60d including the internal heat exchanger for which are supplied data from Table 3. Type 2b-2 is used for the differential controller with upper dead band of 5 and lower dead band 2, the high limit cut-off temperature is set to 100 °C. Between the solar collector and storage tank is connected pipe Type 31 modeled with internal diameter 0.0025 m, length of 10 m and loss coefficient of 0,3 W/m²K to account for the heat losses. The pipe Type 31 beside to account for the

Chapter 4. System and Components validation

heat losses in the pipes also is used in order to increase the thermal capacity of the system and thus increase the simulation stability. Also for the circulating pump is used the Type 3d with mass flow rate 450 kg/h i.e. 7,5 l/min same as in the experimental setup.

Measurements are performed starting from date 18.09.2013 until 28.03.2014 and in parallel are measured two systems with same capacity storage tank of 150l but different type of collectors i.e. flat plate and vacuum tube solar collectors. In the validation process are used the data for the vacuum tube collector and the results from only one day period (18.09.2014) with collection time interval ranging between 20min and 45min interval, starting from 10:40 until 16:05 h.

There is possibility in the TRNSYS software to be inputted specific measured values of the system as the solar radiation but in this case there was no possibility since the measured values for the sun radiation did not provide data for the total the beam and diffuse components which are required by the model. Thus, in the simulations for the solar radiation data was used the weather component from the TRNSYS library the Type 15 which supplies input data in the solar collector numerical model: ambient temperature, beam, sky and diffuse radiation for the tilted surface (calculated regarding the tilt angle of the collector), solar zenith and solar azimuth angle. The weather data in this model are generated in a so called referent year which contains data based on stochastic methods, interpolations where the data for temperatures, wind speed are for the period between 1961 – 2009, while for the sun radiation are for the period 1985 – 2005. In determining this kind of reference year, the typical range of meteorological measurements at hourly intervals are required for a period of several years, a process which results in a complete picture of the climatic conditions that govern the examined area. But this does not mean simply determining the average of all years, because it does not adequately predict the changes that may occur, but is selected representative month for this area. The procedure is as follows: for each month is determined average solar radiation over the entire period of measurement and individual monthly average radiation for each year within the period considered. Monthly value to the average radiation closest or equal to the global monthly average over the period of measurement is chosen as a representative month for typical reference year. This process is repeated for each month of the year where then grouped the selected month and provides hourly average values over the year.

As mentioned previously measurements are performed for the inlet/outlet fluid temperature from the solar collector, inside storage tank temperature and the total solar irradiation.

In the following graphs are presented the result from the comparison between the measurements and simulation data:

Chapter 4. System and Components validation

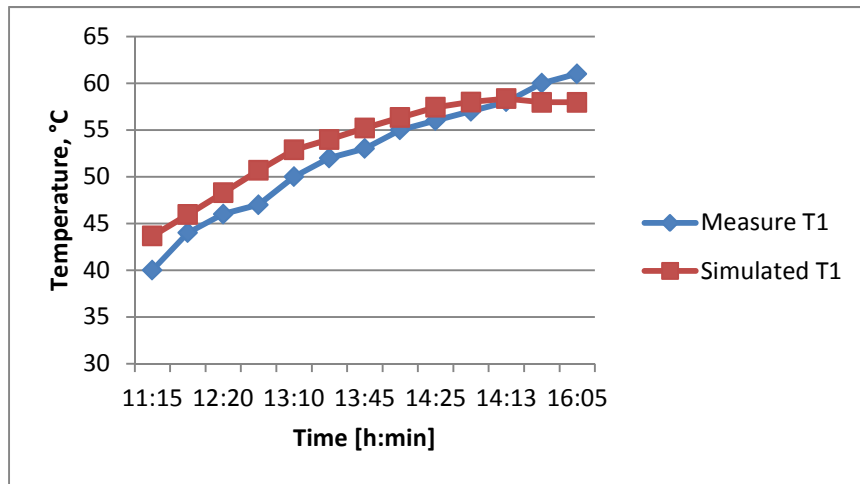


Figure 29. Measured and simulated temperatures for the collector inlet

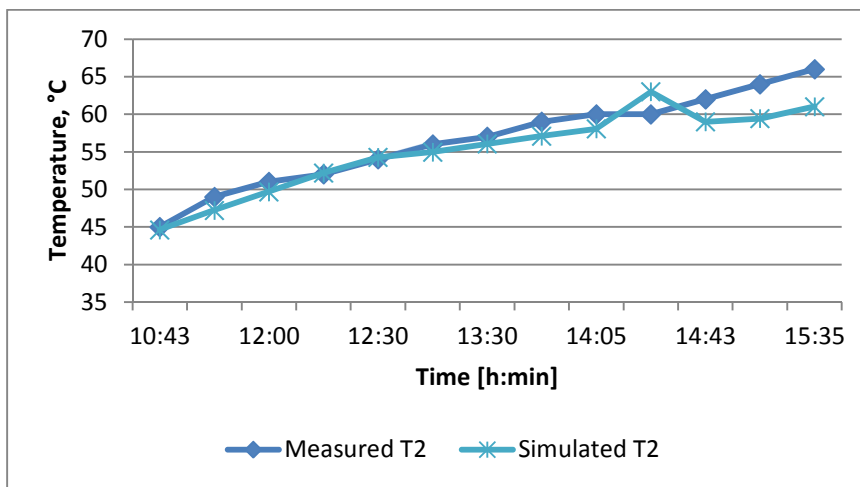


Figure 30. Measured and simulated temperatures at the collector outlet

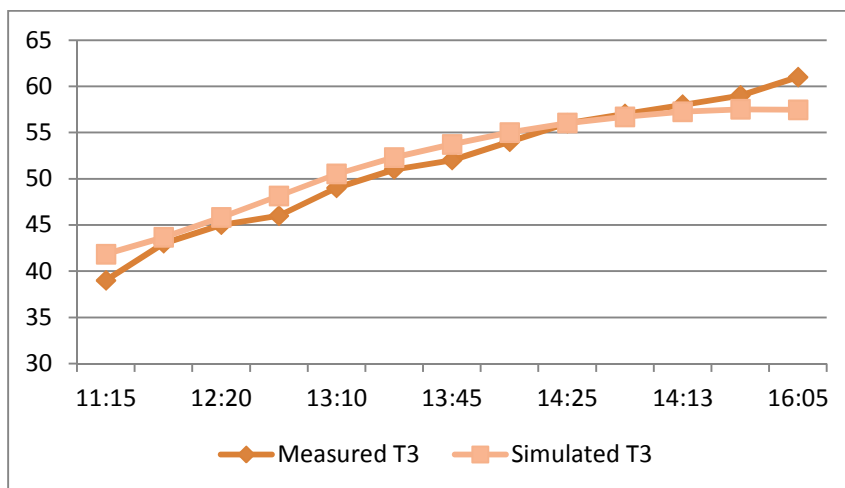


Figure 31. Measured and simulated temperatures inside storage tank

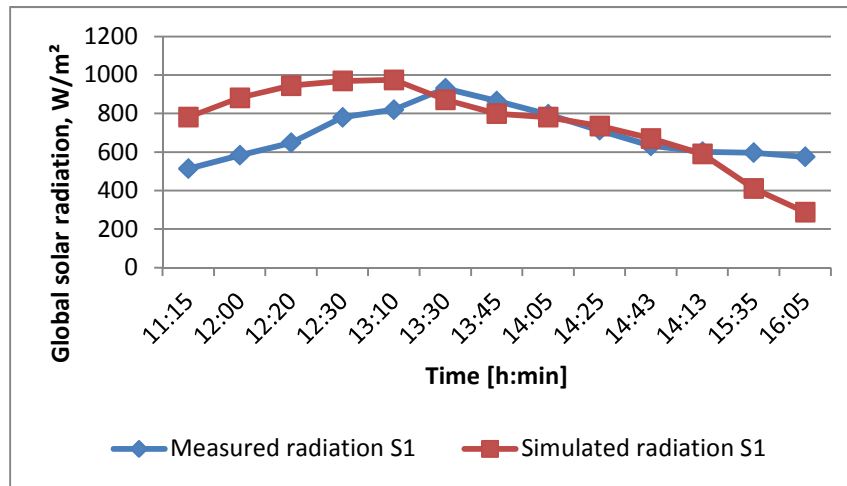


Figure 32. Hourly measured and simulated solar radiation for the specific day

From the above presented data with the diagrams can be concluded that there is acceptable match between the measured and simulated results. The discrepancies that appear between the temperatures of the experimental and simulated results are expected since firstly the solar radiations are measured and simulated which differences clearly appear on Figure 32.

. Another influencing factor are the uncertainty of the measurements error and last but not the least we should consider the transition nature of the solar thermal systems.

The resulting simulations reveal the individual thermal behavior of the solar collector, storage tank, differential controller and circulating pump as well as their assembled thermal behavior. These results were very close to their corresponding experimental data and this fact validates these models for future application in the heating/cooling system.

4.2 Absorption chiller validation

Validation for the absorption chiller is made for the TRNSYS component Type 177, further in detail described.. This component type offers four numerical modes of absorption chiller, and in this simulation is used the mode “a” i.e. Type177a which is standard mode using user supplied characteristic parameters. Since in this thesis will be analyzed solar air-conditioning for residential buildings, in Table 4 are given the technical data for several small absorption chillers. From the presented absorption chillers for the need of the simulation it is selected the absorption chiller H₂O/LiBr produced by Sonnenklima type Suninverse 10.

Numerical modeling for the selected chiller Suninverse is performed by providing the characteristic parameters in the TRNSYS Type 177a. The required characteristic parameters for modeling the absorption chiller within the Type 177a are given in Appendix D with data for several other commercial chillers.

Chapter 4. System and Components validation

Table 4. Technical data for different market available small absorption chillers

Company	Yazaki	EAW	Sonnenklima	Rotarica
Product name	WFC-SC5, chillii WFC 18	Wegral SE 15	Suninverse 10	Solar 045
Technology	Absorption	Absorption	Absorption	Absorption
Working pair	H2O/LiBr	H2O/LiBr	H2O/LiBr	H2O/LiBr
Absorption chiller image		 <small>Source: Schüco</small>	 <small>Source: Sonnenklima</small>	 <small>Source: rotarica</small>
Cooling capacity, kW	17.6	15	10	4.5
Heating temperature, °C	88 / 83	90/80	75/65	90/85
Recooling temperature, °C	31 / 35	30/35	27/35	30/35
Cold water temperature, °C	12.5 / 7	17/11	18/15	13/10
COP	0.70	0.71	0.77	0.67
Dimensions (WxDxH), m	0.60 x 0.80 x 1.94	1.75 x 0.76 x 1.75	1.13 x 0.80 x 1.96	1.09 x 0.76 x 1.15
Weight, kg	420	660	550	290
Electrical power, W	72	300	120	1200 (incl.ventilator)

In the component Type 177a as input parameters are taken the values for Suninverse provided in Table 4 for which with the simulation as output cooling power is obtained value of 10,1 kW which corresponds with the factory value. Thus it can be concluded that this model of absorption chiller provides reliable results and can be used further in simulations.

Validation exists for the Type 177 mode “d” performed by Albers and Ziegler (2011) using the measurement results from Kühn.

The supplied characteristic parameters in the validation of Type 177d are:

Symbol description:

γ	- flow rate ration	
a	- ration of heat transfer coefficient	
\dot{Q}	- heat power	kW
\dot{m}	- mass flow rate	kg/s
Y	- effective heat transimtion	kW K ⁻¹
T, t	- internal, external temperature	°C
$\Delta\Delta t$	- characteristic temperature function	K
Sub- superscript		

Chapter 4. System and Components validation

A	- absorber	ext, int	- external, internal
C	- condenser	i,o	- inlet, outlet
D	- desorber	E	- evaporator
X	- placeholder for component		

An extensive measurement campaign has been carried out by Kühn et al. (2005, 2007) for the investigation of a 10 kW chiller. Here two groups of measurements are used for the verification of the extended calculation method including variable external flow rates:

Measurements under design conditions, i.e. inlet temperatures and flow rates meet the rated values (presented in Table 5 and Table 7. Legend of the performance indicators and framed circles in Figure 34). Also measurements are performed at design inlet temperatures but with non-design external flow rates. The range of flow rate variation was between $0.3 < \gamma_D < 2.3$ of the rated value for hot water and between 0.5 and 1.5 for chilled and cooling water (γ_E and γ_{AC}) (see circles in Figure 34).

The first group of approx. 20 independent measurements of Kühn (2005) at rated conditions has been used to determine the ratios $a_X = \alpha_{ext,X,0} / \alpha_{int,X,0}$: First the external (i.e. tube inside) heat transfer coefficients $\alpha_{ext,X,0}$ have been calculated according to Gnielinski (2006). Then measured values of Q_X and $\Delta T_{log,X}$ have been used together with geometric data of tube bundles to determine $\alpha_{int,X,0}$. The resulting ratios of a_X are given in Table 5 and depicted in variation of inlet temperature and flow rate of hot water (left) and cooling water (right)

Figure 33 as open symbols in together with their uncertainty which is not larger than $\pm 5\%$ to $\pm 10\%$.

Table 5. Averaged measured performance data by Kühn (2005) of a 10kW absorption chiller

X	$m_{X,ext,0}$	tXi	tXo	TX	QX	$Y_{X,0}$	α_X
Unit	kg/s	°C	°C	°C	kW	kW/K	-
D	0.33	74.9	65.1	62.8	13.4	1.9	3.8
E	0.81	18.0	14.9	12.9	10.5	3.0	1.8
C	0.72	31.0	34.9	36.0	11.7	3.7	0.8
A	0.72	27.0	31.0	36.6	12.1	1.7	5.7
S	0.07	31.5	60.8	52.1	4.6	0.8	-

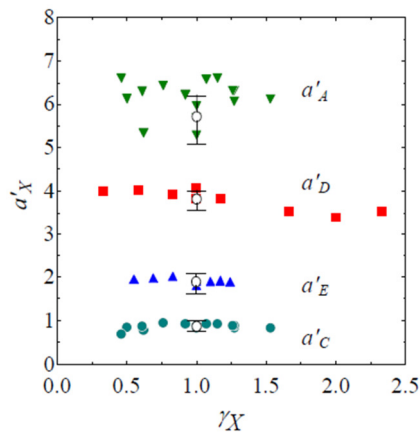


Figure 33. Measured ratios of external to internal heat transfer coefficients

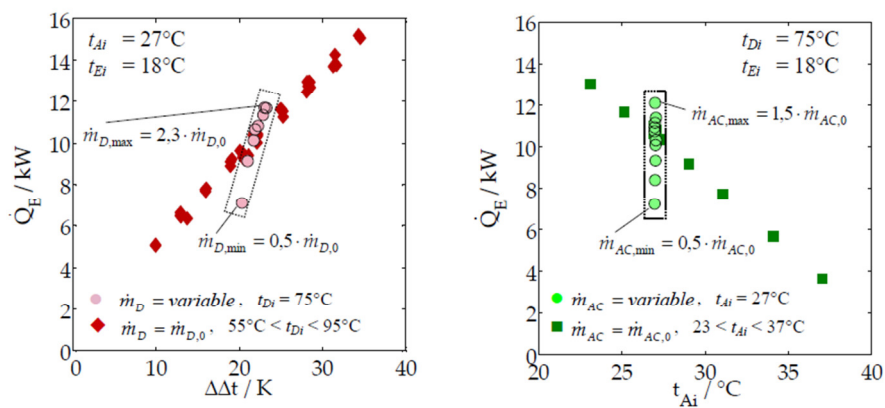


Figure 34. Measured cooling capacity for design and variable flow rates, by Kühn et al. 2005&2007.

According to the previous presented from the Kühn can be concluded that the Type 177d modelled according to the data in Table 5 provides reliable and acceptable output results, further enabling this model to be used in simulation of solar air-conditioning systems.

Chapter 5

5. Performance evaluation of solar air-conditioning system

It has become recognized that, however, solar heating is the product of a collection of components comprising a system and needs to be studied such. Because of the interactions of components, optimal system performance occurs under conditions different from those for optimal behavior of each component. For example optimal collection efficiency would not necessarily be coupled with least auxiliary energy.

In this chapter are presented two schemes for quantification of performance level of a solar heating and cooling plant.

Many different hydraulic schemes are designed which makes difficult to compare the installations performances [43]. Methods used to determine solar heating and/or cooling energy requirements for both active and passive/hybrid systems are described by Feldman and Merriam, Hunn, Nowag and other. In the frame of IEA-TASK 38 a unified monitoring procedure has been developed. For thermally driven systems the scheme on Figure 35 is used to identify main components and energy flows of the system. On Figure 35 is presented small scale system for family houses, small multi dwellings, using a small size packaged ab/adsorption solar system. This configuration is an adaptation of the solar combi system including the cooling function, also called SSC + Solar Combi.

Chapter 5. Performance evaluation of solar air-conditioning system

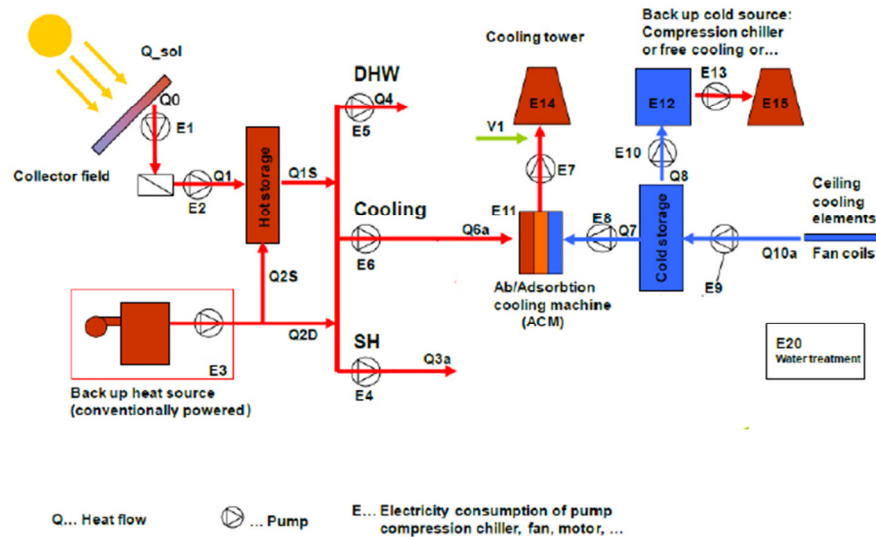


Figure 35. Solar cooling system variables [44]

The description of each variable of the system is presented in Table 6

Table 6. Energy and thermal flows of solar cooling systems

Label	Electricity consumer, kWh
<i>Heating system</i>	
E ₁	pump collector field (primary loop)
E ₂	pump collector field (secondary loop)
E ₃	pump boiler hot-storage (including internal boiler consumption)
E ₄	pump hot-storage to space heating (SH)
E ₅	pump hot-storage to domestic hot water (DHW)
<i>Cooling system</i>	
E ₆	pump hot-storage to cooling machine
E ₇	pump cooling machine (ACM) to cooling tower
E ₈	pump cooling machine (ACM) to cold storage
E ₉	pump cold storage to cold distribution
E ₁₀	pump back-up source -cold storage
E ₁₁	absorption/adsorption cooling machine (ACM)
E ₁₂	compression chiller (back-up system)
E ₁₃	pump compression chiller to fan (back-up system)
E ₁₄	fan, cooling tower
E ₁₅	fan of compression chiller (back-up system)
<i>Water treatment System</i>	
E ₂₀	water treatment for wet cooling tower
Thermal flows, kWh	
Q _{sol}	solar irradiation on total collector aperture area
Q ₀	collector solar thermal output

Chapter 5. Performance evaluation of solar air-conditioning system

Q_1	solar thermal output to hot storage
Q_{1s}	heat output from hot storage
Q_{2s}	boiler thermal output (fossil) into storage
Q_{2D}	fossil boiler thermal input bypassing hot storage (directly used)
Q_{3a}	space heating (SH) consumption (conventional)
Q_{3b}	space heating (SH) consumption (ventilation system)
Q_4	domestic hot water consumption (DHW)
Q_{6a}	hot storage input to cooling machine (ACM)
Q_{6b}	hot storage input to DEC-system (sorption regeneration)
Q_7	cold output ACM to cold storage
Q_8	cold output back-up chiller or free cooling to cold storage
Q_{10a}	cold storage output to cold-distribution

5.1 Performance indicators

There are four generally accepted measures of solar system performance:

1. *Collector efficiency* applies to the performance of the solar energy collection subsystem. It is the energy collected, divided by the radiation incident upon the collectors. The radiation may be the total radiation, or it may be only that incident while the collection subsystem is operating.
2. *System efficiency*, or solar heating performance factor is the solar heat delivered to the load divided by the total radiation incident upon the collector. It is similar to the collector efficiency but also takes into account heat loss from the pipes and storage. The net system efficiency is the solar heat delivered less the electrical inputs to the system, divided by the incident solar radiation. This figure must be used however with the caution that the delivered heat may not have the same economic value as the equivalent energy in the form of electricity.
3. *Solar fraction* is the fraction of the total heat requirement that is met by solar energy. The figure relates the output of the solar system to the size of the system as well as on its efficiency.
4. *Electrical coefficient of performance* is the solar heat delivered to the load, divided by the electrical energy used to operate the system.

Each solar system operates at characteristic efficiency level resulting from the interaction of the subsystems, environmental conditions and system configurations. The net savings per square meter of solar collector indicate the relative performance of each of these systems.

The five categories of system-level design parameters that limit solar system performance. These are:

1. *Solar resource assessment*. This category represents the solar reference weather data values used by the solar design community

Chapter 5. Performance evaluation of solar air-conditioning system

2. *Collection subsystem.* This category represents the solar collection sub-system, including devices used to capture incoming solar radiation

3. *Storage subsystem.* This category deals with all aspects of the system effects caused by storage components.

4. *Controls.* This category refers to equipment and methods for controlling solar components within the solar system.

5. *Load.* This category deals with the types and magnitude of the heat requirements in the buildings.

Also in order to calculate the different performance indicators, some necessary values are defined : the useful solar energy (ESU), the parasitic electricity demand of the whole system (Eaux) and of the solar part (Eaux sol), the thermal losses of the hot and cold storage (Qloss HS and Qloss CS), the thermal losses of the hot storage due to the heating backup system (Qloss HB), the thermal losses of the cold storage due to the cooling backup system (Qloss CB), the final energy consumption of the heating backup system (ConsHB) and of the cooling backup system (ConsCB). Each of this quantities are defined in Table 7.

Table 7. Legend of the performance indicators

Nomenclature		Unit
Qsol	Global irradiation on collector area	kWh
Q1 - Q10	Thermal energy defined according to FIGURE	kWh
E1 at E14	Auxiliary electrical consumptions defined according to Figure	kWh
V1	Water consumption of the heat rejection system	m ³
Eaux & Eaux _{sol}	Parasitic electricity demand of the whole system and of the solar part	kWh
Qloss _{HS} & Qloss _{CS}	Thermal losses of the hot and cold storages	kWh
Qloss _{HB} & Qloss _{CB}	Thermal losses of the storages due to the hot and cold backup system	kWh
ESU	Useful solar energy	kWh
RgHB & RgCB	Generation efficiency of the hot and cold backup system	-
ConsHB & ConsCB	Hot and cold backup system energy consumption	kWh
η _{HS} & η _{CS}	Hot and cold storage efficiency	-
COP _{th}	Thermal coefficient of performance of the sorption chiller -	-
PER	Primary Energy Ratio	-
ε _X	Primary energy conversion factors of the energy X	-
€ _X	Cost per kWh of the energy X	€/kWh
R _{coll} & R _{sol}	Collector thermal yield and solar thermal efficiency of the system	-
PSU	Useful solar thermal productivity	kWh/m ²
COP _{elec_{sol}}	Electrical coefficient of performance for solar energy	-
WC _{spe}	Specific water consumption of the system	l/kWh

Chapter 5. Performance evaluation of solar air-conditioning system

kWhcost	Operation cost of the system	€/kWh
Iconf, Idata & Ifct	Comfort, monitoring data lost and functioning indicators	%
Thot, Tcold	Reference hot and cold storage temperatures	°C
Tamb, Tav, Text	Reference ambient, collector average and external temperatures	°C
Nmonth, Ncool	Number of months in functioning and cooling mode	-
ENS	Average annual daily value of the irradiation on the collector kWh	kWh
Imin, Imax, I, I%	Minimum, maximum, value and percentage value of the considered indicator	-

In some cases the solar fraction can be used as performance index defined as a fraction of required heat for a certain application which is delivered by the solar system. However this parameter is difficult to judge in some cases since it does not reflect the full picture of the energy balance. Particularly for solar cooling systems in which different energy sources may serve as a back-up, it may be difficult to define the solar fraction properly. Therefore since estimation of primary energy is the main goal it is recommended to use the corresponding parameter to quantify the energy performance of a solar air-conditioning assisted system. For complete system performance assessment it is necessary to consider the energy consumption for the entire year.

5.3.1 Thermal efficiency indicators

Losses are inferred from energy flow balances computed for system components. Thus for example the reflection and back-radiation loss from the collector array is calculated as the difference of the solar energy incident on the array and the collected solar energy. Any losses that result in space heating will be indicated in

The thermal efficiency indicators describe the main thermal losses of the system through the hot (1) or (2) and cold (3) storage and the thermal coefficient of performance of the chiller (4).

5.3.2 Global performance indicators

The global performance indicators represent the overall system performances and take into account the solar energy use as well as the heating and cooling backup energy use. The global performance indicator defined is the primary energy ratio. The primary energy savings per unit solar collector area give an indication of the contribution of each square meter of collector field to the energy saving of the entire system.

In the Table 7 are summarized and presented the calculation methods for different performance indicators.

Chapter 5. Performance evaluation of solar air-conditioning system

Table 8. Calculation procedures for solar thermal system performance indicators

Indicators	Calculation method
	$\eta_{hs} = 1 - Q_{lossHS} / (Q_1 + Q_{2s}), \text{ with } Q_{lossHS} = Q_1 - Q_{3a} - Q_4 - Q_{6a} \quad (53)$
	$\eta_{cs} = 1 - Q_{lossHS} / Q_1, \text{ with } Q_{lossHS} = Q_1 + Q_{2s} - Q_{3a} - Q_4 - Q_{6a} \quad (54)$
	$COP_{th} = Q_7 / Q_{6a} \quad (55)$
	$PER = (Q_{10a} + Q_{3a} + Q_4) / (E_{aux} + \epsilon_{elec} + C_{onsCB} \times \epsilon_{CB} + C_{onsCB} \times \epsilon_{CB}), \text{ with} \quad (56)$ $C_{onsCB} = Q_2 / R_{gHB} \text{ and } C_{onsCB} = Q_8 / R_{gCB}$
	$R_{coll} = Q_1 / Q_{sol} \quad (57)$
	$R_{sol} = ESU / Q_{sol} \quad (58)$
	$PSU = ESU / S_{coll} \quad (59)$
	$COP_{elec\ sol} = ESU / E_{aux\ sol} \quad (60)$
	$WC_{spe} = V1 / Q_7 \quad (61)$
	$kWh_{cost} = (E_{aux} \times \epsilon_{elec} + C_{onsSCB} \times \epsilon_{CB} + C_{onsSHB} \times \epsilon_{HB} + V1 \times \epsilon_{water}) / (Q_{10a} + Q_{3a} + Q_4) \quad (62)$
	$ESU = Q_{3a} + Q_4 - Q_{2s} + Q_{lossHB} + (Q_{10} - Q_8 + Q_{lossCB}) / COP_{th}; \text{ with} \quad (63)$ $Q_{lossCB} = Q_{lossCS} \times Q_8 / (Q_8 + Q_7) \text{ and } Q_{lossHB} = Q_{lossHS} \times Q_{2s} / (Q_1 + Q_{2s})$
	$E_{aux} = E_1 + E_2 + E_3 + E_4 + E_5 + E_6 + E_7 + E_8 + E_9 + E_{10} + E_{13} \quad (64)$
	$E_{aux\ sol} = E_1 + E_2 + \sum_{cool} (E_6 + E_7 + E_{11} + E_{14}) \times Q_1 / (Q_1 + Q_{2a}) \quad (65)$

Chapter 6

6. Simulation results and analysis

In this chapter are analyzed multiple scenarios based on which are derived and adopted conclusions on the impact of individual parameters on the system performance, useful energy yield, solar fraction and consumption of primary energy. The analysis can be generally divided into two parts: analysis of the system operating in heating mode and second part in cooling mode.

6.1 Reference building modeling and simulation

Building as energy consumer has a major impact on the overall efficiency of the solar system i.e. can be freely said that the building itself is one of the leading parameter in sizing the system. Since the analyzes are made for climatic conditions in Macedonia also the thermal performance of buildings must be in accordance with the Regulations on energy efficiency in Macedonia. Furthermore the analysis is taken into account the impact of the specific consumption of heating / cooling energy of the building $\text{kWh/m}^2 \text{ a}$ to the response and the performance of the solar collector system. Main indicators based on which system comparison is base are: thermal efficiency of solar collectors, solar fraction and power consumption for the auxiliary devices.

Thus in the simulation / analysis systems are analyzed in conjunction with a reference building with three different specific energy consumption i.e. three types of building are defined.

The building has one floor with a total conditioned area of 150 m^2 . In Table 10 are given data for. surfaces and orientation of exterior walls, windows, floor, roof and coefficients of heat transfer.

In Table 9 are listed three types of the building i.e. the dimensions and orientations are unchanged only the insulation thickness is varied in order to obtain different values for specific annual consumption of thermal energy. The main motive for variations in the thickness of the insulation is to analyze the influence of the thermal performance of buildings on the economic viability of the use of solar thermal systems in air-conditioning.

Chapter 6. Simulation results and analysis

Table 9. Reference building physical and thermal performance data

Surface	Orientation	Area, m ²	Building I	Building II	Building III
			U value, W/m ² K		
Out.wall 1	North	42	0.58	0.33	0.18
Windows 1	North	3	1.40	1.40	1.40
Out.wall 2	East	25.5	0.58	0.33	0.18
Windows 2	East	4.5	1.40	1.40	1.40
Out.wall 3	West	25.5	0.58	0.33	0.18
Windows 3	West	4.5	1.40	1.40	1.40
Out.wall 4	South	42	0.58	0.33	0.18
Windows 4	South	3	1.40	1.40	1.40
Floor	-	150	0.33	0.33	0.24
Roof	-	150	0.54	0.42	0.35
Window type Double glazed TRNSYS library (w4-lib data)					
Windows solar heat gain coefficient;g-value			0.589		
Out.wall construction	2 x Plaster 2cm, brick 25cm	Insulation 5 cm	Insulation 10 cm	Insulation 20 cm	
Floor	Granite tile 6cm, cement mortar 5cm , concrete slab 20cm	Insulation 10 cm	Insulation 10 cm	Insulation 15 cm	
Roof	Concrete slab 20cm, hydro isolation, cement mortar 5cm	Insulation 15 cm	Insulation 20 cm	Insulation 25 cm	
Outside convective heat transfer coefficient			$\alpha_{out} = 25 \text{ W/m}^2\text{K}$		
Inside convective heat transfer coefficient			$\alpha_{in} = 7,7 \text{ W/m}^2\text{K}$		

Constant value of 0.3 1/h is defined for the infiltration of outdoor air, while for the summer when cooling is required in the building is envisaged/modeled mechanical ventilation defined with air mass flow and temperature entered through \the models of fan and heat exchanger air-water which is directly connected with the cooling absorption machine.

Regarding the thermal comfort, in the heating mode the inside temperature is defined to be 20 °C from 05:00 – 22:00 and for the rest is defined setback temperature of 16 °C, for the cooling mode is defined constant inside temperature of 26 °C.

Calculation of energy consumption in the building is obtained directly as output size of the numerical model of the object in kJ / h value which further is integrated for the required period with the quantity integrator. Also as output parameters of the model is the output temperature of floor heating, the temperature of the air entering the fan to the heat exchanger and air-water and the delivered energy from the underfloor heating system into the building.

Monthly analysis is performed for the building heat energy consumption regarding different heat transfer coefficients i.e. different wall, floor and roof isolation thickness thus defining three types of Building I, II and III. as presented in Table 9.

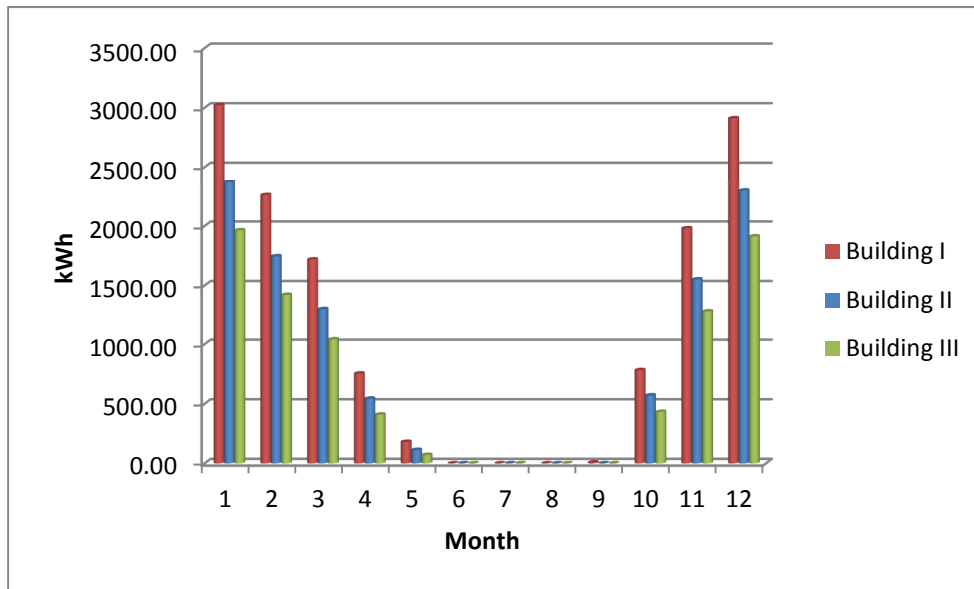


Figure 36. Monthly energy consumption for the three building “types”

Analyzing the presented simulation results on Figure 36 can be noticed that as expected the Building III has the smallest heat consumption i.e. regarding specific annual energy consumption, Building I has $90 \text{ kWh/m}^2\text{a}$, Building II with $70 \text{ kWh/m}^2\text{a}$ and Building III has $57 \text{ kWh/m}^2\text{a}$. Comparing the energy consumption Building III has 42% lower than Building I and 19% than Building II.

On Figure 37 are presented the frequency hourly values of the outside dry bulb temperatures for Skopje, R.Macedonia. All of the meteorological data used in simulations such as temperatures, sun radiation, relative humidity etc., are obtained from the base of Meteonorm software which is a comprehensive meteorological reference. Those values are used as inputs in the simulation to determine the building heat energy consumption.

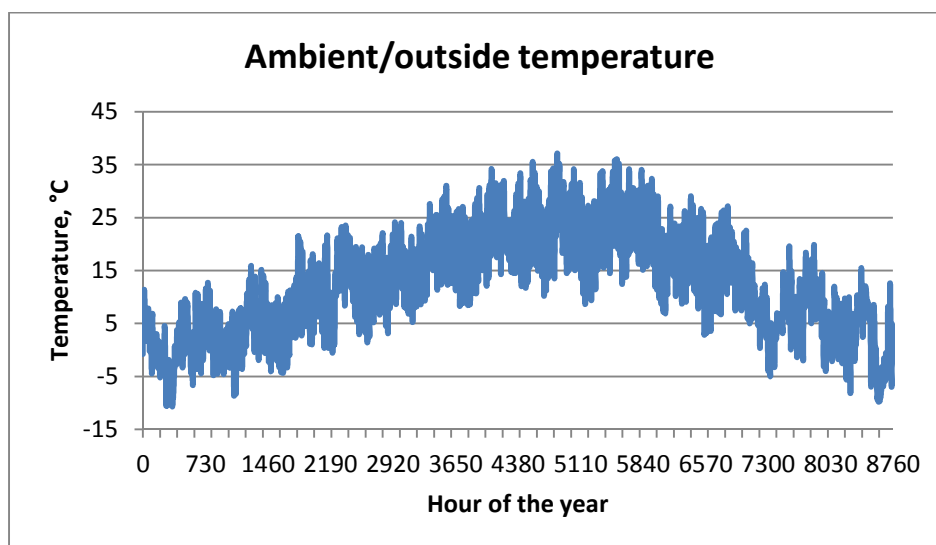


Figure 37. Hourly dry bulb ambient temperatures for Skopje, R.Macedonia

Chapter 6. Simulation results and analysis

The station data used in Meteonorm is supplemented by surface data from five geostationary satellites. This data is available on a global grid with a horizontal resolution of 8 km (3 km in Europe and Northern Africa). Usually, measurement data can only be used in the vicinity of a weather station. Elsewhere, the data has to be interpolated between different stations. The sophisticated interpolation models inside Meteonorm allow a reliable calculation of solar radiation, temperature and additional parameters at any site in the world. From the monthly values (station data, interpolated data or imported data), Meteonorm calculates hourly values of all parameters using a stochastic model. The resulting time series correspond to “typical years” used for system design [45]. Analysis of the solar thermal system in heating mode for the building

In scenario 1 it is analyzed the influence of the heating system type regarding the heat transfer elements (underfloor heating or radiators) regarding the efficiency of solar collectors, solar fraction and the total consumption of heating energy. In the first case analyzed case are set as radiators heating elements. In modeling of the radiator heating system it is defined that radiative part of energy transferred equals to 0.99 which is defined only heating.

This fraction of the heater power is supplied as internal radiative gains and distributed to the walls of the zone. As the set temperature for the heating equipment is related to the air temperature of the zone, the radiative fraction of the heating power RRAD cannot be higher than 0.99 in order to have a convective part remaining to ensure stable control of the heating equipment. The radiators are modeled with Type 1231 from the Tess Library. The heating radiator model is based on the ASHRAE method outlined in the 2004 ASHRAE Handbook - HVAC Systems and Equipment.

Second case is when the heating system i.e. the heat is transferred through underfloor heating. Thus the modeling is performed so that the building model that defines the active layers within the floor area. In this case the floor area is divided into seven active layers in a single area of 21.43 m² in which they are set by the floor heating pipes whose characteristics are defined in the table.

Table 10. Active layer TYPE data

Data description	Unit	
Pipe spacing center to center dx	m	0.2
Pipe outside diameter δ	m	0.02
Pipe wall thickness	m	0.002
Pipe wall conductivity	kJ/h m K	1.26
Specific heat of the fluid	kJ/kg K	4.187

The cross-section of the underfloor heating i.e. the active layers configuration and the pipe disposition is presented in Figure 38

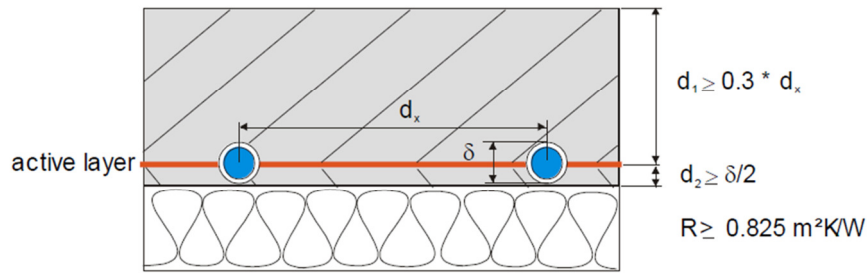


Figure 38. Cross section of the active layer for the underfloor heating

The fluid in the storage tank 4 indirectly is heated by solar collectors which further with the circulating pump mass flow rate of 2000 kg/h is transferred through the auxiliary heater to the underfloor heating. The auxiliary heating temperature i.e. the output fluid temperature is maintained on 50 ° C if the heat transfer elements are radiators while for the underfloor heating is 40 ° C. The system is planned heating and DHW tank with a volume of 200 l of internal heat exchanger and an external electric heater with power of 9 kW. The volume of the storage tank 4 is considered as a parameter in the analysis with values of 1000 l, 1500 and 2000 l. Each of these storage tanks are modeled with an internal heat exchanger which technical characteristics as given in Annex 1. Auxiliary heater power is 12 kW.

Return i.e. exit temperature of the fluid from the heating system is a dynamic variable that depends on several parameters and is output size of the numerical model of radiators i.e. floor heating. If the return temperature of the working fluid is higher than the temperature in the storage tank 4 measured at the highest point 1, it is then redirect directly to the heated auxiliary heater.

The domestic hot water tank 3, differential controller upper band is set to five, lower dead band to two, while for the storage tank 4 both of the values are three.

In Table 12 and Table 13 are presents results from the heating system simulation. As previously mentioned main parameter in this analysis is the type of heating i.e. the left half of the table refers to system with radiators while the right is for a system with underfloor heating. Leading parameters regarding which comparison is made are: solar fraction for the heating system and for the DHW, performance and "real" performance of collectors. Solar fraction is calculated as the ratio between the thermal energy storage tank (calculated with Equation 66) and the sum of the thermal energy storage tank and auxiliary heater.

$$Q_{SH} = m_{sh} c_p (t_o - t_i), \text{ kJ/h} \quad (66)$$

where:

Q_{SH} , kJ/h - extracted heat energy from the storage tank

Chapter 6. Simulation results and analysis

m_{sh} , kg/h - mass flow rate of working fluid from storage tank to system (heating or DHW)

t_o, t_i , K - working fluid outlet and inlet temperatures

The collector thermal efficiency is calculated as ratio between the sum of the useful collector energy and the total tilted solar radiation on the collector surface.

$$\eta_{th} = \frac{\sum Q_{cu}}{\sum G_t} \quad (67)$$

η_{th} - thermal efficiency of the collector array

$\sum Q_{cu}$ - sum of the useful collector array energy transferred to the working fluid

$\sum G_t$ - sum of the total tilted radiation on collector surface

Another parameter in the analysis is so called “real” collector thermal efficiency calculated with which is again ration between the sum of collector useful energy and the sum of the total tilted radiation for the collector surface which in this case are only summed the values of radiation when the circulation pump is on i.e. when the collector is active.

This parameter is inserted in the analysis since it serves as indicator to give sense how long the collector is in function i.e. the bigger the difference between these two efficiencies means that the collector more of the time is in stagnation and vice versa.

The mass flow rate through the solar collectors is selected to be 50 kg/h m² i.e. for the 16 m² is 800 kg/h, for 32 m² is 1600 kg/h and for 64 m² is 3200 kg/h.

The simulations are done with time step of 7.5 min and the result were integrated on monthly basis. Presented results are averaged values from the monthly values and the period of analysis are the heating season months for Skopje i.e. October – April. Analyzing the presented results in Table 11 and Table 12 can be noticed that for different collector area and/or storage tank volume parameters value are the same like the solar fraction, but in the monthly data can be noticed the discrepancies. Thus must be noted that data average is performed since presenting all of the monthly value will be too excessive.

Table 11. Parametric analysis of solar assisted heating system with radiators

Radiator heating system					
	Storage tank volume	Parameter	Collector array area, m ²		
			16	32	64
BUILDING I	1000 L	Sol.fraction.Heat	0.08	0.18	0.28
		Eff_Monthly	0.25	0.18	0.13
		Eff.real	0.55	0.45	0.36
		Sol.frac.DHW	0.75	0.79	0.81
	1500 L	Sol.fraction.Heat	0.07	0.17	0.28
		Eff_Monthly	0.26	0.19	0.14
		Eff.real	0.53	0.41	0.31
		Sol.frac.DHW	0.74	0.79	0.81
	2000 L	Sol.fraction.Heat	0.06	0.16	0.29
		Eff_Monthly	0.27	0.19	0.15
		Eff.real	0.53	0.39	0.30
		Sol.frac.DHW	0.73	0.78	0.81
BUILDING II	1000 L	Sol.fraction.Heat	0.07	0.17	0.27
		Eff_Monthly	0.24	0.17	0.12
		Eff.real	0.55	0.45	0.36
		Sol.frac.DHW	0.76	0.80	0.82
	1500 L	Sol.fraction.Heat	0.06	0.15	0.27
		Eff_Monthly	0.25	0.18	0.13
		Eff.real	0.53	0.4	0.31
		Sol.frac.DHW	0.75	0.8	0.82
	2000 L	Sol.fraction.Heat	0.06	0.16	0.28
		Eff_Monthly	0.25	0.19	0.13
		Eff.real	0.54	0.40	0.30
		Sol.frac.DHW	0.75	0.79	0.82
BUILDING III	1000 L	Sol.fraction.Heat	0.08	0.17	0.28
		Eff_Monthly	0.23	0.17	0.11
		Eff.real	0.55	0.45	0.36
		Sol.frac.DHW	0.76	0.80	0.82
	1500 L	Sol.fraction.Heat	0.07	0.16	0.28
		Eff_Monthly	0.25	0.18	0.12
		Eff.real	0.53	0.40	0.31
		Sol.frac.DHW	0.76	0.80	0.82
	2000 L	Sol.fraction.Heat	0.06	0.17	0.29
		Eff_Monthly	0.26	0.19	0.13
		Eff.real	0.53	0.40	0.30
		Sol.frac.DHW	0.75	0.80	0.82

In the next Table 12 is given analysis for the same parameters as in Table 11 but with difference that as heat transfer devices it is used underfloor heating and the fluid supply temperature is 40 °C.

Table 12. Parametric analysis of solar assisted underfloor heating system

Underfloor heating system					
	Storage tank volume	Parameter	Collector array area, m ²		
			16	32	64
BUILDING I	1000 L	Sol.fraction.Heat	0.19	0.30	0.39
		Eff_Monthly	0.25	0.17	0.11
		Eff.real	0.55	0.45	0.38
		Sol.frac.DHW	0.69	0.75	0.81
	1500 L	Sol.fraction.Heat	0.21	0.34	0.45
		Eff_Monthly	0.28	0.19	0.13
		Eff.real	0.52	0.41	0.31
		Sol.frac.DHW	0.66	0.73	0.78
	2000 L	Sol.fraction.Heat	0.23	0.32	0.44
		Eff_Monthly	0.29	0.21	0.14
		Eff.real	0.51	0.41	0.31
		Sol.frac.DHW	0.64	0.71	0.77
BUILDING II	1000 L	Sol.fraction.Heat	0.22	0.31	0.38
		Eff_Monthly	0.25	0.16	0.10
		Eff.real	0.54	0.44	0.37
		Sol.frac.DHW	0.83	0.78	0.70
	1500 L	Sol.fraction.Heat	0.24	0.35	0.44
		Eff_Monthly	0.27	0.18	0.12
		Eff.real	0.51	0.40	0.31
		Sol.frac.DHW	0.68	0.75	0.81
	2000 L	Sol.fraction.Heat	0.27	0.40	0.49
		Eff_Monthly	0.28	0.20	0.13
		Eff.real	0.51	0.40	0.31
		Sol.frac.DHW	0.66	0.73	0.80
BUILDING III	1000 L	Sol.fraction.Heat	0.24	0.33	0.32
		Eff_Monthly	0.24	0.15	0.10
		Eff.real	0.54	0.45	0.37
		Sol.frac.DHW	0.72	0.79	0.84
	1500 L	Sol.fraction.Heat	0.26	0.35	0.37
		Eff_Monthly	0.26	0.17	0.11
		Eff.real	0.52	0.40	0.31
		Sol.frac.DHW	0.70	0.77	0.82
	2000 L	Sol.fraction.Heat	0.29	0.42	0.52
		Eff_Monthly	0.28	0.19	0.12
		Eff.real	0.51	0.40	0.30
		Sol.frac.DHW	0.68	0.75	0.81

In order to have better insight over the compared systems from the results in Table 11 and Table 12 it is derived diagram presentation of the results given on Figure 39

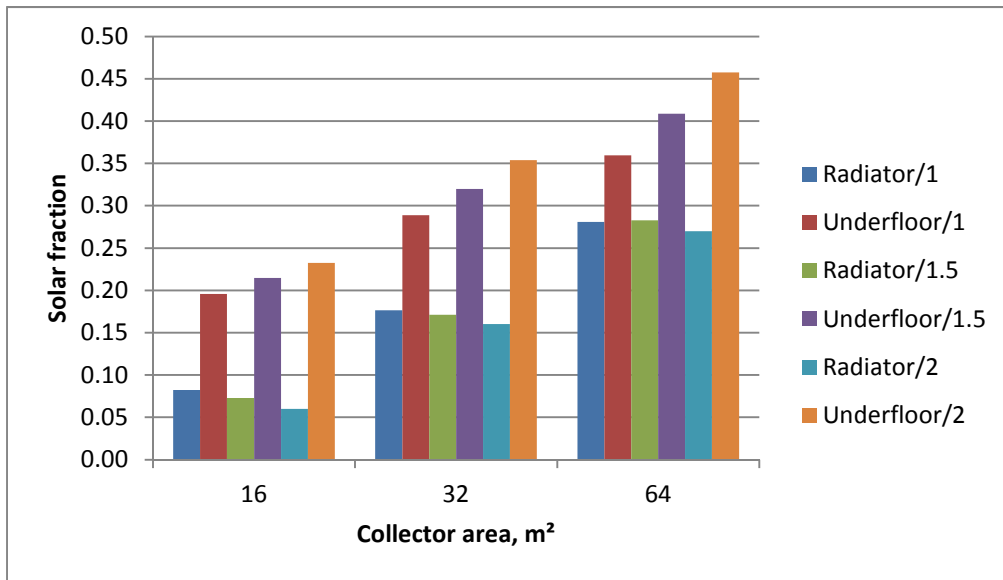


Figure 39. Solar fraction for Building I, radiator and underfloor heating in regard of collector array area and storage volume

The number that is written in the “series” name in the diagram after Radiator and Underfloor indicates the storage tank volume in m³. It’s easily noticeable on the results from Figure 39 that there are differences between the solar fractions i.e. bigger differences are occurring for the combination of lower collector areas and bigger storage volumes. This is because first the analyzed Building I has lowest thermal insulation i.e. highest heat energy consumption which results in high frequency heat energy discharge of the storage tank. The underfloor heating has bigger solar fraction since it uses the thermal mass of the floor which buffers the temperature fluctuations in the building i.e. tank discharge frequencies thus allowing more time the tank to be reheated with solar energy and the second important influencing factor is that the underfloor heating has 10°C lower design driving temperature compared to radiator system.

Another possible analysis is to gain insight for the influence of the specific building energy consumption on the solar fraction. On Figure 40 are presented results from this analysis from which firstly it’s obvious that underfloor heating has bigger solar fractions ranging from 24% up to 73%. This solar fraction differences trend between radiator and underfloor solar assisted heating increases if the building lowers the specific heat energy consumption and lowers the collector area.

This analysis is done for constant volume of storage tank 4, 1500l and internal heat exchanger with parameters given in Appendix A.

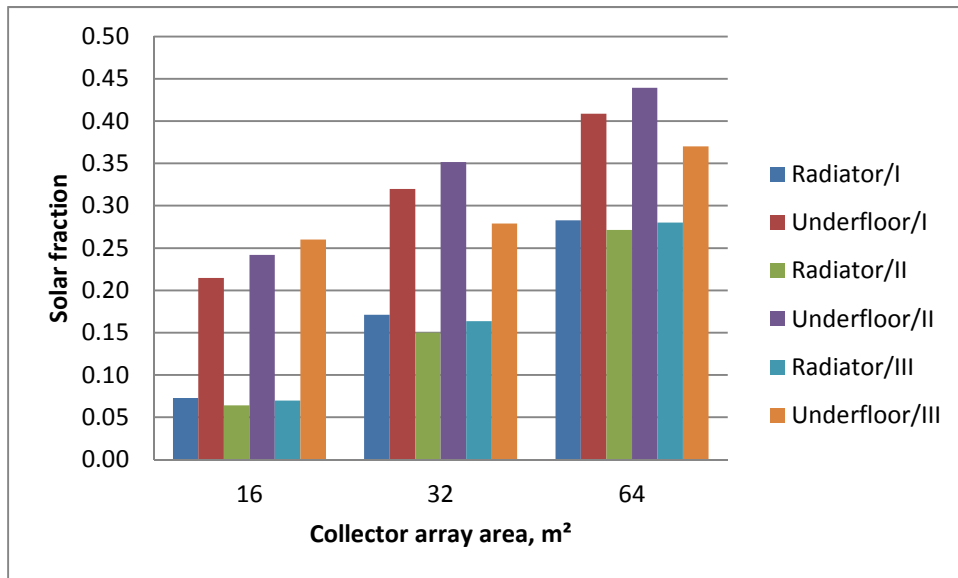


Figure 40. Solar fraction for heating with storage tank 1500l regard of collector array area building type

According to the presented results can be concluded that for buildings with specific heat consumption from 90 kWh/ m² a up to 57 kWh/ m² a, with 0,1 m²/m²_{conditioned} specific collector area per conditioned surface can be achieved between 20 – 25 % solar fraction, with 0,2 m²/m²_{conditioned} range round 35% , and with 0,4 m²/m²_{conditioned} maximum 50 %. It should be noted that the solar fraction also strongly depends from the storage tank volume and for the radiator heating system increasing the storage volume results in decrease of solar fraction while at the underfloor heating its vice versa. It is recommended the storage volume to be in the range 50-60 l/m² collector area in order to optimize between the solar fraction and collector efficiency.

Also during the simulations monthly average space temperature was tracked in order to see if the basic comfort conditions are satisfied and the results are presented on Figure 41.

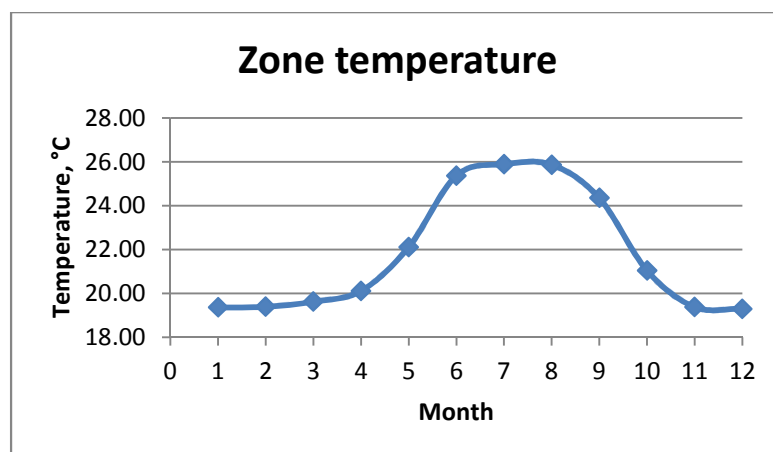


Figure 41. Monthly average zone temperature, only heating analysed

6.3 Analysis of the solar thermal system in cooling mode for the building

This part analyses the performance of solar thermal cooling system i.e. solar driven absorption chiller. As parameters in the analysis are considered: collector type (flat plate and vacuum tube) collector area tilt(slope) and azimuth angle and storage tank volume in regard of solar cooling and DHW fraction, efficiency “ real” efficiency and electrical consumption of the cooling tower fan and the system fan. As mentioned previously for the absorption chiller it is used the component model Type 177a in which input parameters are inserted the data from the LiBr/H₂O Suninverse 10 chiller product of Sonneklima with cooling power of 10 kW with heat driving temperature of 75 °C, cooling water 27 °C and chilled water outlet temperature set at 15°C .

In general are considered two scenarios, first is with flat plate collectors and the second is with vacuum tube collectors.

6.3.1 Scenario 1

The system is simulated as shown on Figure 26 i.e. the solar collectors are used to heat the fluid in storage tank 4 which is connected to the generator of the absorption chiller. In serial connection after the storage tank outlet is installed auxiliary heater used to add heat in periods when the working fluid has lower temperature that the set one. This scenario considers flat plate collectors with characteristic given in Table 1 and the Building II type, which thermal performance described in Table 9. The building internal heat gains consider the lighting power density 5 W/m² and the home appliances with specific power of 2 W/m². The absorption chiller condenser is connected to the wet cooling tower product of Baltimore AirCoil type PF2-0406AA-31-3 (technical details given in Appendix E). It's used Type510 model from Tess library, a closed circuit cooling tower which cools the liquid stream by evaporating water from the outside of coils containing the working fluid. The working fluid is completely isolated from the air and water in this type of system. Data used in the numerical model are given in Table 13.

The control signal of the cooling tower fan is set to have the tower try to maintain the desired outlet water temperature of 26 °C and the fluid flow rate with the circulation pump is set to 2600 kg/h. Also to the circulation of the cooling water are modeled pipe network with diameter 0.04 m and length of 15 m heat transfer coefficient for thermal losses 3 kJ/h m² K which accounts for the heat losses to the environment and also increases the system thermal capacity affecting the simulation stability. Values of the inlet parameters for the cooling tower such as ambient air temperature and relative humidity are read from the weather component respectively for the simulated time and period of the year.

Chapter 6. Simulation results and analysis

The cooling water temperature is parameter which is variable depending from the absorption chiller working conditions.

Table 13. Cooling tower design parameters

Parameter	Unit	Value
Design inlet temperature	°C	35
Design outlet fluid temperature	°C	29.4
Design fluid flow rate	kg/s	1.7
Fluid specific heat	kJ/kg K	4.19
Design ambient air temperature	°C	35
Design wet bulb temperature	°C	25.5
Design air flow rate	kg/s	8
Rated fan power	kW	0.56



The cooling system in the building is modeled using the ventilation air distribution system. Combination among the chilled water from the absorption chiller and the ventilation air is provided with heat exchanger water-air modeled Type 508a which is a cooling coil modeled using a bypass approach in which the user specifies a fraction of the air stream that bypasses the coil. The remainder of the air stream is assumed to exit the coil at the average temperature of the fluid in the coil and at saturated conditions. The two air streams are remixed after the coil. Chilled water flow from the absorption chiller to the cooling coil is set to 2900 kg/h and the air flow rate to the building is 4000 kg/h.

The auxiliary heater power is modeled 12 kW and the outlet temperature is 80 °C, which is the absorption machine driving temperature.

The storage tank 4 in this case is used to store the heat for driving the absorption chiller. With the thermostat Type 108 is regulated the space temperature in the building set to 26 °C, which control signal is directly regulating the function of the circulation pump from the chilled water absorption chiller and the fan distributing the conditioned air.

Simulation time step is 15 min and as cooling period are considered the months from May-September.

The collector efficiencies are calculated same as described in Chapter 5. Solar fraction is calculated as ratio between the useful collector energy transferred to the working fluid and the total radiation on the collector surface. Also there is the DHW storage tank which solar heating control is same as described before in the heating system analysis i.e. the advantage of the solar energy is given to heat the storage tank 4. In this analysis are considered the electrical consumptions of the circulation pumps and fans.

Chapter 6. Simulation results and analysis

Table 14. Monthly average solar fractions and efficiency in regard of collector area and storage volume

Flat plate, Tilt 40°, Azimuth 0° - flow rate 50 l/h m ²									
	1000			1500			2000		
Collector area m ²	16	32	64	16	32	64	16	32	64
Sol.fraction	0.28	0.50	0.67	0.24	0.49	0.69	0.19	0.48	0.70
Avg_Efficiency	0.26	0.19	0.15	0.26	0.20	0.15	0.27	0.21	0.16
Avg_Eff_Real	0.48	0.36	0.32	0.47	0.37	0.33	0.46	0.37	0.30
Sol.DHW	0.98	0.99	0.99	0.98	0.99	0.99	0.98	0.99	0.99

The comparison results between the solar fractions and efficiencies in regard of different collector areas and storage volumes are presented in Table 14. The mass flow rate is set constant according the collector area i.e. it is 50 kg/h m². Solar collectors are tilted on 40° with south orientation i.e. azimuth is 0°. As can be seen the solar fractions increase with the increase of collector area and storage volume and varies in the range between 20% up to 70%. Also the thermal efficiency should not be neglected which for the analyzed cases is in the range between 15% up to 27% monthly averages. Solar fraction for the DHW is almost in every case 100% since the daily consumption is very low compared to the available energy from the solar collectors.

According the above presented results can be concluded that with solar energy regarding the specific collector areas can be covered: 0,1 m² / m²_{conditioned} can cover almost 30% , 0,2 m² / m²_{conditioned} covers 50% and 0,4 m² / m²_{conditioned} can cover 70% of the total required heating energy for driving the absorption chiller. Analyzing the solar fraction for one constant specific collector area and changing only the storage volume can be noticed that biggest fractions are for specific volume per collector area of 30 l/m².

Another analysis is done to estimate the influence of collector interconnections (number in parallel and/or serial) regarding the solar fraction and thermal efficiency. The main idea for this analysis is to check if the higher fluid outlet temperature induced by serial collector connections will increase the solar fraction.

Table 15. Monthly average solar fractions and thermal efficiency in regard of collector array interconnections

1000l, tilt 30° azimuth 0°						
	16/1 - 800 kg/h	16/4 - 400 kg/h	32/1-1600 kgh	32/2-800 kgh	64/1 - 3200 kg/h	64/2 - 1600 kg/h
Sol.fraction	0.30	0.27	0.52	0.55	0.69	0.69
Avg_Efficiency	0.26	0.27	0.20	0.18	0.15	0.15
Avg_Eff_Real	0.50	0.50	0.37	0.38	0.33	0.32
1500l, tilt 30° azimuth 0°						
	16/1 - 800 kg/h	16/2 - 400 kg/h	32/1-1600 kgh	32/2-800 kgh	64/1 - 3200 kg/h	64/2 - 1600 kg/h
Sol.fraction	0.24	0.24	0.51	0.51	0.69	0.69
Avg_Efficiency	0.26	0.26	0.20	0.20	0.15	0.15
Avg_Eff_Real	0.47	0.47	0.38	0.37	0.33	0.32

* 16/2-400 kg/h - total collector array has area of 16 m², each collector module area is 2 m² and two modules each with four collectors are in serial connection as presented on Figure 42.

16/2 - 400 kg/h

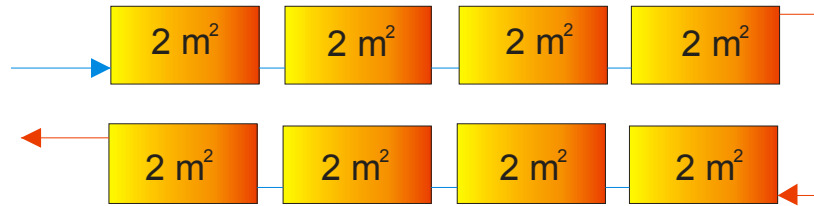


Figure 42. Scheme of the collector array connection 16/2

It is considered that all of the collectors have tilt of 30 ° directed toward south i.e. with azimuth of 0 °. The specific mass flow rate is kept constant with value 50 l/h m².

In Table 15 are presented the results from this simulation of the absorption cooling system where parametric analysis is done varying the number of collector in parallel and serial connection. Regarding the storage tank 4 the analysis is done for 1000 l and 1500 l.

In general analyzing the results can be concluded that serial connection between the collector modules doesn't affect too much on the solar fraction and thermal efficiency i.e. only slight increase at the collector array with 32 m² and storage tank of 1 500 l. Thus recommendation collectors to be in parallel connected since there are no or slight improvements in solar fraction but on the other hand there is decrease in thermal efficiency, increase in “real” efficiency indicating that collector longer stays not in function i.e. it is in stagnation and the last disadvantage is the increase in pressure loss and thus there is increase in pump energy consumption.

Further analyzed the influence of the collector tilt angle with and without azimuth tracking system (one axis-vertical tracking system) to the solar fraction and thermal efficiency. Simulation results are presented in Table 16 .

Table 16. Solar fractions and thermal efficiency for solar assisted cooling system in regard of collector orientation i.e. azimuth

Storage tank 1000l - Collector mass flow rate 50 l/h m ²									
Collector area m ² / tilt °	16/1/40	16/1/30	16/1/30/T	32/1/40	32/1/30	32/1/30/T	64/1/3200/40	64/1/3200/30	64/1/3200/30/T
Sol.fraction	0.28	0.30	0.44	0.53	0.55	0.67	0.67	0.69	0.77
Avg_Efficiency	0.26	0.26	0.24	0.18	0.18	0.19	0.15	0.15	0.16
Avg_Eff_Real	0.48	0.50	0.50	0.38	0.38	0.41	0.32	0.33	0.35
Storage tank 1500l - Collector mass flow rate 50 l/h m ²									
Collector area m ² / tilt °	16/1/40	16/1/30	16/1/30/T	32/1/40	32/1/30	32/1/30/T	64/1/3200/40	64/1/3200/30	64/1/3200/30/T
Sol.fraction	0.22	0.24	0.38	0.49	0.51	0.66	0.67	0.69	0.81
Avg_Efficiency	0.26	0.26	0.26	0.20	0.20	0.20	0.15	0.15	0.15
Avg_Eff_Real	0.46	0.47	0.47	0.37	0.38	0.39	0.32	0.33	0.36

*64/1/3200/30/T - (64) m² collector array , (1) all in parallel connected, (3 200) kg/h mass flow rate, (30) tilt angle, (T) tracking azimuth

Chapter 6. Simulation results and analysis

In order to have better visibility of the parametric influence of the collector tilt angle and azimuth influence, on Figure 43 are presented monthly values for solar fractions from June-September

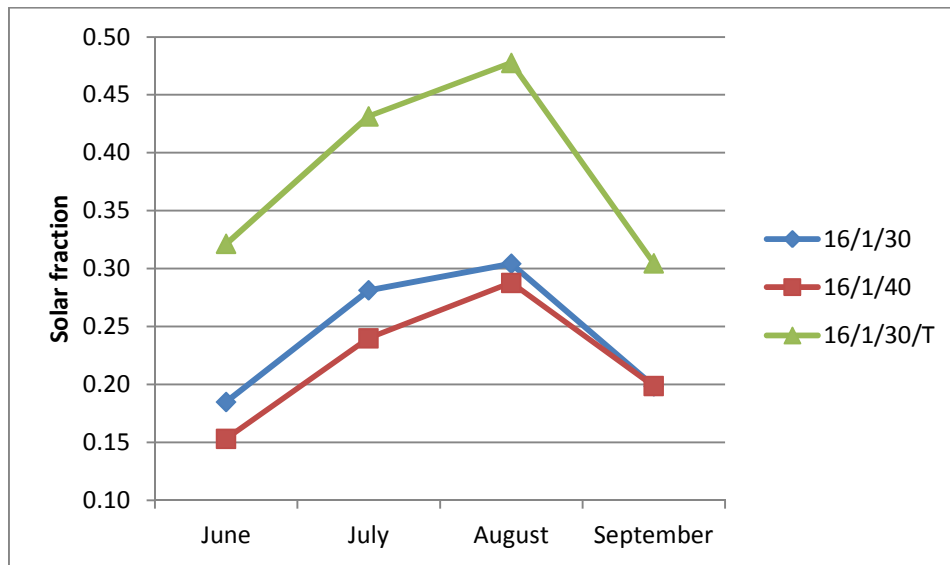


Figure 43. Monthly values of solar fraction for different tilt angles and tracking azimuth for solar assisted cooling system

The presented results indicates that the solar fractions are bigger in average for 2% for collectors tilted on 30° compared to collectors tilted 40°. Much bigger differences can be noticed for collectors with azimuth tracking system, ranging between 10% - 14%.

Another case is analyzed i.e. compared the system presented on Figure 26 with and without cold storage marked with number 8. The analysis is in regard of the solar fraction and cooling tower fan electrical energy consumption since it's the largest energy consumer in the absorption chiller assembly. Analyzed system has 32 m² flat plate solar collector with tilt of 30° south oriented-azimuth 0°, 1500 l hot storage tank and 500 l cold storage tank. Type 534 is used to model the cold storage tank which is divided into isothermal temperature nodes. The degree of stratification is defined through the specification of the number of "nodes" which in this case is five nodes. The building is type II according the description in Table 9 and the control strategy and internal heat gains are in accordance with the previously described.

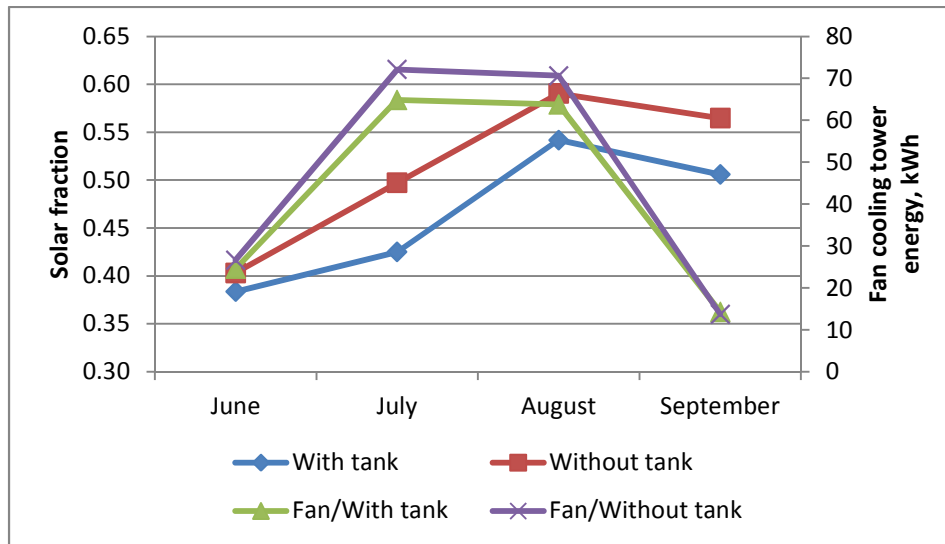


Figure 44. Solar fraction and fan cooling tower energy consumption for system with and without storage tank for solar assisted cooling system

According to the presented results on Figure 44, the conclusion is that installing a cold storage tank between the absorption chiller and building cooling system will cause a decrease in the solar fraction but will also decrease the fan cooling tower electrical consumption. The decrease in solar fraction can be explained by the fact that the stored chilled water causes a decrease in charging/discharging the hot storage tank, thus the collector is in stagnation for more of the time. Graphical presentation of the previous explanation is given with the diagram on Figure 45.

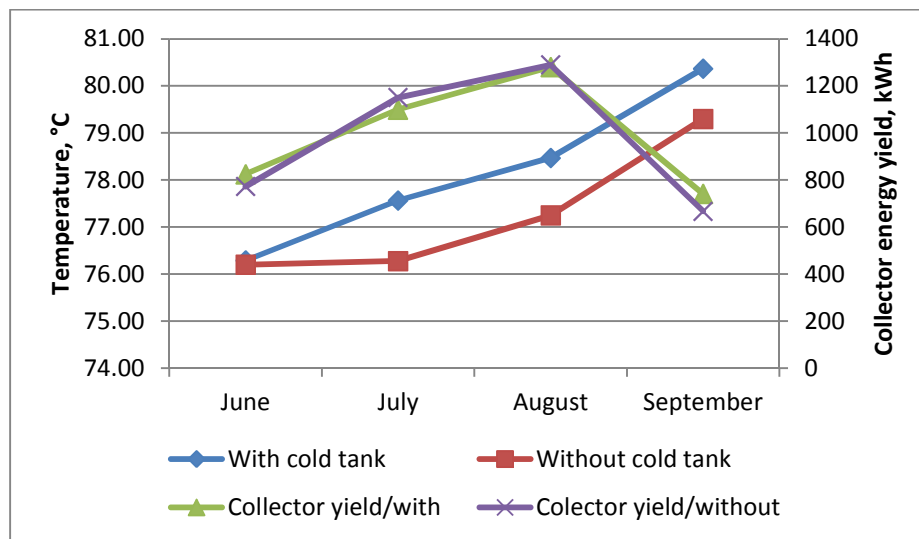


Figure 45. Monthly average storage tank temperature and solar collector yield in regard of system with/without cold storage tank for solar assisted cooling system

6.3.2 Scenario 2

This scenario considers the same system as described in Scenario 1, only the collectors are vacuum type. The analysis is directed toward comparison between the flat plate and vacuum tube collectors regarding the solar fraction and thermal efficiency in a solar cooling system.

Chapter 6. Simulation results and analysis

Vacuum tube collector are product of Camel Solar CS15, with technical data given in Table 2. The reference building is the type II as described in Table 9 and two cases with hot water storage tanks volumes of 1000 l and 1500 l.

Table 17. Average solar fraction and thermal efficiency of solar cooling system in regard of collector area and storage tank volume for solar assisted cooling system

Vacuum tube collector, tank 1 500l, specific flow rate 50 kg/h m ² , tilt 30°, azimuth 0°					
Solar collector area, m ²	10	14	16	18	22
Sol.fraction	0.42	0.60	0.66	0.70	0.77
Avg_Efficiency	0.52	0.44	0.41	0.39	0.35
Vacuum tube collector, tank 1 000l, specific flow rate 50 kg/h m ² , tilt 30°, azimuth 0°					
Solar collector area, m ²	10	14	16	18	22
Sol.fraction	0.46	0.59	0.66	0.71	0.78
Avg_Efficiency	0.48	0.46	0.43	0.41	0.37

Simulations were performed for storage tanks with volumes 1 000 l and 1500 l taking the collector area as parameter with areas of 10, 14, 16, 18 and 22 m² where aperture area one collector module is 1,42 m² which has 15 vacuum tubes. Solar fractions as presented in Table 17 range between 42% for collector array of 10 m² up to 78 % with collector array of 22 m². As expected, for same collector areas thermal efficiency decreases with the decrease of the storage tank volume. Although with 22 m² can be achieved solar fractions of 78% limiting factor is the economic viability of the system which should have reasonable payback meaning it should correspond i.e. lower than the lifetime period of the system .

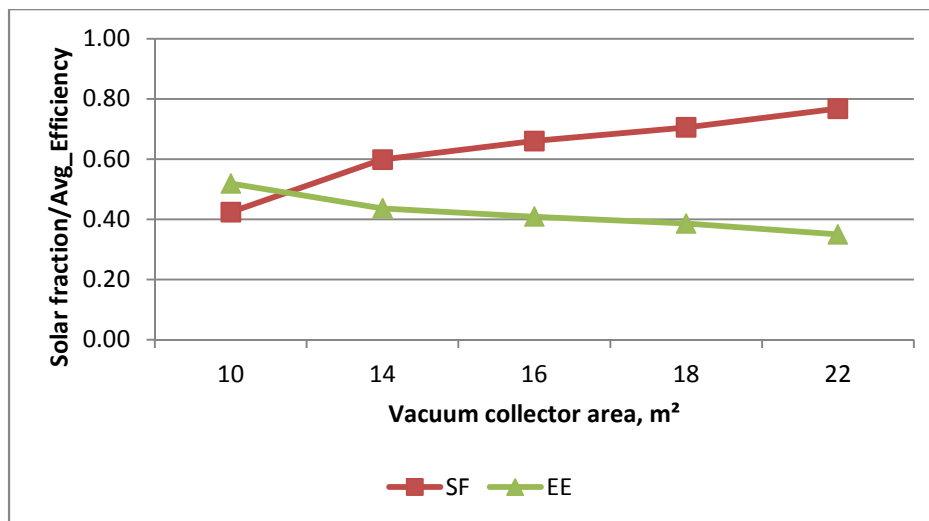


Figure 46. Solar fraction and thermal efficiency in regard of collector area for solar assisted cooling system

Table 18. Solar fraction and thermal efficiency for different specific vacuum collector areas storage volumes for solar assisted cooling system

Vacuum tube collector, tilt 30 °, azimuth 0°			
Specific coll.area	0.1 m ² /m ² _{condit.} 70 l/m ²	0.1 m ² /m ² _{condit.} 105 l/m ²	0.1 m ² /m ² _{condit.} 142 l/m ²
Solar fraction	0.62	0.60	0.59
Avg_efficiency	0.41	0.44	0.46

Chapter 6. Simulation results and analysis

In Table 18 are results for the analyzed cases with specific collector area of 0.1 m^2 per m^2 conditioned area varying the specific storage tank volume per collector area used to determine the solar fractions and thermal efficiency.

According the presented results in Table 18 and Table 19, optimizing between values of the solar fraction and thermal efficiency, results recommendation of 60 l storage volume per square meter vacuum tube collector area. Vacuum tube collectors have bigger specific storage volume compared to the flat plate collectors (30 l/m^2) since they have higher efficiency at higher working fluid temperatures.

6.4 Techno-economic analysis

An important part of the development of any project is the evaluation of its profitability. At the first stage of evaluation the consequences of project financing are normally not considered. Thus, the consequences of loan interest, taxes, grants, subsidies etc. are not taken into account in the project profitability calculations.

The economic viability of a solar energy system depends on two factors: (1) the value of conventional energy displaced (fuel cost savings) and (2) the capital cost of hardware necessary to achieve those savings. There are two principal approaches to economic analysis that are related payback analysis and cost of delivery energy.

There are many factors that affect the decision to adopt a new technology including the real or perceived risks, the economic attractiveness as expressed by some figure of merit and the status as an innovator or trendsetter. The economic evaluation of a solar application includes factors such as the capacity cost of delivering solar energy, the optimum sizing of collectors and other equipment the costs of competing technologies and financial analyses. There figures of merit that are used to accept or reject particular solar application including simple payback, cash flow , capital cost per unit of energy saved, life cycle cost, net present value and levelized energy cost.

To establish cost goals for a future technology the analysis of the economics of active solar systems can be turned around to ask the question: Based on the value on energy savings, how much can be spent on the system? This value becomes the cost goal for the system. For a range of economic assumptions, an analysis considering a 5-year or 7 year simple payback is assumed to be an adequate figure of merit to establish cost goals for active solar cooling and heating technologies. For residential applications, a payback period of 5 - 7 years may consider as acceptable.

Relatively short payback periods required for market acceptance of a new technology, fuel-escalation rates do not greatly change the required cost-goal multiplier. Certainly, for estimating the approximate cost goals for future technologies, the uncertainties generated by assuming a simple

Chapter 6. Simulation results and analysis

payback period are smaller than the uncertainties of future costs of collectors and other components. The actual cost of energy at the time when future systems are proposed and built has a significant impact on the future economic attractiveness of solar options.

6.4.1 Evaluating cost effectiveness

To evaluate the cost effectiveness of system that have not yet been built requires: (1) estimating the load to be served and calculating the contribution of the active solar system to meet the load, (2) calculating the contribution of an efficient conventional system to meet the same load and there by establish the energy and fuel cost savings attributable to the solar system, (3) estimating the cost of active solar system with full back up and the cost of conventional system, (4) comparing the energy cost savings to the incremental solar system cost with suitable economic assumptions.

In the design of a solar system, the performance of a specific application is calculated by use of simplified design methods or it is modeled in detail.

The performance of future conventional space-conditioning systems affects the economic potential of active solar systems. The performance and cost of today's conventional heating, cooling and domestic hot water system can be readily determined, but conventional heating and cooling technology is constantly improving.

As mentioned previously in the text, first should be determined the building heating/cooling loads. In the analysis it is considered the reference Building (type II) with specific energy consumption of $70 \text{ kWh/m}^2 \text{ a}$ for which with the simulation are determined the heating and cooling loads. The time step used in the simulations is 7,5 min and the heating and loads are integrated on hourly basis. On Figure 47 are presented results from the simulation of solar assisted heating with flat plate collectors varying their total area 16 m^2 , 32 m^2 , 64 m^2 , mass flow rates are 50 kg/h m^2 and constant heat storage tank of 1000 l. Collectors are tilted 40° toward south – azimuth 0° also is installed 200l DHW storage tank heating with the same collector array only in period when the heating storage tank is charged or the condition for the circulation pump is not satisfied.

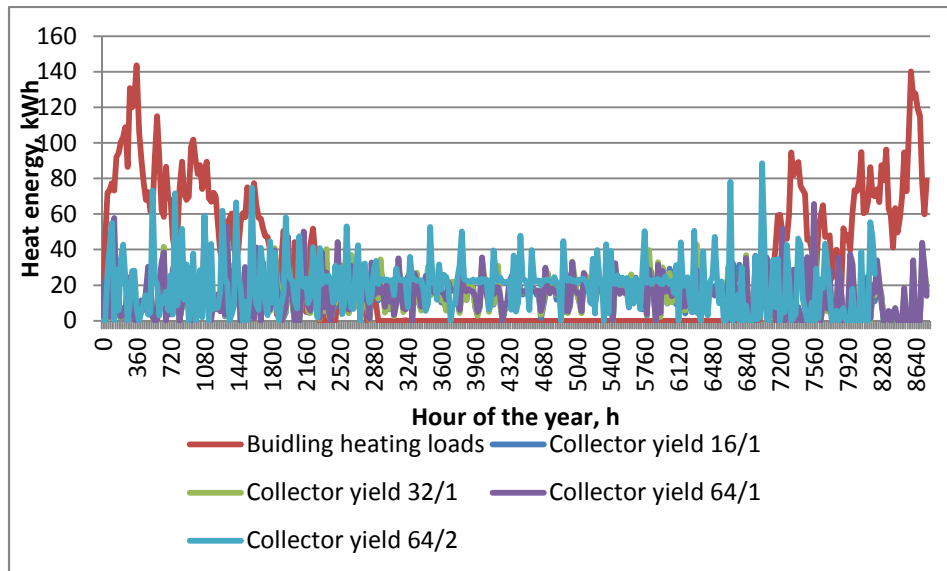


Figure 47. Hourly heating loads and useful heat yield for different collector array areas and constant storage tank of 1000 l and one case for 64 m² with 2000 l

It can be seen that there is no big difference between the solar collector yield of 32 m² and 64 m² since the storage tank capacity is too small to accept the 64 m² collector array solar/heat yield, which results in decrease in solar fraction and stagnation of the collectors.

Since the diagram on Figure 46 is very dense because of the hourly values and cannot be easily noticed the differences, therefore on Figure 47 are also presented collector yields but only for ten days.

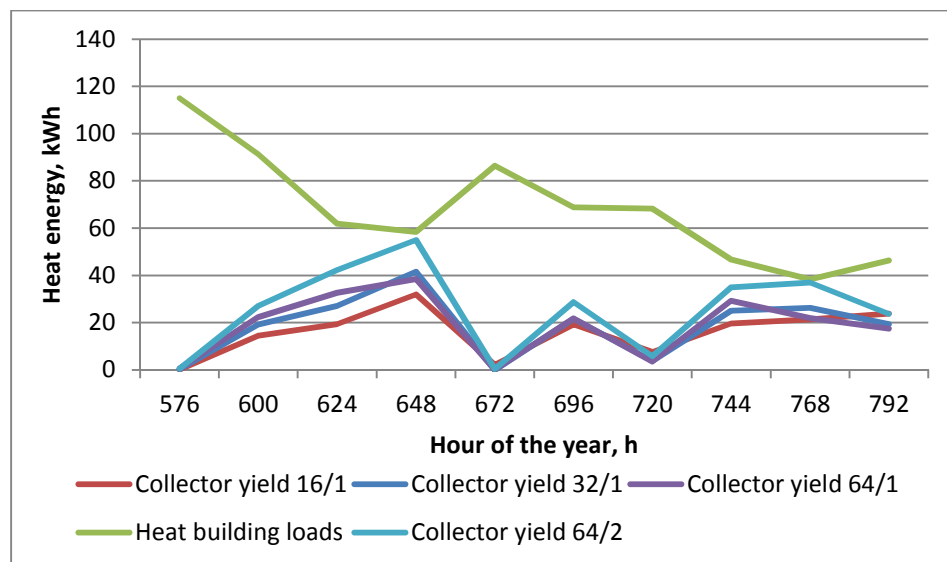


Figure 48. Hourly heating loads and collector energy yield for different areas ten day period

With the obtained building energy heat consumption next step is the LCCA (Life cycle cost analysis) in regard of: auxiliary heat source, collector areas and storage tank. Common for the analyzed systems is that in each of them the heat is distributed through the underfloor heating with

Chapter 6. Simulation results and analysis

flow rate of 2000 kg/h, solar collector array mass flow rate depending from the collector area i.e. 50 kg/h m², auxiliary heat energy is provided by heaters located at the fluid tank outlet with capacity of 12 kW for the heating system and 9 kW for the DHW.

Comparison is performed between different combinations of solar thermal systems and auxiliary heating devices in regard of conventional heating system with electrical boiler. The analyzed solar systems have total solar collector area of 16 m², 32 m² and 64 m² combined with storage tanks of 1000 l, 1500 l and 2000l, and auxiliary heating energy provided by electric heater or heat pump air-water with E.V.I compressors with nominal capacity of 15 kW product of Hidros model Lzti 10.

In Table 19 are presented data for delivered heating energy, annual heating energy cost, system price and the environmental indicator - CO₂ emissions for conventional heating systems with heat sources: electrical energy, wood pellets and heat pump. For the heat pump COP is assumed averaged yearly value of 2,5.

Table 19. Annual energy balance, energy and system costs, CO₂ emissions for conventional heat source systems obtained with simulations, specific heat energy consumption 70 kWh/m² a

Parameter	Unit	Electrical boiler	Pellet boiler	Heat pump
Heat power	kW		12	
Annual delivered heat energy	kWh		13103	
Average thermal efficiency/COP	-	0.99	0.91	2.5
Annual consumed energy	kWh	13235	14399	5241
System electrical energy consumption (circ.pumps)	kWh		144	
Specific energy price	eur/kWh	0.09	0.05	0.09
Total energy price	eur	1203	667	472
Heat source device/system price	eur	800	2000	5000
Annual CO ₂ emissions	kg/year	12177	58	1730

The CO₂ emissions and primary energy consumption factors are provided from the standard “Energy performance of buildings - Overall energy use and definition of energy ratings” EN 15603_2008 [46].

Regarding the energy prices, the electrical energy price (euro/kWh) is provided from the Energy Regulatory Commission of the Republic of Macedonia valid from 01.07.2014 [47], wood pellet energy price is obtained by taking the average market price of 0,2 euro/kg with lower heating value H_d = 4,3 kWh/kg. In Table 20 and Table 21 are given the results for the analyzed solar thermal systems in regard of heat energy consumption, annual energy and system costs and the

Chapter 6. Simulation results and analysis

environmental impact indicator presented by the value for the annual CO₂ (kg/year) annual emissions.

Table 20. Solar thermal system energy performance, costs, parameters and CO₂ emissions, primary energy consumption for building - heat energy consumption 70 kWh/m² a, – part I

<i>Ref. building 70 kWh/m² a</i>		Solar thermal system - Area/Storage tank volume - EH (electric heater) ; HP (heat pump) -						
Parameter	Unit	16/1000-EH	16/1000-HP	32/1000-EH	32/1000-HP	64/1000-EH	64/1000-HP	32/1500-EH
Auxiliary energy - heating system	kWh	8550	8550	7420	7420	6466	6466	6996
Auxiliary energy - DHW	kWh		750		562		428	639
System electrical energy consumption (circ.pumps)	kWh	144	144	114	114	90	90	130
Specific electrical energy price	eur/kWh				0.09			
Total energy price	eur	850	348	729	300	629	256	640
Heat source device/system price	eur	3600	7000	6000	10500	10000	14700	7000
Primary energy consumption	kWh	28777	12790	26798	10946	23117	9426	25702
Annual CO ₂ emissions	kg/year	3069	1275	2672	1091	2305	940	2562
Annual average solar fraction - SF	-		0.19		0.30		0.39	0.34

Table 21. Solar thermal system energy performance, costs, parameters and CO₂ emissions, primary energy consumption for building with specific heat energy consumption 70 kWh/m² a, – part II

Parameter	Unit	32/1500-HP	64/1500-EH	64/1500-HP	32/2000-EH	32/2000-HP	64/2000-EH	64/2000-HP
Auxiliary energy - heating system	kWh	6996	5830	5830	7250	7250	5921	5921
Auxiliary energy - DHW	kWh	639		490				
System electrical energy consumption (circ.pumps)	kWh	130	103	103	138	138	111	111
Specific electrical energy price	eur/kWh				0.09			
Total energy price	eur	287	578	237	665	273	543	223
Heat source device/system price	eur	11500	12000	16500	8000	12500	12800	16700
Primary energy consumption	kWh	10539	21260	8709	24454	10056	19966	8207
Annual CO ₂ emissions	kg/year	1051	2120	868	2438	1003	1991	818
Annual average solar fraction - SF	-	0.34		0.45		0.32		0.44

Further is analyzed how the building energy consumption affects the solar system performance i.e. same systems are applied to building with lower specific heat energy consumption. Thus it is analyzed solar thermal system installed on Building III (as described in Table 9) with specific heat energy consumption on annual basis of 57 kWh/m² a

In order to obtain better insight for the solar thermal system viability, the method of life cycle cost analysis (LCCA) is used to find the cost-effective optimal combination between the solar collector area, storage tank volume and auxiliary heater type. It is obvious that better and feasible combination with heat pump instead of electrical heater although the starting investment is much bigger.

Chapter 6. Simulation results and analysis

Table 22. Solar thermal system energy performance, costs, parameters and CO₂ emissions, primary energy consumption for building with specific heat energy consumption 57 kWh/m² a, – part I

<i>Ref.building 57 kWh/m² a</i>		Solar thermal system - Area/Storage tank volume - EH (electric heater) ; HP (heat pump) -							
Parameter	Unit	16/1000-EH	16/1000-HP	32/1000-EH	32/1000-HP	64/1000-EH	64/1000-HP	32/1500-EH	
Auxiliary energy - heating system	kWh	6708	6708	5762	5762	5418	5418	6192	
Auxiliary energy - DHW	kWh		713		527		402	595	
System electrical energy consumption (circ.pumps)	kWh	139	139	109	109	86	86	115	
Specific electrical energy price	eur/kWh				0.09				
Total energy price	eur	680	280	576	239	532	217	567	
Heat source device/system price	eur	3600	7000	6000	10500	10000	14700	7000	
Primary energy consumption	kWh	22664	10285	21177	8687	19549	7990	22846	
Annual CO ₂ emissions	kg/year	2449	1025	2111	866	1949	797	2278	
Annual average solar fraction - SF			0.22		0.33		0.39	0.28	

Table 23. Solar thermal system energy performance, costs, parameters and CO₂ emissions, primary energy consumption for building with specific heat energy consumption 57 kWh/m² a, – part II

<i>Ref.building 57 kWh/m² a</i>		Solar thermal system - Area/Storage tank volume - EH (electric heater) ; HP (heat pump) -						
Parameter	Unit	32/1500-HP	64/1500-EH	64/1500-HP	32/2000-EH	32/2000-HP	64/2000-EH	64/2000-HP
Auxiliary energy - heating system	kWh	6192	5600	5600	5074	5074	4042	4042
Auxiliary energy - DHW	kWh	595		457		630		488
System electrical energy consumption (circ.pumps)	kWh	115	94	94	118	118	97	97
Specific electrical energy price	eur/kWh				0.09			
Total energy price	eur	255	554	227	524	216	416	172
Heat source device/system price	eur	11500	12000	16500	8000	12500	12800	16700
Primary energy consumption	kWh	9367	20360	8331	19271	7943	15315	6319
Annual CO ₂ emissions	kg/year	934	2030	831	1921	792	1527	630
Annual average solar fraction - SF		0.28		0.36		0.41		0.53

In the following analysis will be considered collector areas of 16 m², 32 m² and 64 m², storage tank volumes of 1000 l, 1500l and 2000l, and for auxiliary heater are considered electrical heater and air-water heat pump.

6.4.2 Life cycle cost analysis

Life Cycle Cost (LCC) analysis is an economic method of project evaluation in which all costs occurring from building, owning, operating, maintaining and ultimately demolishing/disposing of the project are taken into consideration. In a LCC analysis the costs occurring at different time is discounted to their present value.

The investment includes all expenses connected to the realization of the project, normally the following elements: Design/Planning, project Management / quality assurance, components installation, control and testing, as-built document, commissioning, training, other expenses, taxes, VAT.

Chapter 6. Simulation results and analysis

Technical life is the physical lifetime of the investment/equipment, i.e. for how long the equipment technically can operate. Economic life is the practical lifetime for the investment/equipment, i.e. the lifetime before it is profitable to change into new equipment.

If components/products are being replaced before they are worn out as a result of new and more efficient components available on the market, then the economic lifetime is shorter than the technical lifetime. Changes in standards and regulations, energy prices, comfort levels, etc. may also lead to replacing equipment prior to the end of their technical life.

Inflation “b”, is defined as the yearly average price increase for all consumer goods. In this analysis the inflation is considered to be 2 %.

A discount rate n_r , is used to calculate the present value of, for instance, future energy savings, adjusted for the cost of capital. Discount rates could be in nominal or real terms, where the real discount rate is adjusted to eliminate the effects of expected inflation. The nominal discount rate includes the expected general inflation. The real discount rate is the nominal rate corrected for inflation, relative increase of energy price, and other possible relative price increases. In this case the nominal discount rate is 6 % and the real discount rate calculated with Equation 68 is:

$$r = \frac{n_r - b}{1 + b} \quad (68)$$

6.4.3 Calculation of Profitability

There are a number of methods to calculate the profitability of investments:

- Payback
- Net Present Value
- Net Present Value Quotient
- Pay-Off
- Internal Rate of Return

The discounted value (present value) concept is the basis for several of these methods. The following parameters are used for the calculations:

- Investment I_0 [€]
- Annual net savings B [€/year]
- Economic lifetime n [year]
- Real discount rate $r \cdot 100$ [%]

The simple payback is the time it takes to pay back the investment, based on equal annual net savings. If the payback is longer than economic lifetime of the measure, the measure is not

Chapter 6. Simulation results and analysis

profitable. The Payback method is useful for quick calculations, but there are limitations: It should be used when the real discount rate is low, if payback period is less than 4 - 5 years and if the method ignores the value of annual savings after the payback period.

In order to summarize the discounted value of the future annual savings, it is necessary to define a reference year, to which all investments and savings should be related. All in- and outgoing payments should be related to the same reference year. Normally, the selected year is the one in which the investments are made (year 0). The Net Present Value (NPV) of a measure or project is today's value of all the future annual net savings during the economic life time minus the initial investment. The NPV of a measure or project is today's value of all the future annual net savings during the economic life time minus the initial investment. The NPV value must be positive in order the measure to be profitable.

The Pay-off is the time it takes to repay the investment, considering the real discount rate. This means the number of years that makes the NPV equal to 0.

The IRR is the interest rate that equates the net present value of future savings/cash flow over the economic lifetime of the assets to the cost of the investment.

The Net Present Value Quotient, NPVQ, is the ratio between the Net Present Value and the total investment. The highest NPVQ indicates the most profitable measure. The NPVQ could be used for internal ranking of energy efficiency measures

The LCC method provides a better assessment of the long-term cost-effectiveness of the project/measure than other economic methods which only focus on initial investment costs and operation costs for the first years. At the same time, a LCC analysis requires more information than other profitability evaluation methods. The lowest Life Cycle Costs indicates the most profitable investment, measure or solution.

Chapter 6. Simulation results and analysis

Table 24. LCCA for solar thermal system assisted building heating with specific heat energy consumption 70 kWh/m² a

Real interest rate 3,9% ; Building 70 kWh/m² a

Measures	Investment	Net savings	Lifetime	PB	PO	IRR	NPV	NPVQ	ax.Investment	
	EUR	EUR/Year	Year	Year	Year	%	EUR		EUR	Year
Pellet boiler	2000	506	20	4	4.4	25	4.93	2.46	4.12	12
Heat pump	5000	671	20	7.5	9	12	4.18	0.84	6.34	12
HP 16/1-1000	7000	814	20	8.6	10.7	10	4.14	0.59	7.687	12
HP 32/1-1000	9700	849	20	11.4	15.5	6	1.919	0.20	8.017	12
EH 16/1-1000	3600	312	20	11.5	15.7	6	670	0.19	2.946	12
HP 32/1-1500	10700	864	20	12.4	17.3	5	1.125	0.11	8.159	12
EH 32/1-1500	7000	511	20	13.7	20	4	-7	0.00	4.825	12
EH 32/1-1000	6000	421	20	14.3	21.3	3	-239	-0.04	3.975	12
EH 32/1-2000	8000	487	20	16.4	26.9	2	-1.335	-0.17	4.599	12
HP 64/1-1000	14700	881	20	16.7	27.6	2	-2.643	-0.18	8.319	12
HP 64/1-1500	16500	902	20	18.3	32.9	1	-4.156	-0.25	8.518	12
HP 32/1-2000	16500	868	20	19	35.6	0	-4.621	-0.28	8.196	12
HP 64/1-2000	17300	896	20	19.3	36.8	0	-5.038	-0.29	8.461	12
EH 64/1-1000	10000	509	20	19.7	38.3	0	-3.034	-0.30	4.806	12
EH 64/1-1500	12000	560	20	21.4	47.7	0	-4.336	-0.36	5.288	12
EH 64/1-2000	12800	596	20	21.5	48	0	-4.644	-0.36	5.628	12

PB=Payback, PO=Pay-off, IRR=Internal Rate of Return, NPV=Net Present Value, NPVQ=Net Present Value Quotient,
 * Maximum investment [EUR] with [Years] pay-off

According to the presented results several conclusions can be drawn. As most profitable measure according to the LCC analysis is the measure with the highest NPVQ. Thus, most profitable would be installing pellet boiler as unique heating source with payback period of 4 years. Next profitable measure would be solar system with total collector area of 16 m² and heat pump as additional auxiliary heat source. Further follow the systems with collector array areas of 32 m² and 64 m² with different storage tank volumes in combination with auxiliary heat device electric heater (EH) or heat pump (HP). LCC analysis reveals that for same collector area and storage tank volume more profitable is the combination solar collectors with heat pump instead with electric heater although the starting investment is far lower for electric heater but energy savings contribute to have lower payback period for the heat pump system.

It can be noticed from Table 24 that the net present values for all of the system combinations with 64 m² collectors, have negative values which indicates that those systems are not profitable for buildings with specific heat energy consumption of 70 kWh / m² a.

Next is LCC analysis for the same solar thermal systems but applied to building with lower specific heat consumption of 57 kWh/m² a, represented with the Building type III described in Table 9.

Chapter 6. Simulation results and analysis

Table 25. LCCA for solar thermal system assisted building heating with specific heat energy consumption 57 kWh/m² a

Real interest rate 3,9% ; Building 70 kWh/m² a

Measures	Investment	Net savings	Lifetime	PB	PO	IRR	NPV	NPVQ	ax. Investment	
	EUR	EUR/Year	Year	Year	Year	%	EUR		EUR	Year
Pellet boiler	2000	314	20	6.4	7.5	15	2.297	1.15	2.965	12
Heat pump	5000	571	20	8.8	10.9	10	2.814	0.56	5.392	12
HP 16/1-1000	7000	702	20	10	12.9	8	2.607	0.37	6.629	12
EH 16/1-1000	3600	301	20	12	16.5	6	519	0.14	2.842	12
HP 32/1-1000	9700	730	20	13.3	19.1	4	290	0.03	6.893	12
HP 32/1-1500	10700	715	20	15	23	3	-915	-0.09	6.752	12
EH 32/1-1000	6000	393	20	15.3	23.7	3	-622	-0.10	3.711	12
HP 32/1-2000	12500	754	20	16.6	27.3	2	-2.181	-0.17	7.12	12
EH 32/1-1500	7000	393	20	17.8	31.2	1	-1.622	-0.23	3.711	12
EH 32/1-2000	8000	446	20	17.9	31.6	1	-1.896	-0.24	4.212	12
HP 64/1-1000	14700	768	20	19.1	36.1	0	-4.19	-0.29	7.252	12
HP 64/1-2000	17300	786	20	22	51.7	0	-6.453	-0.38	7.422	12
EH 64/1-1000	10000	454	20	22	51.8	0	-3.787	-0.38	4.287	12
HP 64/1-1500	16500	731	20	22.6	56.3	0	-6.496	-0.39	6.903	12
EH 64/1-2000	12800	542	20	23.6	67.7	0	-5.383	-0.42	5.118	12
EH 64/1-1500	12000	404	20	29.7	99	0	-6.471	-0.54	3.815	12

PB=Payback, PO=Pay-off, IRR=Internal Rate of Return, NPV=Net Present Value, NPVQ=Net Present Value Quotient,
 * Maximum investment [EUR] with [Years] pay-off

In order to obtain better visibility of the results presented in Table 24 and Table 25 it is constructed diagram Figure 49 between the heating system/source type and the simple payback period for the two building types and only the system with positive NPV are taken into account.

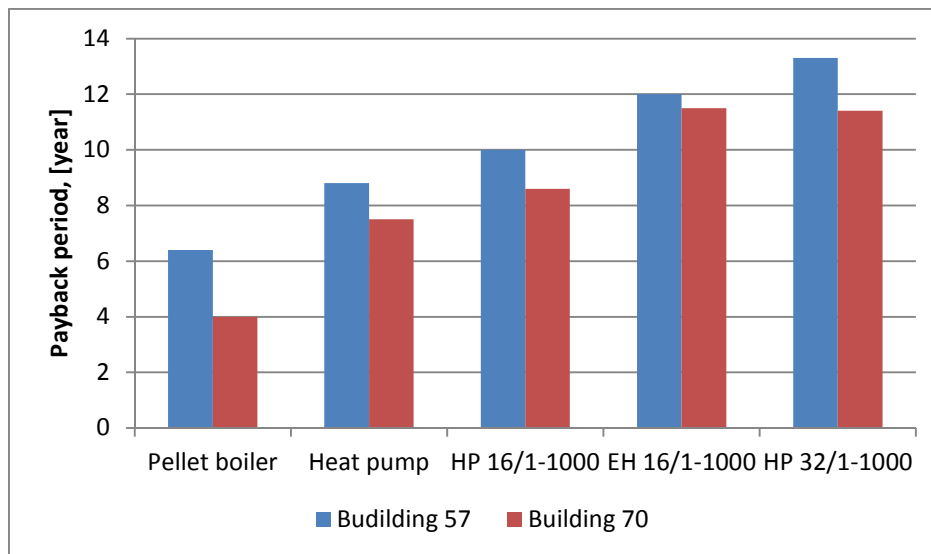


Figure 49. Payback time for solar thermal systems for two building types regarding the specific heat energy consumption

It's interesting to be noticed that same solar thermal systems for the building with the higher specific energy consumption have lower payback period since they have bigger energy consumption thus generating bigger energy differences between the basic scenario with electrical boiler and the solar system. This is comparison between same systems but also should be noticed that with same systems at the building with lower specific heat consumption are achieved bigger

Chapter 6. Simulation results and analysis

solar fractions. Another comparison is performed for the same solar thermal systems in regard of the primary energy consumption given on Figure 48.

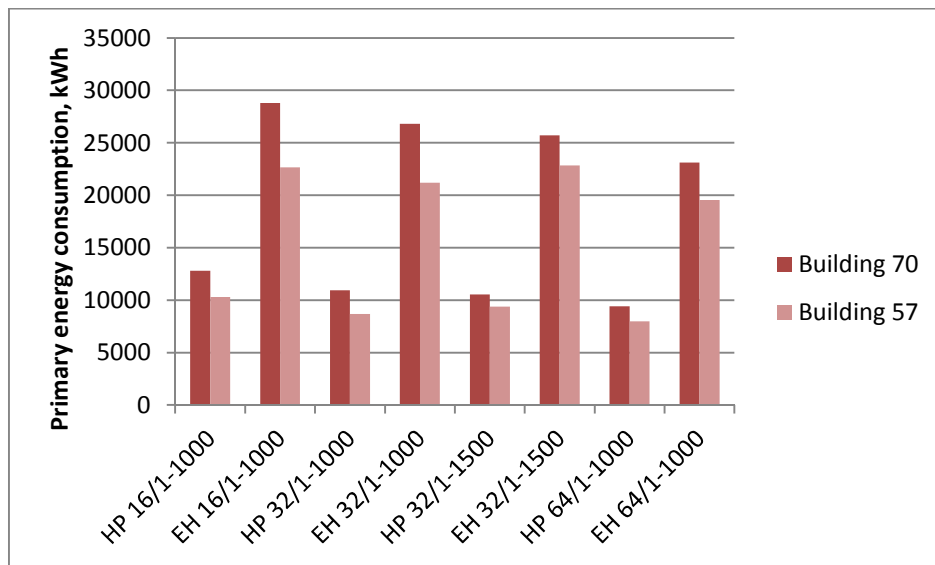


Figure 50. Primary energy consumption for solar thermal systems in regard of two buildings with different specific heat energy consumption $57 \text{ kWh/m}^2 \text{ a}$ and $70 \text{ kWh/m}^2 \text{ a}$

Differences in primary energy consumptions are noticeable for the same solar systems applied in the two buildings i.e. logically much lower primary energy consumption and lower CO_2 emissions for the building with lower specific heat energy but it's interesting that especially the differences are expressed at the smaller collector areas with electrical heater as auxiliary device. Also from the presented LCC analysis can be concluded that for same collector areas it is more cost-effective the auxiliary source to be heat pump instead of electrical heater although the investment is higher for the HP but on longer period is more feasible. On Figure 51 are given specific costs per kW cooling power for absorption chillers. The costs are from manufacturers based on Germany and from a survey of the international energy agency. According the presented costs for the analysis is chosen that the absorption chiller as ne assembly with the cooling tower costs 1500 eur/kW i.e. total $15\,000 \text{ eur}$.

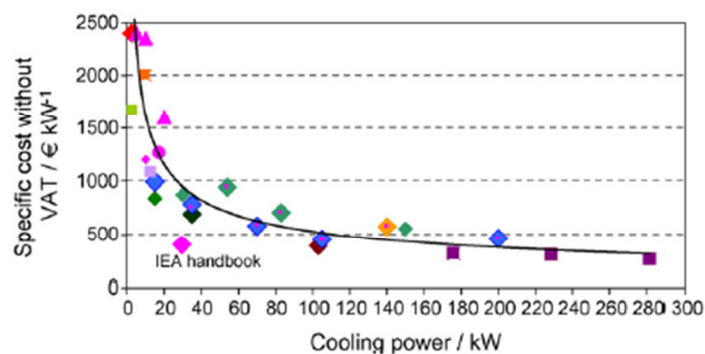


Figure 51. Specific absorption chiller costs per kW cooling power [48]

Chapter 6. Simulation results and analysis

In the next Table 26 are presented results from the comparison between the energy consumption, system costs, primary energy consumption and CO₂ emissions for the chiller conventional system and the solar assisted absorption cooling.

Table 26. Solar thermal system energy performance, costs, parameters and CO₂ emissions, primary energy consumption for building with cooling energy consumption 12 kWh/m²a

Conventional chiller cooling - average EER 3 - 600 kWh/year		Solar thermal system - Area/Storage tank volume = 1000 l					
Parameter	Unit	Chiller	10/1000-EH	14/1000-EH	16/1000-EH	18/1000-EH	22/1000-EH
Auxiliary energy - cooling system	kWh	600	324	246	204	174	132
Auxiliary energy - DHW	kWh	835			0		
Absorption electrical energy	kWh				461		
System electrical energy consumption (circ.pumps)	kWh	293			90		
Specific electrical energy price	eur/kWh				0.09		
Total energy price	eur	156	79	22	18	16	12
Heat source device/system price	eur	6500			15000		
Primary energy consumption	kWh	5720	2896	2638	2499	2400	2261
Annual CO ₂ emissions	kg/year	570	289	263	249	239	225
Annual average solar fraction - SF	%		46	59	66	71	78

The performance data for absorption cooling machine are given in Appendix D. It is assumed that the chiller average cooling coefficient of performance is 3 and regarding the building cooling loads in the simulations is used the Building type II for which the annual cooling load is 1800 kWh. The DHW in the case of conventional chiller is heated 100% by electrical heater while in the case of absorption machine the area of solar collectors are sufficient to provide 100% solar fraction for the DHW i.e. it is not used any additional auxiliary energy.

The cooling period considers four months starting from June until September and the inside temperature is set to be constant 26 °C.

The primary energy and CO₂ factors are the same as previously i.e. are used from the standard “Energy performance of buildings - Overall energy use and definition of energy ratings” EN 15603_2008 [46].

According the presented results can be concluded that there is no need to be performed LCC analysis since the simple payback period is bigger than 20 years. Main reasons for the non-feasibility of these solar-assisted air-conditioning systems mainly is the low electricity price of 0.09 eur/kWh but also is the low cooling energy demand since it is analyzed residential building which usually have small internal gains. Nevertheless according the results in Table 26 the solar – assisted cooling systems provides big possibilities for decrease in primary energy consumption and CO₂ emissions.

Chapter 7

7. Summary and recommendations for further work

A solar system can be designed to satisfy any particular space and water heating application. Technically considered it is feasible to design a system which can satisfy 100% of the heating needs of a building, but generally it is economically not profitable solution. In practice solar heating systems are designed to displace up to about 50% of conventional fuel needs and require auxiliary heating systems that are fully capable of supplying the total heating load when no solar energy is being collected and when solar energy has been depleted.

When solar heating is designed for space heating systems it is economical to include solar heating of domestic hot water (DHW) in the system. In the residential systems during the summer, when there is no space heating load, the entire solar system can be devoted to water heating so that solar can supply a substantial portion if not all of the DHW heating needs. However, for large commercial systems, summer operation to provide a relatively small DHW demand may not be worthwhile.

The size of a solar system (primarily the storage volume and collector area) for a particular building depends on the portion of the total load of the system is expected to provide. Size is also strongly dependent from the climate and location

In this thesis were analyzed the thermal performances of solar assisted heating and cooling systems. Main leading parameters for assessment of the system are the solar fraction of the heating and DHW systems i.e. energy provided by solar collectors and auxiliary heat energy and the collector efficiencies. Thus for the needs of assessment, simulation model of solar assisted air-conditioning system was developed in TRNSYS. The analyzed system main components are: solar collectors, storage tank, auxiliary heater building and hydraulic components.

First analysis was performed to examine the influence of the heating system type (radiator and underfloor heating) to the system thermal performance i.e. to the solar fraction, collector efficiency and “real” efficiency. In the analysis also were considered different: collector areas (16 m², 32 m²

Chapter 7. Summary

and 64 m^2), storage tank volumes (1000 l, 1500l, 2000 l) and three types of buildings (I, II, III) with different specific heat consumptions $90 \text{ kWh/m}^2 \text{ a}$, $70 \text{ kWh/m}^2 \text{ a}$ and $57 \text{ kWh/m}^2 \text{ a}$ respectively. Results from the simulation showed that for building type I i.e. specific heat consumption of $90 \text{ kWh/m}^2 \text{ a}$, 16 m^2 collector area, storage tank 1000 l and radiator heating solar energy can cover 8% from the annual heat energy needs while the maximum solar fraction of 52% is achieved for Building III ($57 \text{ kWh/m}^2 \text{ a}$) with underfloor heating system 64 m^2 collector area and 2000l storage tank. with $0,1 \text{ m}^2/\text{m}^2_{\text{conditioned}}$ specific collector area per conditioned surface can be achieved between 20 – 25 % solar fraction, with $0,2 \text{ m}^2/\text{m}^2_{\text{conditioned}}$ range round 35% , and with $0,4 \text{ m}^2/\text{m}^2_{\text{conditioned}}$ maximum 50 %. It should be noted that the solar fraction also strongly depends from the storage tank volume and for the radiator heating system increasing the storage volume results in decrease of solar fraction while at the underfloor heating its vice versa. It is recommended the storage volume to be in the range 50-60 l/ m^2 collector area in order to optimize between the solar fraction and collector efficiency.

Further, analysis is done for solar assisted cooling system with vacuum tube collectors and same volumes of storage tanks and building types as described previously. Obtained results show that solar fractions increase with the increase of collector area and storage volume and vary in range between 20% up to 70%. Also the thermal efficiency should not be neglected which in the analyzed cases is in the range between 15% up to 27% monthly averages. Solar fraction for the DHW is almost in every case 100% since the daily consumption is very low compared to the available energy from the solar collectors.

Specific indicators for solar fraction in regard of the ratio between solar collector area and conditioned area are: $0,1 \text{ m}^2 / \text{m}^2_{\text{conditioned}}$ can cover almost 30% , $0,2 \text{ m}^2 / \text{m}^2_{\text{conditioned}}$ covers 50% and $0,4 \text{ m}^2 / \text{m}^2_{\text{conditioned}}$ can cover 70% of the total required heating energy for driving the absorption chiller. Analyzing the solar fraction for one constant specific collector area and changing only the storage volume can be noticed that biggest fractions are for 30 l/ m^2 specific storage tank volume per collector area for vacuum tube collectors.

Installing cold storage tank between the absorption chiller and building cooling system will cause decrease in the solar fraction but also will decrease the fan cooling tower electrical consumption. The decrease in solar fraction can be explained with the fact that the stored chilled water causes decrease in charging/discharging the hot storage tank thus collector more of the time is in stagnation.

The analysis is separated in two parts: first is solar collectors only for heating and second analysis is solar collectors for cooling with absorption chillers. As referent system for comparison

Chapter 7. Summary

is selected electrical boiler i.e. all of the savings and payback periods are calculated against electrical energy costs. Also in the comparison are considered pellet boiler and heat pump.

Results show that most profitable would be installing pellet boiler as heating source 100% covering the heating needs, with payback period of 4 years. Second profitable measure would be solar system with total collector area of 16 m² and heat pump as additional auxiliary heat source. Further follows the systems with collector array areas of 32 m² and 64 m² with different storage tank volumes in combination with auxiliary heat device electric heater (EH) or heat pump (HP). LCC analysis reveal that for same collector area and storage tank volume more profitable is the combination solar collectors with heat pump instead with electric heater although the starting investment is far lower for electric heater but energy savings contribute to have lower payback period for the heat pump system.

Solar cooling is not yet feasible solution for the residential sector. Main reasons are the low specific cooling energy consumption, low electricity price and high investment cost for the absorption chiller. However, solar energy showed that can be achieved big primary energy savings resulting with more than 50% compared with the conventional energy sources i.e. electrical energy. Thus can be said that solar energy is environmental friendly also decreasing to a high extent the greenhouse gasses emissions.

Further recommendation is to be researched the technical and economic feasibility of implementation solar assisted air-conditioning systems in commercial buildings since they have high internal loads thus offering potential for big energy savings.

Bibliography

1. *Communication energy 2020—A strategy for competitive sustainable and secure energy*, E.C. Brussels, Editor. 2010.
2. (ESTIF), E.S.T.I.F., *The Spanish Technical Building Code (Royal Decree 314/2006)*. 2006. p. 42.
3. ESTIF, E.S.I., *Best practice regulations for solar thermal*. 2007. p. 61.
4. International Energy Agency, I., *Technology Roadmap-Solar Heating and Cooling*. 2012.
5. Ampatzi, E., I. Knight, and R. Wiltshire, *The potential contribution of solar thermal collection and storage systems to meeting the energy requirements of North European Housing*. *Solar Energy*, 2013. **91**(0): p. 402-421.
6. Argiriou, A.A., *CSHPSS systems in Greece: Test of simulation software and analysis of typical systems*. *Solar Energy*, 1997. **60**(3-4): p. 159-170.
7. Henning, H.-M. and J. Döll, *Solar Systems for Heating and Cooling of Buildings*. *Energy Procedia*, 2012. **30**(0): p. 633-653.
8. Pinel, P., et al., *A review of available methods for seasonal storage of solar thermal energy in residential applications*. *Renewable and Sustainable Energy Reviews*, 2011. **15**(7): p. 3341-3359.
9. H-M, H., *Primary energy and economic analysis of combined heating, cooling and power systems*. *Energy and Buildings*, 2011. **36**: p. 575-85.
10. CRES. "Market Study", D.D.p.a.p.o.t.E.p., *High solar fraction heating and cooling systems with Combination of innovative components and methods*. 2011: Athens.
11. Papadopoulos, A.M., S. Oxizidis, and N. Kyriakis, *Perspectives of solar cooling in view of the developments in the air-conditioning sector*. *Renewable and Sustainable Energy Reviews*, 2003. **7**(5): p. 419-438.
12. Lamp, P. and F. Ziegler, *European research on solar-assisted air conditioning*. *International Journal of Refrigeration*, 1998. **21**(2): p. 89-99.
13. Karagiorgas, M., et al., *HOTRES: renewable energies in the hotels. An extensive technical tool for the hotel industry*. *Renewable and Sustainable Energy Reviews*, 2006. **10**(3): p. 198-224.
14. Federation, E.S.T.I. *Trends and Market Statistics 2012*. 2013.
15. ASHRAE, *HAVC APPLICATIONS*, in *ENERGY-RELATED APPLICATIONS*. 2007, ASHRAE: Atlanta.
16. Henning, H.-M., *Solar assisted air conditioning of buildings – an overview*. *Applied Thermal Engineering*, 2007. **27**(10): p. 1734-1749.
17. Bilgili, M., *Hourly simulation and performance of solar electric-vapor compression refrigeration system*. *Solar Energy*, 2011. **85**(11): p. 2720-2731.
18. Henning, H.-M., *Air-Conditioning in Buildings, A Handbook for Planners*. 2007, New York: Springer. 150.
19. García Casals, X., *Solar absorption cooling in Spain: Perspectives and outcomes from the simulation of recent installations*. *Renewable Energy*, 2006. **31**(9): p. 1371-1389.
20. Srihirin, P., S. Aphornratana, and S. Chungpaibulpatana, *A review of absorption refrigeration technologies*. *Renewable and Sustainable Energy Reviews*, 2001. **5**(4): p. 343-372.
21. Ayyash, S., *An assessment of the feasibility of solar absorption and vapor compression cooling systems*. *Energy Conversion and Management*, 1981. **21**(2): p. 163-169.
22. Butz, L.W., W.A. Beckman, and J.A. Duffie, *Simulation of a solar heating and cooling system*. *Solar Energy*, 1974. **16**(3-4): p. 129-136.
23. Eicker, U. and D. Pietruschka, *Design and performance of solar powered absorption cooling systems in office buildings*. *Energy and Buildings*, 2009. **41**(1): p. 81-91.
24. Haim, I., G. Grossman, and A. Shavit, *Simulation and analysis of open cycle absorption systems for solar cooling*. *Solar Energy*, 1992. **49**(6): p. 515-534.

25. Kalogirou, S.A., *Chapter six - Solar Space Heating and Cooling*, in *Solar Energy Engineering*, S.A. Kalogirou, Editor. 2009, Academic Press: Boston. p. 315-389.
26. Klein, S.A., W.A. Beckman, and J.A. Duffie, *A design procedure for solar air heating systems*. *Solar Energy*, 1977. **19**(5): p. 509-512.
27. Kumar, P. and S. Devotta, *Analysis of solar absorption cooling systems with low generator temperatures*. *International Journal of Refrigeration*, 1985. **8**(6): p. 356-359.
28. Oonk, R.L., W.A. Beckman, and J.A. Duffie, *Modeling of the CSU heating/cooling system*. *Solar Energy*, 1975. **17**(1): p. 21-28.
29. Vargas, J.V.C., et al., *Modeling, simulation and optimization of a solar collector driven water heating and absorption cooling plant*. *Solar Energy*, 2009. **83**(8): p. 1232-1244.
30. Zhai, X.Q. and R.Z. Wang, *A review for absorption and adsorption solar cooling systems in China*. *Renewable and Sustainable Energy Reviews*, 2009. **13**(6-7): p. 1523-1531.
31. Herold, K.E., Radermacher, R., Klein, S.A., *Absorption chillers and heat pumps* 1996, Boca Raton, FL: CRC Press.
32. Filipe Mendes, L., M. Collares-Pereira, and F. Ziegler, *Supply of cooling and heating with solar assisted absorption heat pumps: an energetic approach*. *International Journal of Refrigeration*, 1998. **21**(2): p. 116-125.
33. Eisa, M.A.R., et al., *Thermodynamic design data for absorption heat pump systems operating on water-lithium bromide part II: Heating*. *Applied Energy*, 1986. **25**(1): p. 71-82.
34. Chua, H.T., et al., *Improved thermodynamic property fields of LiBr-H₂O solution*. *International Journal of Refrigeration*, 2000. **23**(6): p. 412-429.
35. Macriss, R.A., T.S.Zawacki, *Absorption fluid data survey* 1989, Institute of gas technology: Chicago, Illinois. p. 286.
36. Braun, R.J., et al., *Chapter 7 - Analysis, Optimization, and Control of Solid-Oxide Fuel Cell Systems*, in *Advances in Chemical Engineering*, S. Kai, Editor. 2012, Academic Press. p. 383-446.
37. S.A.Klein, *A Design Procedure for Solar Heating Systems*, in *Department of Chemical engineering* 1976, University of Wisconsin-Madison.
38. Jan Albers, F.S., *HEAT TRANSFER CALCULATION FOR ABSORPTION HEAT PUMPS UNDER VARIABLE FLOW RATE CONDITIONS*, in *International Sorption Heat Pump Conference*. 2011: Italy. p. 9.
39. Eicker, U., et al., *Façades and summer performance of buildings*. *Energy and Buildings*, 2008. **40**(4): p. 600-611.
40. Mei, L., et al., *Cooling potential of ventilated PV façade and solar air heaters combined with a desiccant cooling machine*. *Renewable Energy*, 2006. **31**(8): p. 1265-1278.
41. Mei, L., et al., *Thermal modelling of a building with an integrated ventilated PV façade*. *Energy and Buildings*, 2003. **35**(6): p. 605-617.
42. Laboratory, L.b., *WINDOW 4.1*. 1994. p. Program for Analyzing Window Thermal Performance in Accordance with Standard NFRC Procedures.
43. A.Napolitano, W.S., *Monitored installation and results, report of Subtask B Task 38 IEA SHC, AIT Austrian Institute of Technology*. 2010, Institute for Renewable Energy, EURAC: Italy.
44. THOMAS, S., *Analysis of solar air-conditioning systems and their integration in buildings*, in *Environmental sciences and management*. 2013, University of Liege: Belgium.
45. Meteonorm. *Meteonorm Features*. [cited 2014 05.07.2014].
46. European commission for standardization., *Energy performance of buildings - Overall energy use and definition of energy ratings*, in *Primary energy factors ; Carbon dioxide emissions*. 2008, European Committee for standardization: Brussels. p. 62.
47. Energy Regulatory Commission of R.Macedonia. *Pricing-Electricity*. 2014 [cited 2014 14.07].
48. Eicker, U., et al., *Economic evaluation of solar thermal and photovoltaic cooling systems through simulation in different climatic conditions: An analysis in three different cities in Europe*. *Energy and Buildings*, 2014. **70**(0): p. 207-223.

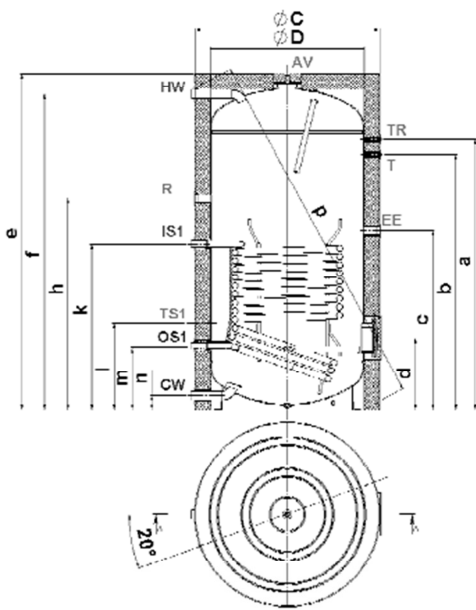
APPENDICIES

Appendix A

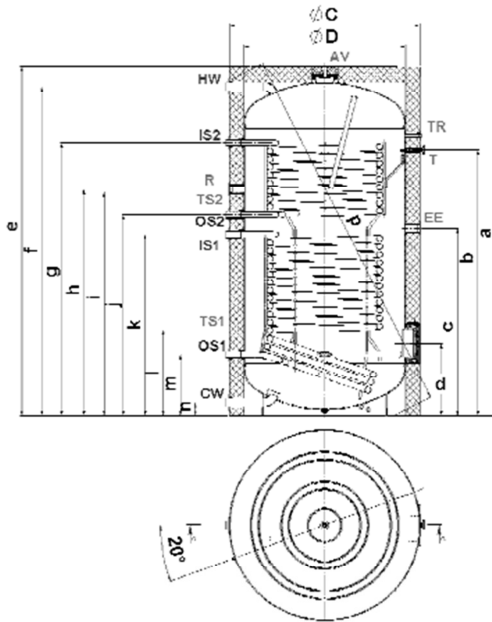
Technical data solar thermal storage, type: 15/9 S2, 12/8 S2, 13/7 S2



Тип серпентина	Coil heat exchanger type:	Tipul serpentinei		15/9 S2	15S	12/8 S2	12S	13S	13/7 S2	12S	12/9 S2
Номинален обем	Total capacity (EN 12897)	Volum nominal	l	1928	1950	1500	1500	988	977	800	800
Действителен обем	Actual capacity (EN 12897)	Volum real	l	1836	1867	1430	1455	941	931	774	762
Тегло нето	Net Weight	Greutate	kg	501	454	421	382	233	279	221	252
Изолация „Мек“ PU	Insulation „Soft“ PU	Izolatie „Soft“ PU	mm	100	100	100	100	100	100	100	100
Площ серпентина (S1 - долна)	Heat exchanger surface (S1 –lower HE)	Suprafata serpentinei (S1 – de jos)	m ²	4,5	4,5	3,47	3,47	3,45	3,45	2,89	2,89
Площ серпентина (S2 - горна)	Heat exchanger surface (S2 –upper HE)	Suprafata serpentinei (S2 – de sus)	m ²	2,7		2,3			1,31		1,54
Обем на серпентината (S1)	Heat exchanger content (S1)	Volumul serpentinei (S1)	l	41,6	41,6	31,4	31,4	31,3	31,3	26,2	26,2
Обем на серпентината (S2)	Heat exchanger content (S2)	Volumul serpentinei (S2)	l	25,2		20,5			7,9		9,4
Мощност на S1 в проточен режим	Exchanged power of HE S1 in continuous mood	Puterea serpentinei S1 in regim de functionare									
70-90 °C	70-90 °C	70-90 °C	kW	250	250	175	175	175	175	148	148
60-80 °C	60-80 °C	60-80 °C		195	195	140	140	130	130	107	107
50-70 °C	50-70 °C	50-70 °C		130	130	100	100	85	85	70	70
50-60 °C	50-60 °C	50-60 °C		68	68	80	80	56	56	50	50
Мощност на S2 в проточен режим	Exchanged power of HE S2 in continuous mood	Puterea serpentinei S2 in regim de functionare									
70-90 °C	70-90 °C	70-90 °C	kW	117	-	120			72		87
60-80 °C	60-80 °C	60-80 °C		83		95			50		57
50-70 °C	50-70 °C	50-70 °C		51		68			30		36
50-60 °C	50-60 °C	50-60 °C		24		51			17		20
Макс. дебит топла вода с ΔT35 °C (S1)	Max. flow rate of DHW with ΔT35 °C (S1); continuous mood	Cantitate apa calda cu ΔT35 °C (S1)									
70-90 °C	70-90 °C	70-90 °C	l/min	102	102	72	72	72	72	61	61
60-80 °C	60-80 °C	60-80 °C		80	80	57	57	53	53	44	44
50-70 °C	50-70 °C	50-70 °C		53	53	41	41	35	35	29	29
50-60 °C	50-60 °C	50-60 °C		26	2	33	33	23	23	20	20
Макс. дебит топла вода с ΔT35 °C (S2)	Max. flow rate of DHW with ΔT35 °C (S2); continuous mood	Cantitate apa calda cu ΔT35 °C (S2)									
70-90 °C	70-90 °C	70-90 °C	l/min	46		49			29		36
60-80 °C	60-80 °C	60-80 °C		34		39			20		23
50-70 °C	50-70 °C	50-70 °C		21		28			12		15
50-60 °C	50-60 °C	50-60 °C		10		21			7		8
Макс. количество вода MIX45 °C (S1)	Quantity of hot water MIX45 °C (S1)	Cantitate max. de apa MIX45 °C (S1)	l	2080	2145	1650	1728	1081	1055	845	823
Макс. количество вода MIX45 °C (S2)	Quantity of hot water MIX45 °C (S2)	Cantitate max. de apa MIX45 °C (S2)	l	991		611			503		401
Загуба на топлина (ΔT45K)	Heat loss (ΔT45K)	Pierdere de caldura (ΔT45K)	kW/24h	8.3	8.3	6.5	6.5	5.3	5.3	5.1	5.1
Макс. работна температура	Max. working temperature	Max. temperatura de lucru	°C	95	95	95	95	95	95	95	95
	Max. working temperature Coil HE	Max. temperatura de lucru a serpentinei	°C	110	110	110	110	110	110	110	110
Макс. работно налягане водосъдържател	Max. pressure of water tank	Presiune de lucru a vasului de apa	MPa	0.8	0.8	0.8	0.8	0.8	0.8	0.8	0.8
Работно налягане за серпентините	Max. pressure of coil heat exchanger	Presiune de lucru a serpentinei	MPa	0.6	0.6	0.6	0.6	0.6	0.6	0.6	0.6



EV (X) S 1500; 2000



EV (X/X) S2 1500; 2000

Dimensions

	15/9S2	12/8S2
mm	2000	1500
a	1927	1768
b	1827	1666
c	1287	1168
d	497	468
e	2399	2193
f	2263	2061
g	1875	-
h	1560	1378
i	1537	-
j	1380	-
k	1244	1081
l	587	579
m	420	421
n	90	90
p	2565	2361
ΦC	1300	1200
ΦD	1100	1000

Legend

R	Recirculation
TS1	Thermo pocket 1
TS2	Thermo pocket 2
EE	Electric heating element
T	Thermometer
TR	Thermoregulator
CW	Inlet cold water
IS2	Inlet heat exchanger 2
OS2	Outlet heat exchanger 2
IS1	Inlet heat exchanger 1
OS1	Outlet heat exchanger 1
HW	Outlet hot water
AV	Air ventilation

Appendix B

Technical data flat plate solar collector

Camel Solar, type CS Full Plate 2.0-4



Flat plate collector "Camel Solar" CS full plate 2.0-4

Dimensions L x W x H	2005 x 1005 x 85 mm
Absorber	
Material	Aluminum sheet and copper piping
Joint absorber risers	Additional aluminum sheet (0.2mm) ultrasonic welded on back side, two times with absorber sheet one time and once with riser tube
Thickness	0.5mm
Surface treatment	TiNOX
Absorptance	0.95
Emittance	0.05
Heat transfer fluid content	1.5 liter
Flow pattern	Harp
Dimension absorber tubes	8 x 0.4 mm
Number of absorber tubes	10
Distance between absorber tubes	94 mm
Dimensions of the header	22 x 0.8 mm
Number of connections	2
Transparent cover	
Number	1
Outer diameter glass tube	High borosilicate 3.3 glass
Material	Tempered low iron glass
Transmittance	0.92
Thickness	3.2mm
Insulation	
Material	Rockwool
Thermal conductivity	0.035 W/mK

Density	100 kg/m ³
Thickness of insulation	back side 50 mm, sideways 20 mm

Limitations

Stagantion temperature	197 °C
Max. pressure	10 bar
Allowed heat transfer fluid	Glycol/water mixture
Nominal flow rate per collector	90 kg/h

Thermal performance data

Conversion factor of the beam irradiance, $F'(\tau\alpha)_{en}$	0.795
Factor to determine the incidence angle modifier of the beam irradiance, b_0	0.138
Optical efficiency, η_0	0.791
Heat transfer coefficient a_1	4.176 W/m ² K
Temperature depending heat transfer coefficient a_2	0.008 W/m ² K ²
Incidence angle modifier diffuse radiaton $K_{\theta d}$	0.988
Incidence angle modifier $K_{\theta} = 50^\circ$	0.935
Area related heat capacity c	13.19 kJ/m ² K
Volume flow rate,	72 l/m ² h
Peak power per collector unit $G=1000$ W/m ²	1448 W

Appendix C

Technical data vacuum tube collector

“Camel Solar”, type CS 15



Dimensions L x W x H	1990 x 1180 x 158 mm
Absorber	
Material	Glass Aluminium heat transfer sheet
Joint absorber risers	sheet
Thickness	1.5mm
Surface treatment	CU/SS-ALN(H)/SS-ALN(L)ALN
Absorptance	0.92-0.96
Emittance	0.04-0.06
Heat transfer fluid content	2.95 Liter
Flow pattern	Parallel
Dimension absorber tubes	8 x 0.4 mm (U pipe)
Number of absorber tubes	15
Distance between absorber tubes	76 mm
Dimensions of the header	22 x 0.8 mm
Number of connections	2
Transparent cover	
Number	1
Outer diameter glass tube	58 mm
Material	High borosilicate 3.3 glass
Transmittance	0.92
Thickness	1.5mm
Insulation	
Material	Rockwool
Thermal conductivity	0.035 W/mK
Density	100 kg/m ³
Thickness of insulation	20 cm

Limitations

Stagnation temperature	250 °C
Max. pressure	10 bar
Allowed heat transfer fluid	Glycol/water mixture
Nominal flow rate per collector	90 kg/h
Conversion factor of the beam irradiance, $F'(\tau\alpha)_n$	0.695
Factor to determine the incidence angle modifier of the beam irradiance, b_0	0.138
Optical efficiency, η_0	0.738
Heat transfer coefficient a_1	1.725 W/m ² K
Temperature depending heat transfer coefficient a_2	0.01 W/m ² K ²
Incidence angle modifier diffuse radiation $K_{\theta d}$	1.203
Incidence angle modifier $K_{\theta} = 50^\circ$	0.935
Area related heat capacity c	58.4 kJ/m ² K
Volume flow rate,	72 l/m ² h
Aperture area per collector unit	1.42 m ²
Peak power per collector unit $G=1000$ W/m ²	1048 W

Appendix D

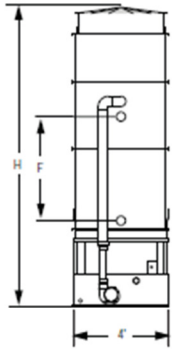
Parameters value for the absorption chillers

Numerical model Type 177 for different commercial available absorption chillers

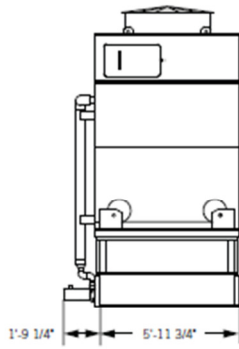
Par.	Description	Unit	YIA 1A1	Suninverse	Wegra 15
1	Calculation mode	-	1	1	1
2	$r_{D,0}$ Zero order parameter for axis interval (desorber)	kJ/h	-214163	-756	-15654
3	$r_{D,1}$ First order parameter for axis interval (desorber)	kJ/h K	4443	398	978
4	$s_{D,0}$ Zero order parameter for slope calculation (desorber)	kJ/h K	47555	2359	3203
5	$s_{D,1}$ First order parameter for slope calculation (desorber)	kJ/h K ²	7	-27	-60
6	$r_{E,0}$ Zero order parameter for axis interval (evaporator)	kJ/h	-47405	10233	-1855
7	$r_{E,1}$ First order parameter for axis interval (evaporator)	kJ/h K	-4039	-420	55
8	$s_{E,0}$ Zero order parameter for slope calculation (evaporator)	kJ/h K	32134	1710	2384
9	$s_{E,1}$ First order parameter for slope calculation (evaporator)	kJ/h K ²	140	-14	-41
10	B Dühring parameter	-	1.2	1.2	1.2
11	Minimum cooling water inlet temperature (i.e. range of validity for parameter	°C	26	22	26
12	Maximum cooling water inlet temperature (i.e. range of validity for parameter 2 to 13)	°C	47	42	37
13	Minimum hot water inlet temperature (i.e. range of validity for parameter 2 to 13)	°C	74	49	59
14	Maximum hot water inlet temperature (i.e. range of validity for parameter 2 to 13)	°C	116	106	96
15	Minimum chilled water inlet temperature (i.e. range of validity for parameter 2 to 13)	°C	5	7	5
16	Maximum chilled water inlet temperature (i.e. range of validity for parameter 2 to 13)	°C	13	22	25
17	$m_{D,0}$ Rated mass flow rate hot water (parameters 2 to 9 are valid in a range of +/- 10%)	kg/h	36935	1171	1940
18	$m_{E,0}$ Rated mass flow rate chilled water (parameters 2 to 9 are valid in a range of +/- 10%)	kg/h	65641	2898	1999
19	$m_{AC,0}$ Rated mass flow rate cooling water (parameters 2 to 9 are valid in a range of +/- 10%)	kg/h	89137	2590	4975

Appendix E

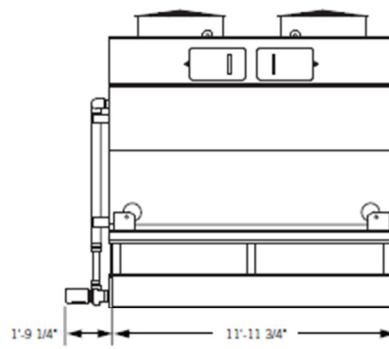
Cooling tower performance data – Baltimore aircoil model PF2-0406AA-31-3



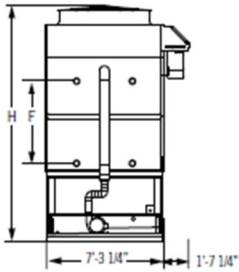
Face A:
PF2-0406 and PF2-0412 Units



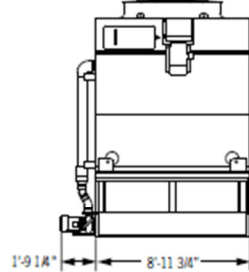
Face D:
PF2-0406 Units



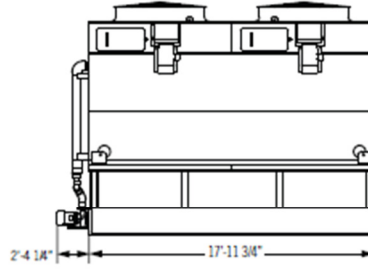
Face D:
PF2-0412 Units



Face A:
PF2-0709 and PF2-0718 Units



Face D:
PF2-0709 Units



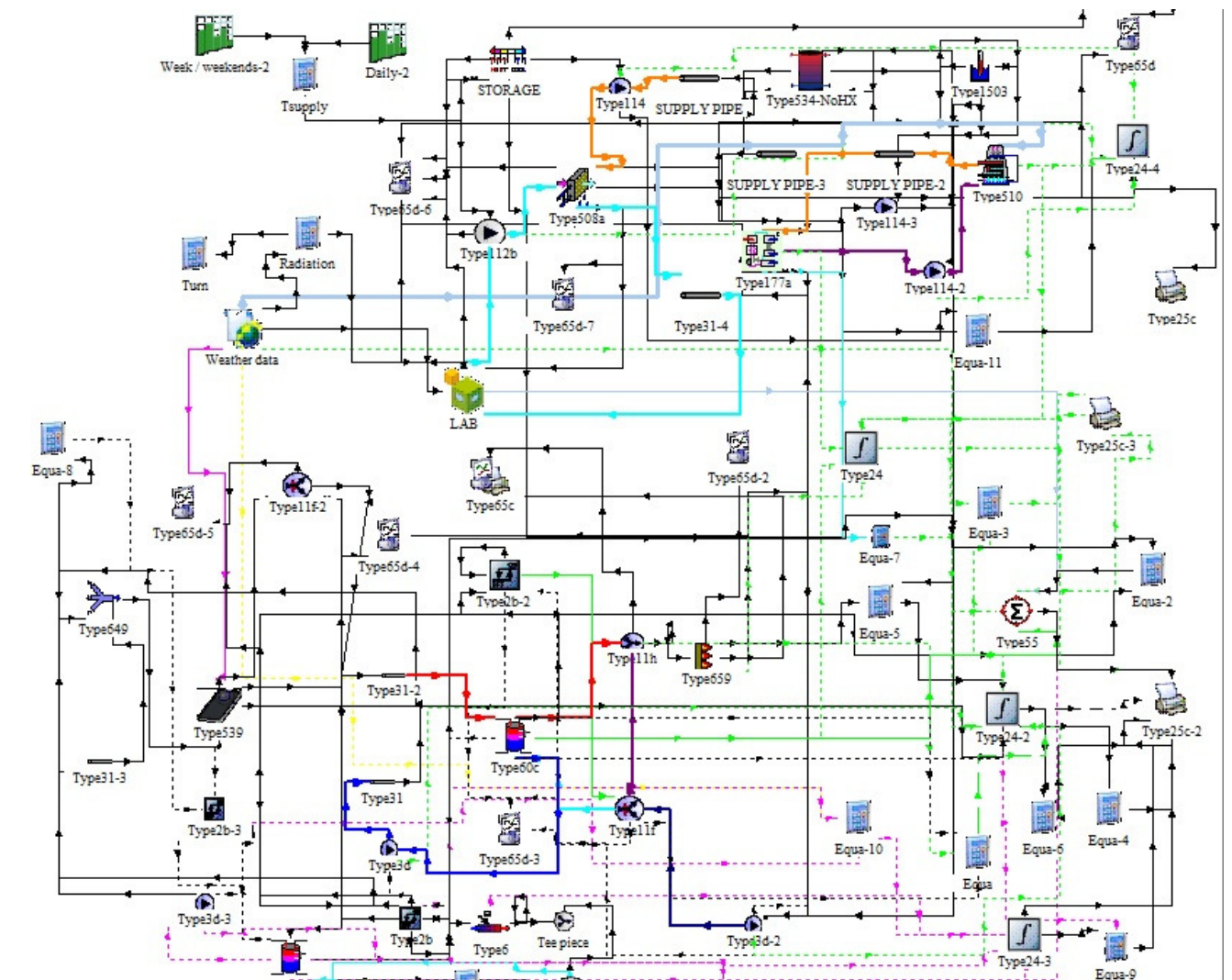
Face D:
PF2-0718 Units

Model Number	Pump Motor HP	CFM ¹	Approximate Weight (lbs)			Dimensions					Connection Size ^{5,6}		Integral Coil Volume (gal)	Riser Pipe Dia.	
			Operating Weight ²	Shipping Weight	Roundest Section	L	W	H	F	P	Make-Up Water	Coil			
PF2-0406A-31-z	0.75	10,300	4,130	2,630	2,000	6'-0"	4'-0"	10'-0"	2'-0"	1'-0"	1'-0"	4	00	48	4
PF2-0406A-32-z			4,600	3,050	2,420			10'-0"	2'-10"						
PF2-0406A-41-z			5,270	3,540	2,910			11'-4"	3'-2"						
PF2-0406A-51-z			5,740	3,890	3,260			12'-3"	4'-4"						
PF2-0406A-61-z			6,210	4,240	3,610			13'-3"	5'-4"						
PF2-0406A-62-z			6,680	4,590	3,960			14'-3"	6'-4"						
PF2-0412A-31-z	1	20,600	7,860	4,900	3,900	12'-0"	4'-0"	10'-0"	2'-0"	1'-0"	1'-0"	4	120	4	
PF2-0412A-32-z			8,750	5,550	4,520			10'-0"	2'-10"						
PF2-0412A-41-z			9,640	6,210	5,200			11'-4"	3'-2"						
PF2-0412A-51-z			10,540	6,870	5,900			12'-3"	4'-4"						
PF2-0412A-61-z			11,430	7,530	6,600			13'-3"	5'-4"						
PF2-0412A-62-z			12,320	8,190	7,300			14'-3"	6'-4"						
PF2-0709A-41-z	1.5	42,160	11,900	7,130	6,000	9'-0"	7'-4"	12'-4"	2'-10"	1'-0"	1'-0"	4	180	C	
PF2-0709A-42-z			13,300	8,800	7,610			13'-1"	3'-2"						
PF2-0709A-51-z			14,700	9,900	8,700			13'-10"	4'-4"						
PF2-0709A-61-z			16,100	10,900	9,600			14'-2"	5'-1"						
PF2-0709A-62-z			17,500	11,900	10,500			15'-0"	6'-10"						
PF2-0718A-41-z			3	86,810	22,250			14,550	11,890						18'-0"
PF2-0718A-51-z	26,750	17,700			15,100	13'-0"	3'-2"								
PF2-0718A-61-z	27,800	18,040			15,300	14'-2"	4'-4"								
PF2-0718A-71-z	32,300	21,820			18,170	15'-4"	5'-1"								

NOTES:

- Nominal tons of cooling represents 3 USGPM of water cooled from 95°F to 85°F at a 78°F entering wet-bulb temperature.
- CFM listed is for the highest fan motor HP and vary with the fan HP.
- Operating weight is for the unit with the water level in the cold water basin at the overflow.
- The actual size of the coil inlet and outlet connection may vary with the design flow rate. Consult unit print for dimensions.
- Coil inlet and outlet connections are beveled for welding.
- Models with Whisper Quiet Fans may have heights up to 5 1/2" greater than shown.
- Standard make-up, drain and overflow connections are located near the bottom of the unit. Make-up connection is 1 1/2" MPT standpipe, drain is 2" FPT, and overflow is 3" FPT. Standard make-up, drain, and overflow connections are MPT.

Appendix F - TRNSYS model of the analyzed solar assisted air-conditioning system



Appendix G - Draft proposal for scientific paper

Techno-economic feasibility analysis for application of small solar-assisted air conditioning systems in Macedonia

Igor Shesho^{a*1}, Laurent Georges^b, Vojislav Novakovic^{b,1}, Done Tashevski^a

^aUniversity "SS.Cyril and Methodius University of Skopje", Faculty of Mechanical Engineering Skopje, Karpos II bb, 1000 Skopje, R.Macedonia

^bNorwegian University of Science and Technology, Department Energy and Process Engineering, Kolbjørn Hejes vei 1, Trondheim 7491 Norway,

Abstract

This paper has objective, due to climatic conditions in Macedonia, to estimate the thermal performance of solar assisted air conditioning systems in regard of solar fraction, primary energy and perform life cycle cost analysis to assess the feasibility of their implementation in residential sector. The analysis is performed using numerical methods within TRNSYS software, since the solar processes are transient in nature been driven by time dependent forcing functions and loads represented with component models. Validation is made for the used TRNSYS components models i.e. the simulation results are compared with experimental measurements where the modelled and measured solar collectors are Macedonian product. Reference building is modelled representing the heating and cooling energy consumer. The building is modelled in three types regarding the annual specific heating and cooling energy consumption. The obtained results reveals that the solar fraction for heating and for driving absorption chiller as ratio between the total collector and conditioned area. Solar collector systems applied only for heating and DHW with heat pump as auxiliary heat source and building with specific heat consumption of 57 kWh/m²a, have payback period starting from 7,5 years for 16 m² collector area and 1000l heat storage tank, while the solar assisted cooling system all of the NPV values are negative indicating that economically without subsidies is not profitable measure. Solar assisted cooling is not feasible since the electricity price in Macedonia has low price and also the absorption chiller has relatively high investment cost offsetting the payback period to higher values. But it must be noted that regarding primary energy consumption solar assisted air conditioning systems for conditions in Macedonia can provide more than 50 % savings compared to conventional energy sources i.e. electrical energy.

Keyword: Solar assisted air conditioning, primary energy, solar fraction, simulation, TRNSYS

1. Introduction

In the past twenty years the uncontrolled or mildly said "demanded" industry development accompanied by the increased thermal comfort demand and the limited energy resources naturally activated and imposed the need of the forgotten term of energy efficiency. In the past, the cheap/affordable energy sources, high building energy consumption and the modest technology development were the main limiting factors for the viability of utilization renewable energy sources.

Undertaken measures started with limiting the energy consumption through different directives and regulations which translated into actions meant: improving efficiencies of existing systems, decreasing the energy demand, up to developing new technologies, and all of that with one purpose - doing more with less. Now with the implementation of the buildings directives such as the Energy Performance Building Directive 2002/91/EC the EU 2020 strategy, technology development enabled the renewable energy sources to be feasible for implementation in buildings air-conditioning systems. European commission adopted communication "Energy 2020" that defines new strategy toward 2020 for a competitive, sustainable and secure energy [1]. A significant contribution to the primary energy consumption of first and second world countries is being made by the rapidly increasing use of electrical air-conditioning units worldwide. Worldwide sales of room air-conditioners of all types amount to approximately 50 Mio. units p.a., with the U.S. China and Japan being the three main markets. In Europe, commercial air conditioning has a share of 4% of the total annual electricity consumption while residential air conditioning accounts only for 0.4%. Although the latter number is still comparatively low, Europe has seen a seven-fold increase of residential air-conditioning sales between 1990 and 2004. The reasons for the growing use of air-conditioning are twofold. First, the comfort demands from both building users and owners have increased. The standard of living of the present generation is higher than in the past, especially in private buildings. . Second, the trend towards commercial buildings with large glazed facades has increased the internal heat load to be removed by air-conditioning. Third, electricity prices are

¹ Corresponding author. Tel: +38923099200,
e-mail address: igor.seso@mf.edu.mk (I.Shesho)

On Figure 1 is presented the analyzed i.e. modeled and simulated solar assisted air-conditioning system. The main system components are: the solar collector array, two storage tanks, auxiliary heater, absorption chiller and the energy consumer i.e. the building which also incorporates the heating/cooling system components.

The working fluid from the solar collectors indirectly through heat exchangers is used to heat the domestic hot water in tank 3 or heat the fluid in the storage tank 4 further used as part of the heating energy in the building or part of the driving heat for the absorption chiller in summer. The circulation of the solar collectors working fluid for the storage tanks 3 and 4 is done by two separate circulating pumps P1 and P2, controlled by two differential controllers having mutual predefined control function further explained. First condition for the pumps to be switched on is the temperature difference between the collector outlet temperature and the fluid temperature in storage tank (3 or 4) to be greater than the set upper dead band. The control logic for switching between the two tanks is solved using the two controllers Type 2b (K1 and K2) one flow diverter Type 11f. The advantage has the controller K2 of the tank 4 i.e. the initial input control signal (on/off) for the controller of the DHW tank K1 is received from the controller K2 i.e. when the controller K2 is on, then the controller K1 is off.

In the analyses are considered vacuum tube and flat plate collectors and the Building II type, with thermal performance described in Table 4. The building internal heat gains consider the lighting power density 5 W/m^2 and the home appliances with specific power of 2 W/m^2 . The absorption chiller condenser is connected to the wet cooling tower product of Baltimore AirCoil type PF2-0406AA-31-3. Numerical modelling of the cooling tower is provided by the TRNSYS Type510 model from Tess library, a closed circuit cooling tower which cools the liquid stream by evaporating water from the outside of coils containing the working fluid. The working fluid is completely isolated from the air and water in this type of system.

The control signal of the cooling tower fan is set to have the tower try to maintain the desired outlet water temperature of $26 \text{ }^\circ\text{C}$ and the fluid flow rate with the circulation pump is set to 2600 kg/h . Also to the circulation of the cooling water are modeled pipe network with diameter 0.04 m and length of 15 m heat transfer coefficient for thermal losses $3 \text{ kJ/h m}^2 \text{ K}$ which accounts for the heat losses to the environment and also increases the system thermal capacity affecting the simulation stability. Values of the inlet parameters for the cooling tower such as ambient air temperature and relative humidity are read from the weather component respectively for the simulated time and period of the year. The cooling water temperature is parameter which is variable depending from the absorption chiller working conditions.

The cooling system in the building is modeled using the ventilation air distribution system. The combination among the chilled water from the absorption chiller and the ventilation air is provided with heat exchanger water-air modeled Type 508a which is a cooling coil modeled using a bypass approach in which the user specifies a fraction of the air stream that bypasses the coil. The remainder of the air stream is assumed to exit the coil at the average temperature of the fluid in the coil and at saturated conditions. The two air streams are remixed after the coil. Chilled water flow from the absorption chiller to the cooling coil is set to 2900 kg/h and the air flow rate to the building is 4000 kg/h . The auxiliary heater power is modeled 12 kW and the outlet temperature is $80 \text{ }^\circ\text{C}$, which is the absorption machine driving temperature.

The storage tank 4 in this case is used to store the heat for driving the absorption chiller. With the thermostat Type 108 is regulated the space temperature in the building set to $26 \text{ }^\circ\text{C}$, which control signal is directly regulating the function of the circulation pump from the chilled water absorption chiller and the fan distributing the conditioned air.

Simulation time step is 15 min and as cooling period are considered the months from May-September.

The collector(s) thermal efficiency in the simulation is determined using the equation component from the TRNSYS library. The equation considers ratio between the useful energy gain from the all of the collectors transferred to the fluid and the total tilted radiation for the collector surface. The data for the quantity of useful energy gain and total radiation in the equation is read from the quantity integrator which integrates these values in the predefined period defined from the required value period thermal efficiency and energy i.e. daily, weekly, monthly, yearly or any other time interval.

2.1 System component models definition and validation

2.1.1 Solar system component validation

The validation is performed for the following solar thermal system components: solar collector, storage tank and differential controller. The system consist one flat plate solar collector connected with the internal heat exchanger of the storage tank. Control is provided by differential controller which is set to turn the circulation pump on, when the temperature difference between the collector outlet temperature and the tank temperature is greater than five. The water from the storage tank is not discharged and the electric heater is turned off during the measurements. The fluid (water) flow rate is set to $7,5 \text{ lit/min}$.

The measurements are made on an hour interval for the fluid inlet T1 and outlet T2 temperatures from the solar collector, tank fluid temperature T3 and the solar radiation measured with the pyrometer S. The experimental setup of

the analyzed solar thermal system is placed in Skopje, R.Macedonia, northern latitude of 42° and 21.43° east longitude. The temperature measurements are performed with temperature data logger thermocouple probes type K. The solar collector is evacuated tubular direct flow product of Camel Solar type Vacuum CS 15 Solar KeyMark certified. It is installed under tilt of 45° , south orientated i.e. azimuth angle of 0° . The collector thermal performance test results made according EN 12975 are presented in Table 1 while the storage tank technical data are given in Table 2

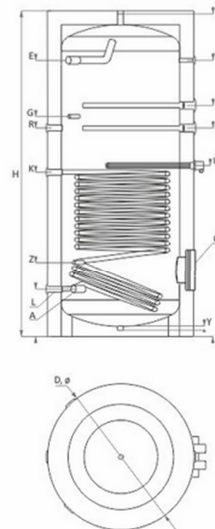
Table 1. Technical data for collector type Camel Solar Vacuum tube SC 15 (“U” type)

Dimensions L x W x H	mm	1990 x 1180 x 158
Number of absorber tubes	-	15
Absorptance, α	-	0.92-0.96
Emittance, ϵ	-	0.04-0.06
Conversion factor of the beam irradiance, $F'(\tau\alpha)_{en}$	-	0.695
Factor to determine the incidence angle modifier of the beam irradiance, b_0	-	0.138
Optical efficiency, η_0	-	0.738
Heat transfer coefficient a_1	W/m^2K	1.725
Temperature depending heat transfer coefficient a_2	W/m^2K^2	0.01
Incidence angle modifier diffuse radiation $K_{\theta,d}$	-	1.203
Incidence angle modifier $K_{\theta} = 50^\circ$	-	0.935
Area related heat capacity c	kJ/m^2K	58.4
Volume flow rate,	l/m^2h	72
Aperture area per collector unit	m^2	1.42
Peak power per collector unit $G=1000$	W/m^2	1048



Table 2. Storage tank technical details

Capacity	l	150
Height	H, mm	1210
Diameter	D, mm	560
Insulation, rigid PU	mm	50
Coil capacity	l	4.56
Heat exchanger surface	m^2	0.74
Prolonged power according DIN 4708 80/60/45	kW	25
	m^3/h	0.61
NL-power coefficient at $60^\circ C$	-	2.5
Coil outlet	L, mm	202
Cold water inlet	A, mm	202
Sensor sleeve for thermostat	G, mm	822
Coil inlet	K, mm	592
Hot water outlet	E, mm	868



In the TRNSYS model for the solar collector model is used the collector Type 538 from the Tess library modeled with the technical data given in Table 1. The storage tank is modeled with the Type 60d including the internal heat exchanger for which are supplied data from Table 2. Type 2b-2 is used for the differential controller with upper dead band of 5 and lower dead band 2, the high limit cut-off temperature is set to $100^\circ C$. Between the solar collector and storage tank is connected pipe Type 31 modeled with internal diameter 0.025 m, length of 10 m and loss coefficient of $0,3 W/m^2K$ to account for the heat losses. The pipe Type 31 beside to account for the heat losses in the pipes also is used in order to increase the thermal capacity of the system and thus increase the simulation stability. Also for the circulating pump is used the Type 3d with mass flow rate 450 kg/h i.e. 7,5 l/min same as in the experimental setup. Measurements are performed starting from date 18.09.2013 until 28.03.2014 and in parallel are measured two systems with same capacity storage tank of 150l but different type of collectors i.e. flat plate and vacuum tube solar collectors. In the validation process are used the data for the vacuum tube collector and the results from only one day period (18.09.2014) with collection time interval ranging between 20min and 45min interval, starting from 10:40 until 16:05 h.

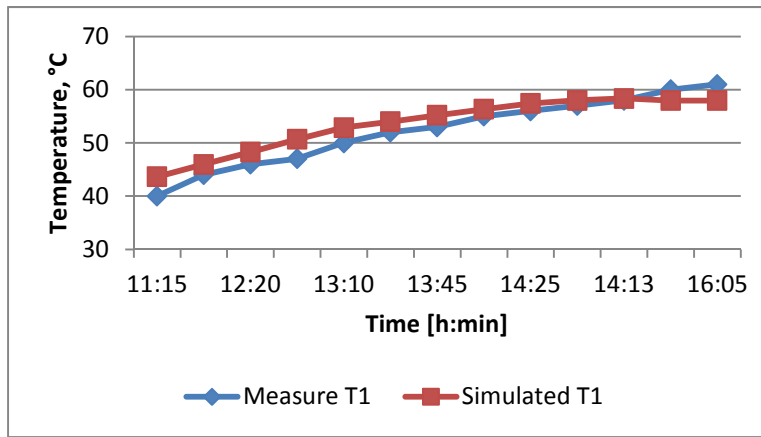


Figure 2. Measured and simulated temperatures for the collector inlet

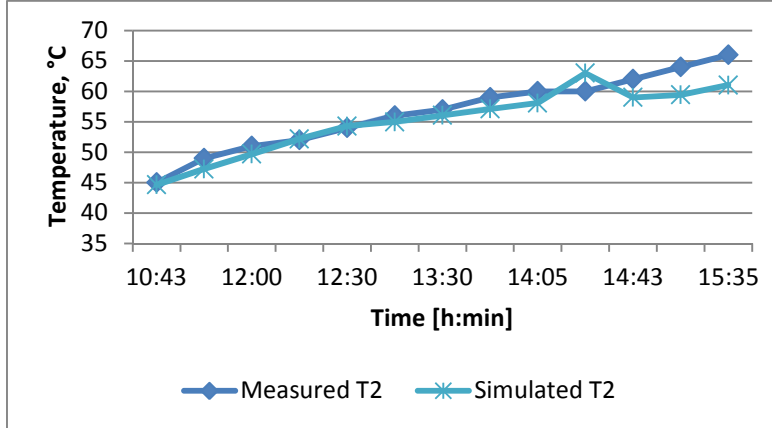


Figure 3. Measured and simulated temperatures at the collector outlet

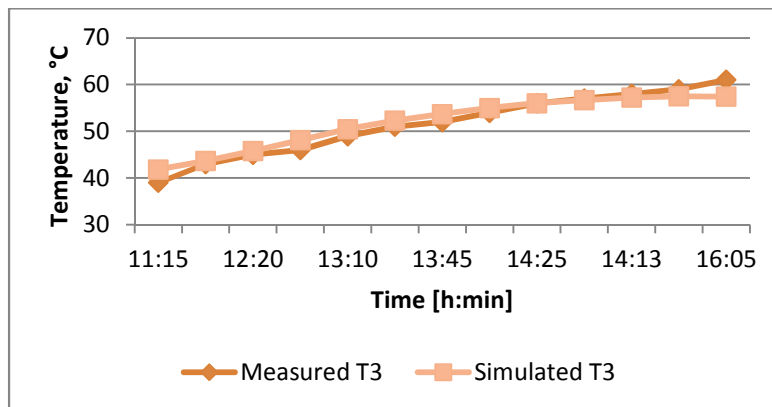


Figure 4. Measured and simulated temperatures inside storage tank

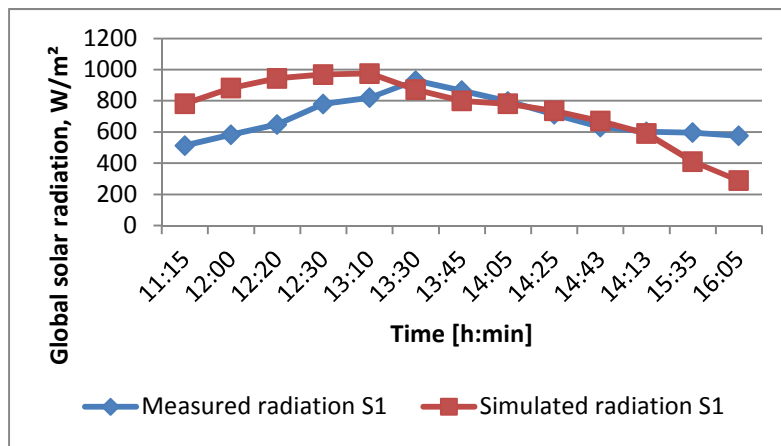


Figure 5. Hourly measured and simulated solar radiation for the specific day

According to the above presented data i.e. diagrams, it can be concluded that there is an acceptable match between the measured and simulated results. The discrepancies that appear between the temperatures of the experimental and simulated results are expected since the solar radiations have different values because one value is obtained with measurements and the others are from the Meteoronorm database for the selected location. Another influencing factor is the uncertainty of the measurement error and last but not the least, it should not be neglected that the transition nature of the solar thermal systems.

The resulting simulations reveal the individual thermal behaviour of the solar collector, storage tank, differential controller and circulating pump as well as their assembled thermal behaviour. These results were very close to their corresponding experimental data and this fact validates these models for future application in the heating/cooling system.

2.1.2 Absorption chiller component validation

Validation for the absorption chiller is made for the TRNSYS component Type 177. This component type offers four numerical modes of absorption chiller, and in this simulation, the mode "a" i.e. Type177a, which is standard mode using user-supplied characteristic parameters. Since in this paper, only solar air-conditioning for residential buildings is considered, in Table 3, technical data for several small absorption chillers are given. From the presented absorption chillers, in the simulation, the absorption chiller H₂O/LiBr produced by Sonnenklima type Suninverse 10 is modeled as component Type 177a. As input parameters, the values for Suninverse provided in Table 3 are taken, for which the simulation as output cooling power is obtained a value of 10.1 kW, corresponding to the factory value. Validation exists for the Type 177 mode "d" performed by Albers and Ziegler [10], using the measurement results from Kühn [11]. According to this, it can be concluded that this numerical model of absorption chiller provides reliable results and can be used further in simulations.

Table 3. Technical data for different market available small absorption chillers

Company	Yazaki	Sonnenklima	Rotarica
Product name	WFC-SC5, chillii WFC 18	Suninverse 10	Solar 045
Technology	Absorption	Absorption	Absorption
Working pair	H ₂ O/LiBr	H ₂ O/LiBr	H ₂ O/LiBr
Cooling capacity, kW	17.6	10	4.5
Heating temperature, °C	88 / 83	75/65	90/85
Recooling temperature, °C	31 / 35	27/35	30/35
Cold water temperature, °C	12.5 / 7	18/15	13/10
COP	0.70	0.77	0.67
Weight, kg	420	550	290 1200
Electrical power, W	72	120	(incl.ventilator)

2.1.3 Reference building model description

Building as energy consumer has a major impact on the overall efficiency of the solar system i.e. can be freely said that the building itself is one of the leading parameter in sizing the system. Since the analyses are made for climatic conditions in Macedonia also the thermal performance of buildings must be in accordance with the Regulations on energy efficiency in Macedonia. Furthermore the analysis is taken into account the impact of the specific consumption of heating / cooling energy of the building kWh/m² a to the response and the performance of the solar collector system. In Table 4 are listed three types of the building i.e. the dimensions and orientations are unchanged only the insulation thickness is varied in order to obtain different values for specific annual consumption of thermal energy. The main motive for variations in the thickness of the insulation is to analyze the influence of the thermal performance of buildings on the economic viability of the use of solar thermal systems in air-conditioning. Constant value of 0.3 1/h is defined for the infiltration of outdoor air, while for the summer when cooling is required in the building is envisaged/modeled mechanical ventilation defined with air mass flow and temperature entered through \the models of fan and heat exchanger air-water which is directly connected with the cooling absorption machine. Regarding the thermal comfort, in the heating mode the inside temperature is defined to be 20 °C from 05:00 – 22:00 and for the rest is defined setback temperature of 16 °C, for the cooling mode is defined constant inside temperature of 26 °C.

Table 4. Reference building physical and thermal performance data

Surface	Orientation	Area, m ²	Building I Building II Building III		
			U value, W/m ² K		
Out.wall 1	North	42	0.58	0.33	0.18
Windows 1	North	3	1.40	1.40	1.40
Out.wall 2	East	25.5	0.58	0.33	0.18
Windows 2	East	4.5	1.40	1.40	1.40
Out.wall 3	West	25.5	0.58	0.33	0.18
Windows 3	West	4.5	1.40	1.40	1.40
Out.wall 4	South	42	0.58	0.33	0.18
Windows 4	South	3	1.40	1.40	1.40
Floor	-	150	0.33	0.33	0.24
Roof	-	150	0.54	0.42	0.35
Window type		Double glazed TRNSYS library (w4-lib data)			
Windows solar heat gain coefficient;g-value		0.589			
Out.wall construction	2 x Plaster 2cm, brick 25cm	Insulation 5 cm	Insulation 10 cm	Insulation 20 cm	
Floor	Granite tile 6cm, cement mortar 5cm , concrete slab 20cm	Insulation 10 cm	Insulation 10 cm	Insulation 15 cm	
Roof	Concrete slab 20cm, hydro isolation, cement mortar 5cm	Insulation 15 cm	Insulation 20 cm	Insulation 25 cm	
Outside convective heat transfer coefficient		$\alpha_{out} = 25 \text{ W/m}^2\text{K}$			
Inside convective heat transfer coefficient		$\alpha_{in} = 7,7 \text{ W/m}^2\text{K}$			

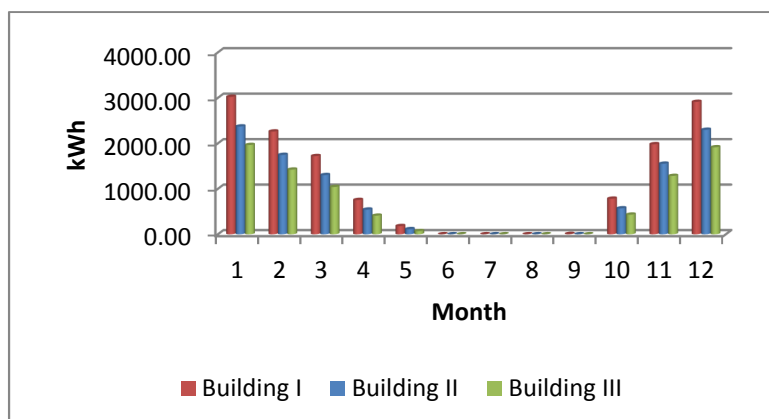


Figure 6. Monthly energy consumption for Building I, II and III

Analyzing the presented simulation results on Calculation of energy consumption in the building is obtained directly as output size of the numerical model of the object in kJ / h value which further is integrated for the required period with the quantity integrator. Also as output parameters of the model is the output temperature of floor heating, the

temperature of the air entering the fan to the heat exchanger and air-water and the delivered energy from the underfloor heating system into the building.

Monthly analysis is performed for the building heat energy consumption regarding different heat transfer coefficients i.e. different wall, floor and roof isolation thickness thus defining three types of Building I, II and III. as presented in Figure 6.

It can be noticed that as expected the Building III has the smallest heat consumption i.e. regarding specific annual energy consumption, Building I has 90 kWh/m²a, Building II with 70 kWh/m²a and Building III has 57 kWh/m²a. Comparing the energy consumption Building III has 42% lower than Building I and 19% than Building II.

As mentioned previously for the absorption chiller it is used the component model Type 177a in which input parameters are inserted the data from the LiBr/H₂O Suninverse 10 chiller product of Sonneklima with cooling power of 10 kW with heat driving temperature of 75 °C, cooling water 27 °C and chilled water outlet temperature set at 15°C.

3. Simulation results and discussion

The comparison results between the solar fractions and efficiencies in regard of different collector areas (flat plate collectors) and storage volumes are presented in Table 5. The mass flow rate is set constant according the collector area i.e. it is 50 kg/h m². Solar collectors are tilted on 40° with south orientation i.e. azimuth is 0°. As can be seen the solar fractions increase with the increase of collector area and storage volume and varies in the range between 20% up to 70%. Also the thermal efficiency should not be neglected which for the analyzed cases is in the range between 15% up to 27% monthly averages. Solar fraction for the DHW is almost in every case 100% since the daily consumption is very low compared to the available energy from the solar collectors.

Table 5. Monthly average solar fractions and efficiency in regard of collector area and storage volume

Flat plate, Tilt 40°, Azimuth 0° - flow rate 50 l/h m ²									
	1000			1500			2000		
Collector area m ²	16	32	64	16	32	64	16	32	64
Sol.fraction	0.28	0.50	0.67	0.24	0.49	0.69	0.19	0.48	0.70
Avg_Efficiency	0.26	0.19	0.15	0.26	0.20	0.15	0.27	0.21	0.16
Avg_Eff_Real	0.48	0.36	0.32	0.47	0.37	0.33	0.46	0.37	0.30
Sol.DHW	0.98	0.99	0.99	0.98	0.99	0.99	0.98	0.99	0.99

According the above presented results can be concluded that with solar energy regarding the specific collector areas can be covered: 0,1 m² / m² conditioned can cover almost 30%, 0,2 m²/m² conditioned covers 50% and 0,4 m²/m² conditioned can cover 70% of the total required heating energy for driving the absorption chiller. Analyzing the solar fraction for one constant specific collector area and changing only the storage volume can be noticed that biggest fractions are for specific volume per collector area of 30 l/m².

Further analyzed the influence of the collector tilt angle with and without azimuth tracking system (one axis-vertical tracking system) to the solar fraction and thermal efficiency. Simulation results are presented in

Table 6. Solar fractions and thermal efficiency for solar assisted cooling system in regard of collector orientation i.e. azimuth

Storage tank 1000l - Collector mass flow rate 50 l/h m ²									
Collector area m ² / tilt °	16/1/40	16/1/30	16/1/30/T	32/1/40	32/1/30	32/1/30/T	64/1/3200/40	64/1/3200/30	64/1/3200/30/T
Sol.fraction	0.28	0.30	0.44	0.53	0.55	0.67	0.67	0.69	0.77
Avg_Efficiency	0.26	0.26	0.24	0.18	0.18	0.19	0.15	0.15	0.16
Avg_Eff_Real	0.48	0.50	0.50	0.38	0.38	0.41	0.32	0.33	0.35
Storage tank 1500l - Collector mass flow rate 50 l/h m ²									
Collector area m ² / tilt °	16/1/40	16/1/30	16/1/30/T	32/1/40	32/1/30	32/1/30/T	64/1/3200/40	64/1/3200/30	64/1/3200/30/T
Sol.fraction	0.22	0.24	0.38	0.49	0.51	0.66	0.67	0.69	0.81
Avg_Efficiency	0.26	0.26	0.26	0.20	0.20	0.20	0.15	0.15	0.15
Avg_Eff_Real	0.46	0.47	0.47	0.37	0.38	0.39	0.32	0.33	0.36

*64/1/3200/30/T - (64) m² collector array, (1) all in parallel connected, (3 200) kg/h mass flow rate, (30) tilt angle, (T) tracking azimuth

In order to have better visibility of the parametric influence of the collector tilt angle and azimuth influence, on Figure 7 are presented monthly values for solar fractions from June-September

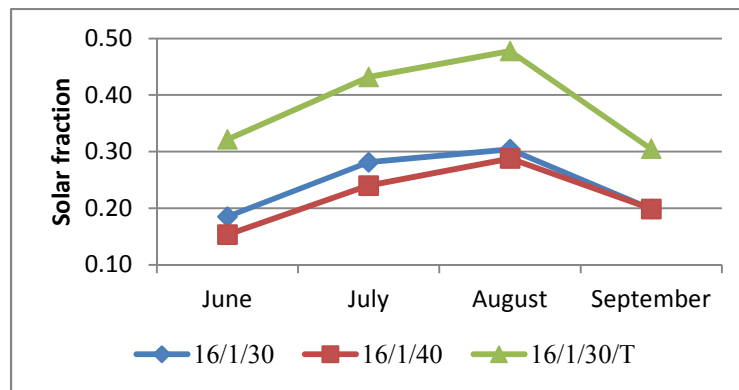


Figure 7. Monthly values of solar fraction for different tilt angles and tracking azimuth for solar assisted cooling system

3.1 Life cycle cost analysis of solar cooling system

The economic evaluation of a solar application includes factors such as the capacity cost of delivering solar energy, the optimum sizing of collectors and other equipment the costs of competing technologies and financial analyses. There figures of merit that are used to accept or reject particular solar application including simple payback, cash flow , capital cost per unit of energy saved, life cycle cost, net present value and levelized energy cost. For a range of economic assumptions, an analysis considering a 5-year or 7 year simple payback is assumed to be an adequate figure of merit to establish cost goals for active solar cooling and heating technologies. For residential applications, a payback period of 5 - 7 years may consider as acceptable.

Comparison is performed between different combinations of solar thermal systems and auxiliary heating devices in regard of conventional heating system with electrical boiler. The analyzed solar systems have total solar collector area of 16 m², 32 m² and 64 m² combined with storage tanks of 1000 l, 1500 l and 2000l , and auxiliary heating energy provided by electric heater or heat pump air-water with E.V.I compressors with nominal capacity of 15 kW product of Hidros model Lzti 10 [12].

In Table 7 are presented data for delivered heating energy, annual heating energy cost, system price and the environmental indicator - CO₂ emissions for conventional heating systems with heat sources: electrical energy, wood pellets and heat pump. The heat pump COP is assumed with averaged yearly value of 2,5.

Table 7. Annual energy balance, energy and system costs, CO₂ emissions for conventional heat source systems obtained with simulations, specific heat energy consumption 70 kWh/m² a

Parameter	Unit	Electrical boiler	Pellet boiler	Heat pump
Heat power	kW	12	12	12.5
Annual delivered heat energy	kWh	13103	13103	13103
Average thermal efficiency/COP	-	0.99	0.91	2.5
Annual consumed energy	kWh	13235	14399	5241
System electrical energy consumption (circ.pumps)	kWh	144	144	144
Specific energy price	eur/kWh	0.09	0.05	0.09
Total energy price	eur	1203	667	472
Heat source device/system price	eur	800	2000	5000
Annual CO ₂ emissions	kg/year	12177	58	1730

The CO₂ emissions and primary energy consumption factors are provided from the standard “Energy performance of buildings - Overall energy use and definition of energy ratings” EN 15603_2008 [13].

Regarding the energy prices, the electrical energy price (euro/kWh) is provided from the Energy Regulatory Commission of the Republic of Macedonia valid from 01.07.2014 , wood pellet energy price is obtained by taking the average market price of 0,2 euro/kg with lower heating value H_d = 4,3 kWh/kg.

In Table 8 and Table 9 are given results from the analyzed solar thermal systems in regard of heat energy consumption, annual energy and system costs and the environmental impact indicator presented by the value for the annual CO₂ (kg/year) annual emissions.

Table 8. Solar thermal system energy performance, costs, parameters and CO₂ emissions, primary energy consumption for building with specific heat energy consumption 70 kWh/m² a, – part I

<i>Ref.building 70 kWh/m² a</i>		Solar thermal system - Area/Storage tank volume - EH (electric heater) ; HP (heat pump) -							
Parameter	Unit	16/1000-EH	16/1000-HP	32/1000-EH	32/1000-HP	64/1000-EH	64/1000-HP	32/1500-EH	
Auxiliary energy - heating system	kWh	8550	8550	7420	7420	6466	6466	6996	
Auxiliary energy - DHW	kWh		750		562		428	639	
System electrical energy consumption (circ.pumps)	kWh	144	144	114	114	90	90	130	
Specific electrical energy price	eur/kWh				0.09				
Total energy price	eur	850	348	729	300	629	256	640	
Heat source device/system price	eur	3600	7000	6000	10500	10000	14700	7000	
Primary energy consumption	kWh	28777	12790	26798	10946	23117	9426	25702	
Annual CO ₂ emissions	kg/year	3069	1275	2672	1091	2305	940	2562	
Annual average solar fraction - SF	-		0.19		0.30		0.39	0.34	

Table 9. Solar thermal system energy performance, costs, parameters and CO₂ emissions, primary energy consumption for building with specific heat energy consumption 70 kWh/m² a, – part II

<i>Ref.building 70 kWh/m² a</i>		Solar thermal system - Area/Storage tank volume - EH (electric heater) ; HP (heat pump) -							
Parameter	Unit	32/1500-HP	64/1500-EH	64/1500-HP	32/2000-EH	32/2000-HP	64/2000-EH	64/2000-HP	
Auxiliary energy - heating system	kWh	6996	5830	5830	7250	7250	5921	5921	
Auxiliary energy - DHW	kWh	639		490					
System electrical energy consumption (circ.pumps)	kWh	130	103	103	138	138	111	111	
Specific electrical energy price	eur/kWh				0.09				
Total energy price	eur	287	578	237	665	273	543	223	
Heat source device/system price	eur	11500	12000	16500	8000	12500	12800	16700	
Primary energy consumption	kWh	10539	21260	8709	24454	10056	19966	8207	
Annual CO ₂ emissions	kg/year	1051	2120	868	2438	1003	1991	818	
Annual average solar fraction - SF	-	0.34		0.45		0.32		0.44	

Table 10. Solar thermal system energy performance, costs, parameters and CO₂ emissions, primary energy consumption for building with specific heat energy consumption 57 kWh/m² a, – part I

<i>Ref.building 57 kWh/m² a</i>		Solar thermal system - Area/Storage tank volume - EH (electric heater) ; HP (heat pump) -							
Parameter	Unit	16/1000-EH	16/1000-HP	32/1000-EH	32/1000-HP	64/1000-EH	64/1000-HP	32/1500-EH	
Auxiliary energy - heating system	kWh	6708	6708	5762	5762	5418	5418	6192	
Auxiliary energy - DHW	kWh		713		527		402	595	
System electrical energy consumption (circ.pumps)	kWh	139	139	109	109	86	86	115	
Specific electrical energy price	eur/kWh				0.09				
Total energy price	eur	680	280	576	239	532	217	567	
Heat source device/system price	eur	3600	7000	6000	10500	10000	14700	7000	
Primary energy consumption	kWh	22664	10285	21177	8687	19549	7990	22846	
Annual CO ₂ emissions	kg/year	2449	1025	2111	866	1949	797	2278	
Annual average solar fraction - SF	-		0.22		0.33		0.39	0.28	

Table 11. Solar thermal system energy performance, costs, parameters and CO₂ emissions, primary energy consumption for building with specific heat energy consumption 57 kWh/m² a, – part II

<i>Ref.building 57 kWh/m² a</i>		Solar thermal system - Area/Storage tank volume - EH (electric heater) ; HP (heat pump) -							
Parameter	Unit	32/1500-HP	64/1500-EH	64/1500-HP	32/2000-EH	32/2000-HP	64/2000-EH	64/2000-HP	
Auxiliary energy - heating system	kWh	6192	5600	5600	5074	5074	4042	4042	
Auxiliary energy - DHW	kWh	595		457		630		488	
System electrical energy consumption (circ.pumps)	kWh	115	94	94	118	118	97	97	
Specific electrical energy price	eur/kWh				0.09				
Total energy price	eur	255	554	227	524	216	416	172	
Heat source device/system price	eur	11500	12000	16500	8000	12500	12800	16700	
Primary energy consumption	kWh	9367	20360	8331	19271	7943	15315	6319	
Annual CO ₂ emissions	kg/year	934	2030	831	1921	792	1527	630	
Annual average solar fraction - SF	-	0.28		0.36		0.41		0.53	

Further is analyzed the building energy consumption influence on the solar system performance i.e. same solar air-conditioning system is applied to building with lower specific heat energy consumption. Analysing the presented results is indicative that improved and feasible combination would be with heat pump instead of electrical heater which

is further verified with LCC analysis. The LCC method provides a better assessment of the long-term cost-effectiveness of the project/measure than other economic methods which only focus on initial investment costs and operation costs for the first years.

Same time, a LCC analysis requires more information than other profitability evaluation methods. The lowest Life Cycle Costs indicates the most profitable investment, measure or solution

Table 12. Life Cycle Cost Analysis for solar thermal system assisted building heating with specific heat energy consumption 70 kWh/m² a

Real interest rate 3,9% ; Building 70 kWh/m² a

Measures	Investment	Net savings	Lifetime	PB	PO	IRR	NPV	NPVQ	*Max.Investment	
	EUR	EUR/Year	Year	Year	Year	%	EUR		EUR	Year
Pellet boiler	2000	506	20	4	4.4	25	4.93	2.46	4.12	12
Heat pump	5000	671	20	7.5	9	12	4.18	0.84	6.34	12
HP 16/1-1000	7000	814	20	8.6	10.7	10	4.14	0.59	7.687	12
HP 32/1-1000	9700	849	20	11.4	15.5	6	1.919	0.20	8.017	12
EH 16/1-1000	3600	312	20	11.5	15.7	6	670	0.19	2.946	12
HP 32/1-1500	10700	864	20	12.4	17.3	5	1.125	0.11	8.159	12
EH 32/1-1500	7000	511	20	13.7	20	4	-7	0.00	4.825	12
EH 32/1-1000	6000	421	20	14.3	21.3	3	-239	-0.04	3.975	12
EH 32/1-2000	8000	487	20	16.4	26.9	2	-1.335	-0.17	4.599	12
HP 64/1-1000	14700	881	20	16.7	27.6	2	-2.643	-0.18	8.319	12
HP 64/1-1500	16500	902	20	18.3	32.9	1	-4.156	-0.25	8.518	12
HP 32/1-2000	16500	868	20	19	35.6	0	-4.621	-0.28	8.196	12
HP 64/1-2000	17300	896	20	19.3	36.8	0	-5.038	-0.29	8.461	12
EH 64/1-1000	10000	509	20	19.7	38.3	0	-3.034	-0.30	4.806	12
EH 64/1-1500	12000	560	20	21.4	47.7	0	-4.336	-0.36	5.288	12
EH 64/1-2000	12800	596	20	21.5	48	0	-4.644	-0.36	5.628	12

Table 13. Life Cycle Cost Analysis for solar thermal system assisted building heating with specific heat energy consumption 57 kWh/m² a

Real interest rate 3,9% ; Building 70 kWh/m² a

Measures	Investment	Net savings	Lifetime	PB	PO	IRR	NPV	NPVQ	ax.Investment	
	EUR	EUR/Year	Year	Year	Year	%	EUR		EUR	Year
Pellet boiler	2000	314	20	6.4	7.5	15	2.297	1.15	2.965	12
Heat pump	5000	571	20	8.8	10.9	10	2.814	0.56	5.392	12
HP 16/1-1000	7000	702	20	10	12.9	8	2.607	0.37	6.629	12
EH 16/1-1000	3600	301	20	12	16.5	6	519	0.14	2.842	12
HP 32/1-1000	9700	730	20	13.3	19.1	4	290	0.03	6.893	12
HP 32/1-1500	10700	715	20	15	23	3	-915	-0.09	6.752	12
EH 32/1-1000	6000	393	20	15.3	23.7	3	-622	-0.10	3.711	12
HP 32/1-2000	12500	754	20	16.6	27.3	2	-2.181	-0.17	7.12	12
EH 32/1-1500	7000	393	20	17.8	31.2	1	-1.622	-0.23	3.711	12
EH 32/1-2000	8000	446	20	17.9	31.6	1	-1.896	-0.24	4.212	12
HP 64/1-1000	14700	768	20	19.1	36.1	0	-4.19	-0.29	7.252	12
HP 64/1-2000	17300	786	20	22	51.7	0	-6.453	-0.38	7.422	12
EH 64/1-1000	10000	454	20	22	51.8	0	-3.787	-0.38	4.287	12
HP 64/1-1500	16500	731	20	22.6	56.3	0	-6.496	-0.39	6.903	12
EH 64/1-2000	12800	542	20	23.6	67.7	0	-5.383	-0.42	5.118	12
EH 64/1-1500	12000	404	20	29.7	99	0	-6.471	-0.54	3.815	12

According the presented results several conclusions can be drawn. As most profitable measure according the LCC analysis is the measure with the highest NPVQ. Thus, most profitable would be installing pellet boiler as unique heating source with payback period of 4 years. Next profitable measure would be solar system with total collector area of 16 m² and heat pump as additional auxiliary heat source. Further follows the systems with collector array areas of 32 m² and 64 m² with different storage tank volumes in combination with auxiliary heat device electric heater (EH) or heat pump (HP). LCC analysis reveal that for same collector area and storage tank volume more profitable is the combination solar collectors with heat pump instead with electric heater although the starting investment is far lower for electric heater but energy savings contribute to have lower payback period for the heat pump system.

It can be noticed from Table 12 that the net present values for all of the system combination with 64 m² collectors, have negative values which indicates that those systems are not profitable for buildings with specific heat energy consumption of 70 kWh / m² a.

Next is LCCA for the same solar thermal systems but applied to building with lower specific heat consumption of 57 kWh/m² a, represented with the Building type III described in Table 4.

It's interesting to be noticed that same solar thermal systems for the building with the higher specific energy consumption have lower payback period since they have bigger energy consumption thus generating larger energy differences compared with the scenario with electrical boiler and the solar system. This is comparison between same systems but also should be noticed that with same systems at the building with lower specific heat consumption are achieved bigger solar fractions.

Further is analyzed the building energy consumption influence on the solar system performance i.e. same solar air-conditioning system is applied to building with lower specific heat energy consumption. Analysing the presented results is indicative that improved and feasible combination would be with heat pump instead of electrical heater which is further verified with LCC analysis. The LCC method provides a better assessment of the long-term cost-effectiveness of the project/measure than other economic methods which only focus on initial investment costs and operation costs for the first years. Another comparison is performed for the same solar thermal systems in regard of the primary energy according the results presented in Table 10 and Table 11. Differences in primary energy consumptions are noticeable for the same solar systems applied in the two buildings i.e. logically much lower primary energy consumption and lower CO₂ emissions for the building with lower specific heat energy but it's interesting that especially the differences are expressed at the smaller collector areas with electrical heater as auxiliary device. Also from the presented LCC analysis can be concluded that for same collector areas it is more cost-effective the auxiliary source to be heat pump instead of electrical heater although the investment is higher for the HP but on longer period is more feasible.

The specific absorption chiller costs per kW cooling power are taken from [14]. The costs are from manufacturers based on Germany and from a survey of the international energy agency. According the presented costs for the analysis is chosen that the absorption chiller as ne assembly with the cooling tower costs 1500 eur/ kW i.e. total 15 000 eur.

In the next Table are presented results from the comparison between the energy consumption, system costs, primary energy consumption and CO₂ emissions for the chiller conventional system and the solar assisted absorption cooling.

It is assumed that the chiller average cooling coefficient of performance is 3 and regarding the building cooling loads in the simulations is used the Building type II for which the annual cooling load is 1800 kWh. The DHW in the case of conventional chiller is heated 100% by electrical heater while in the case of absorption machine the area of solar collectors are sufficient to provide 100% solar fraction for the DHW i.e. it is not used any additional auxiliary energy. According the presented results can be concluded that there is no need to be performed LCC analysis since the simple payback period is bigger than 20 years i.e. bigger than the system lifetime. Main reasons for the non-feasibility of these solar-assisted air-conditioning systems mainly is the low electricity price of 0.09 eur/kWh but also is the low cooling energy demand since it is analyzed residential building which usually have small internal gains. Nevertheless according the results in Table the solar – assisted cooling systems provides big possibilities for decrease in primary energy consumption and CO₂ emissions

Table 14. Solar thermal system energy performance, costs, parameters and CO₂ emissions, primary energy consumption for building with specific cooling energy consumption 12 kWh/m² a

Parameter	Unit	Solar thermal system - Area/Storage tank volume = 1000 l					
		Chiller	10/1000-EH	14/1000-EH	16/1000-EH	18/1000-EH	22/1000-EH
Auxiliary energy - cooling system	kWh	600	324	246	204	174	132
Auxiliary energy - DHW	kWh	835			0		
Absorption electrical energy	kWh				461		
System electrical energy consumption (circ.pumps)	kWh	293			90		
Specific electrical energy price	eur/kWh				0.09		
Total energy price	eur	156	79	22	18	16	12
Heat source device/system price	eur	6500			15000		
Primary energy consumption	kWh	5720	2896	2638	2499	2400	2261
Annual CO ₂ emissions	kg/year	570	289	263	249	239	225
Annual average solar fraction - SF	%		46	59	66	71	78

4. Conclusion

Results show that most profitable would be installing pellet boiler as heating source 100% covering the heating needs, with payback period of 4 years. Second profitable measure would be solar system with total collector area of 16 m² and heat pump as additional auxiliary heat source. Further follows the systems with collector array areas of 32 m² and 64 m² with different storage tank volumes in combination with auxiliary heat device electric heater (EH) or heat pump (HP). LCC analysis reveal that for same collector area and storage tank volume more profitable is the combination solar collectors with heat pump instead with electric heater although the starting investment is far lower for electric heater but energy savings contribute to have lower payback period for the heat pump system.

Solar cooling is not yet feasible solution for the residential sector. Main reasons are the low specific cooling energy consumption, low electricity price and high investment cost for the absorption chiller. However, solar energy showed that can be achieved big primary energy savings resulting with more that 50% compared with the conventional energy sources i.e. electrical energy. Thus can be said that solar energy is environmental friendly also decreasing to a high extent the greenhouse gasses emissions.

Further recommendation is to be researched the technical and economic feasibility of implementation solar assisted air-conditioning systems in commercial buildings since they have high internal loads thus offering potential for big energy savings.

Literature:

1. Communication energy 2020—A strategy for competitive sustainable and secure energy, E.C. Brussels, Editor. 2010.
2. ESTIF, The Spanish Technical Building Code (Royal Decree 314/2006). 2006. p. 42.
3. ESTIF, E.S.I., Best practice regulations for solar thermal. 2007. p. 61.
4. International Energy Agency , I., Technology Roadmap-Solar Heating and Cooling. 2012.
5. Ampatzi, E., I. Knight, and R. Wiltshire, The potential contribution of solar thermal collection and storage systems to meeting the energy requirements of North European Housing. *Solar Energy*, 2013. 91(0): p. 402-421.
6. Argiriou, A.A., CSHPSS systems in Greece: Test of simulation software and analysis of typical systems. *Solar Energy*, 1997. 60(3–4): p. 159-170.
7. Henning, H.-M. and J. Döll, Solar Systems for Heating and Cooling of Buildings. *Energy Procedia*, 2012. 30(0): p. 633-653.
8. Pinel, P., et al., A review of available methods for seasonal storage of solar thermal energy in residential applications. *Renewable and Sustainable Energy Reviews*, 2011. 15(7): p. 3341-3359.
9. Jan Albers, F.S., HEAT TRANSFER CALCULATION FOR ABSORPTION HEAT PUMPS UNDER VARIABLE FLOW RATE CONDITIONS, in International Sorption Heat Pump Conference. 2011: Italy. p. 9.
10. H.-M.Hellman, C.S., F.Ziegler, The characteristics equations of absorption chillers, in International sorption heat pump conference. 1999: Germnay.
11. www.hidros.eu. Heat pump. Heat pumps air/water DC inverter compressor with vapor injection (EVI) 2014 [cited 2014 04.07.2014]; Heat pumps air/water DC inverter compressor with vapor injection (EVI)].
12. European Commitee for standardization., Energy performance of buildings - Overall energy use and definition of energy ratings, in Primary energy factors ; Carbon dioxide emissions. 2008, European Commitee for standardization: Brussels. p. 62.
13. www.erc.org.mk. Macedonia, Energy Regulatory Comission. Pricing-Electricity. 2014 [cited 2014 14.07].
14. Eicker, U., et al., Economic evaluation of solar thermal and photovoltaic cooling systems through simulation in different climatic conditions: An analysis in three different cities in Europe. *Energy and Buildings*, 2014. 70(0): p. 207-223.